

Dissertation
Submitted to the
Combined Faculties for Natural Sciences and Mathematics
Of the Ruperto-Carola university of Heidelberg, Germany
For the degree of the
Doctor of Natural Sciences

Presented by
Diplom- Rahul Dhandapani
Born in: Hyderabad, India
Oral-examination: 6th March 2017

Identification of primary sensory neurons that mediate mechanical allodynia

Referees:

Prof. Dr. Cornelius Gross

Prof. Dr. Stephan Frings

Abstract

Mechanical allodynia is a type of neuropathic pain in which innocuous touch evokes severe pain. Despite several years of research, the primary sensory neurons that mediate allodynia still remain unidentified. In this study, we demonstrate that a population of low threshold mechanoreceptors expressing TrkB mediates the input that produces pain from light touch after nerve injury. Using an inducible Cre line driven from the TrkB gene locus, we show that TrkB is expressed in D-hairs and RA A β -mechanoreceptors. Ablation of TrkB positive neurons leads to reduction in sensitivity to the gentle touch under naïve conditions, and failure to develop mechanical allodynia in a nerve injury model of neuropathic pain. Also, selective optogenetic activation of these neurons evokes marked nocifensive behavior after nerve injury. Furthermore, we develop a phototherapeutic strategy based on the ligand for TrkB to perform ligand-mediated photo-ablation of TrkB positive afferents. Using this approach we show that selective photo-ablation of TrkB afferents in the skin results in a pronounced rescue of mechanical allodynia in multiple models of neuropathic pain. We thus identify the peripheral neurons which transmit pain from light touch and establish a novel therapeutic strategy for its treatment.

Zusammenfassung

Mechanische Allodynie ist eine Klasse von neuropathischem Schmerz, bei der eine sanfte Berührung einen heftigen Schmerz auslöst. Trotz intensiver Forschung konnten bisher die primären sensorischen Neuronen, die für die Allodynie verantwortlich sind, nicht identifiziert werden. In dieser Studie zeigen wir, dass eine Gruppe von TrkB exprimierenden niedrigschwelligen Mechanorezeptoren als Auslöser für den Schmerz durch sanfte Berührung nach einer Nervenverletzung verantwortlich sind. Mit Hilfe einer induzierbaren Cre Linie, die aus dem TrkB Genlokus abstammt, zeigen wir, dass TrkB im D-Haar und in RA A β -Mechanorezeptoren exprimiert wird. Die Entfernung von TrkB-positiven Neuronen führt zu einer Reduktion der Sensitivität der sanften Berührung unter naiven Bedingungen und die Nerven sind in einem Modell mit einer Nervenverletzung nicht in der Lage, eine mechanische Allodynie zu entwickeln. Auch ruft eine selektive optogenetische Aktivierung dieser Neuronen ein deutliches nozifensives Verhalten nach einer Nervenverletzung hervor. Des Weiteren entwickeln wir eine phototherapeutische Strategie, die auf dem Liganden für TrkB beruht, um eine Liganden-abhängige Photoablation von TrkB-positiven afferenten Neuronen durchzuführen. Durch diesen Ansatz zeigen wir, dass selektive Photoablation von TrkB afferenten Neuronen in der Haut zu einer ausgeprägten Auslösung von mechanischer Allodynie in multiplen Modellen von neuropathischen Schmerz führt. Auf diese Weise können wir die peripheren Neuronen identifizieren, welche die leichte Berührung in Schmerz verwandeln, und können einen neuen therapeutischen Ansatz hierfür entwickeln.

Acknowledgements

I would like to first convey my gratitude to Paul for giving me an opportunity to work in his lab and on this project. His mentorship and guidance throughout this work has been of immense help.

Next I would like to thank the Heppenstall lab for their inputs through all these years. My sincere thanks to the facilities at EMBL Monterotondo, the collaborators who are part of this work and my TAC committee for their help.

Finally, I would like to thank my parents and all friends, especially the EMBL Monterotondo family for their support.

1 Table of Contents

2	Introduction.....	11
2.1	Somatosensation	11
2.2	The peripheral nervous system	12
2.3	Nociceptors	15
2.4	Mechanoreceptors.....	16
2.4.1	Hairy skin mechanoreceptors.....	17
2.4.2	Glabrous skin mechanoreceptors	18
2.5	Diversification of mechanoreceptors	20
2.6	Genetic labelling of mechanoreceptor subtypes.....	21
2.7	Mechano-transductive channels.....	25
2.7.1	Piezo2	25
2.7.2	Acid Sensing Ion Channels	26
2.7.3	Transient Receptor Potential channels	27
2.7.4	K ⁺ channel family	27
2.7.5	Stomatin.....	28
2.7.6	aTAT1.....	28
2.8	Neuropathic pain	29
2.8.1	Primary hyperalgesia	30
2.8.2	Secondary hyperalgesia and mechanical allodynia	30
2.8.3	Central mechanisms of mechanical allodynia.....	33
2.9	Treatment of Neuropathic pain.....	34
2.10	Mouse models of neuropathic pain	35
2.10.1	Sciatic nerve transection.....	35
2.10.2	Partial nerve ligation (PNL).....	36
2.10.3	Chronic constriction injury (CCI).....	36
2.10.4	Spared nerve injury (SNI)	36
2.10.5	Spinal nerve ligation.....	37
2.10.6	Inflammatory pain.....	37
2.10.7	Diabetic neuropathy.....	37

2.10.8	Drug-induced neuropathy.....	37
2.11	TrkB and BDNF: involvement in neuropathic pain.....	38
2.12	General aims.....	39
3	Materials and methods.....	40
3.1	Generation of TrkB ^{CreERT2} mice.....	40
3.2	Generation of Avil ^{mCherry} mice.....	40
3.3	Avil ^{iDTR} mice.....	41
3.4	Tamoxifen treatment.....	41
3.5	Immunofluorescence.....	42
3.6	In-situ Hybridization.....	44
3.7	Ex-vivo skin nerve preparation.....	44
3.8	Diphtheria toxin injection.....	45
3.9	Behavioral testing.....	46
3.9.1	Acetone drop test.....	46
3.9.2	Hot plate test.....	46
3.9.3	Grip strength test.....	46
3.9.4	Pin-prick test.....	47
3.9.5	Tape-test.....	47
3.9.6	Cotton swab test.....	47
3.9.7	Von Frey test.....	47
3.9.8	Dynamic brush test.....	48
3.10	Models of neuropathic pain.....	48
3.10.1	Spared nerve injury model.....	48
3.10.2	CFA model.....	48
3.10.3	Chemotherapy induced neuropathic pain.....	49
3.10.4	Diabetes induced peripheral neuropathy.....	49
3.11	Light activation using channelrhodopsin.....	50
3.12	C-fos labelling of the spinal cord.....	50
3.13	Production of recombinant BDNF ^{SNAP}	51
3.14	Synthesis of BG-IR700.....	51
3.15	In-vitro labeling of BDNF ^{SNAP}	51

3.15.1	HEK293T labeling.....	51
3.15.2	DRG labelling	52
3.16	In-vitro photo-ablation	52
3.17	In-vivo photo-ablation.....	53
3.18	Statistical analysis	53
4	Results.....	54
4.1	Molecular characterization of TrkB ⁺ sensory neurons in adult mice.....	54
4.1.1	TrkB expression in the DRG.....	54
4.1.2	TrkB expression in the skin.....	56
4.1.3	TrkB expression in the spinal cord	58
4.1.4	TrkB expression in human DRG and skin	58
4.1.5	Ex-vivo skin nerve electrophysiology	60
4.2	Functional characterization of TrkB ⁺ neurons.....	62
4.2.1	Ablation of TrkB ⁺ neurons leads to reduction in responses to gentle touch.....	62
4.3	Role in mechanical allodynia.....	64
4.3.1	Inflammatory pain unaffected in TrkB ablated mice.....	64
4.3.2	TrkB ⁺ neurons contribute to allodynia after nerve injury	66
4.3.3	c-fos induction increases in lamina I after SNI.....	67
4.4	BDNF ^{SNAP} as a target for TrkB ⁺ neurons.....	67
4.4.1	BDNF ^{SNAP} labels TrkB ⁺ neurons in-vitro	68
4.4.2	BDNF ^{SNAP} mediated ablation in-vitro	68
4.4.3	BDNF ^{SNAP} mediated ablation in-vivo.....	69
4.4.4	BDNF ^{SNAP} mediated rescue of mechanical allodynia	72
4.4.5	BDNF ^{SNAP} mediated rescue of diabetic peripheral neuropathy	74
4.4.6	BDNF ^{SNAP} mediated rescue of chemotherapy induced neuropathic pain	75
5	Discussion.....	76
5.1	TrkB is expressed in LTMR subsets	76
5.2	TrkB ⁺ neurons are required to detect gentle mechanical stimuli.....	77
5.3	TrkB ⁺ neurons drive mechanical allodynia after injury.....	79
5.4	BDNF ^{SNAP} as a therapeutic molecule for allodynia in mice.....	81
5.5	BDNF ^{SNAP} mediated photo-ablation reverses mechanical allodynia	83

5.6	Future perspectives.....	83
6	Conclusion.....	87
7	References	88
8	Supplementary figures.....	100

Table of Figures

FIGURE 1: SCHEMATIC OF SENSORY AFFERENTS	13
FIGURE 2: SCHEMATIC OF CUTANEOUS RECEPTORS	16
FIGURE 3: CLASSIFICATION OF SENSORY NEURON SUBTYPES	21
FIGURE 4: EXPRESSION OF TRKB IN DRG	54
FIGURE 5: CO-LOCALIZATION OF TRKB WITH KNOWN MOLECULAR MARKERS	56
FIGURE 6: TRKB INNERVATES HAIR FOLLICLES IN THE SKIN	57
FIGURE 7: TRKB INNERVATES MEISSNER'S CORPUSCLES IN GLABROUS SKIN	57
FIGURE 8: TRKB TERMINATES IN LAMINAE III/IV OF THE DORSAL HORN	58
FIGURE 9: TRKB-IR IN HUMAN DRG MARKS MECHANORECEPTORS	59
FIGURE 10: TRKB-IR IN MEISSNER'S CORPUSCLES OF HUMAN PALMAR SKIN	60
FIGURE 11: SKIN-NERVE ELECTROPHYSIOLOGY OF TRKB ⁺ AFFERENTS	61
FIGURE 12: DIPHTHERIA TOXIN MEDIATED ABLATION OF TRKB ⁺ NEURONS	63
FIGURE 13: TRKB ⁺ NEURONS DRIVE MECHANICAL ALLODYNIA	65
FIGURE 14: BDNF ^{SNAP} LABELLING ON CELLS IN-VITRO	68
FIGURE 15: BDNF ^{SNAP} MEDIATED ABLATION IN-VITRO	69
FIGURE 16: BDNF ^{SNAP} MEDIATED ABLATION IN DRG SECTIONS	70
FIGURE 17: BDNF ^{SNAP} MEDIATED ABLATION IN-VIVO	71
FIGURE 18: PHOTOABLATION USING BDNF ^{SNAP} RESCUES MECHANICAL ALLODYNIA	72
FIGURE 19: VISUALIZATION OF BDNF ^{SNAP} MEDIATED ABLATION IN-VIVO	73
FIGURE 20: BDNF ^{SNAP} MEDIATED RESCUE OF DIABETIC AND CHEMOTHERAPY INDUCED NEUROPATHY	75
FIGURE 21: MANUAL PICKING OF CELLS FOR SEQUENCING	86
SUPPLEMENTARY FIGURE 22: GENERATION OF TRKB ^{CREERT2} AND AVILM ^{CHERRY-HM3DQ} MICE	100
SUPPLEMENTARY FIGURE 23: IN-SITU HYBRIDIZATION FOR TRKB	101
SUPPLEMENTARY FIGURE 24: STAINING FOR MOLECULAR MARKERS ON TRKB ABLATED MICE	101
SUPPLEMENTARY FIGURE 25: INNERVATION OF HIND-PAW AFTER BDNF ^{SNAP} PHOTOABLATION	102

Table of abbreviations

DRG	Dorsal Root Ganglia
GCT	Gate Control Theory
LTMR	Low Threshold Mechanoreceptors
HTMR	High Threshold Mechanoreceptors
RA	Rapidly Adapting
SA	Slowly Adapting
TRKA	Tropomyosin Receptor Kinase A
TRKB	Tropomyosin Receptor Kinase B
TRKC	Tropomyosin Receptor Kinase C
NGF	Nerve Growth Factor
BDNF	Brain Derived Neurotrophic Factor
NT3	Neurotrophin-3
NT4	Neurotrophin-4
TRP	Transient Receptor Potential
ASIC	Acid Sensing Ion Channel
MRGPR	Mas Related G-Protein like Receptor
IB4	Isolectin B4
CGRP	Calcitonin Gene Related Peptide
TH	Tyrosine Hydroxylase
NF200	Neuro Filament 200
VGLUT	Vesicular Glutamate Transporter
SOM	Somatostatin
PKC	Protein Kinase C
GABA	Gamma Amino Butyric Acid
DTR	Diphtheria Toxin Receptor
DTX	Diphtheria Toxin

2 Introduction

2.1 Somatosensation

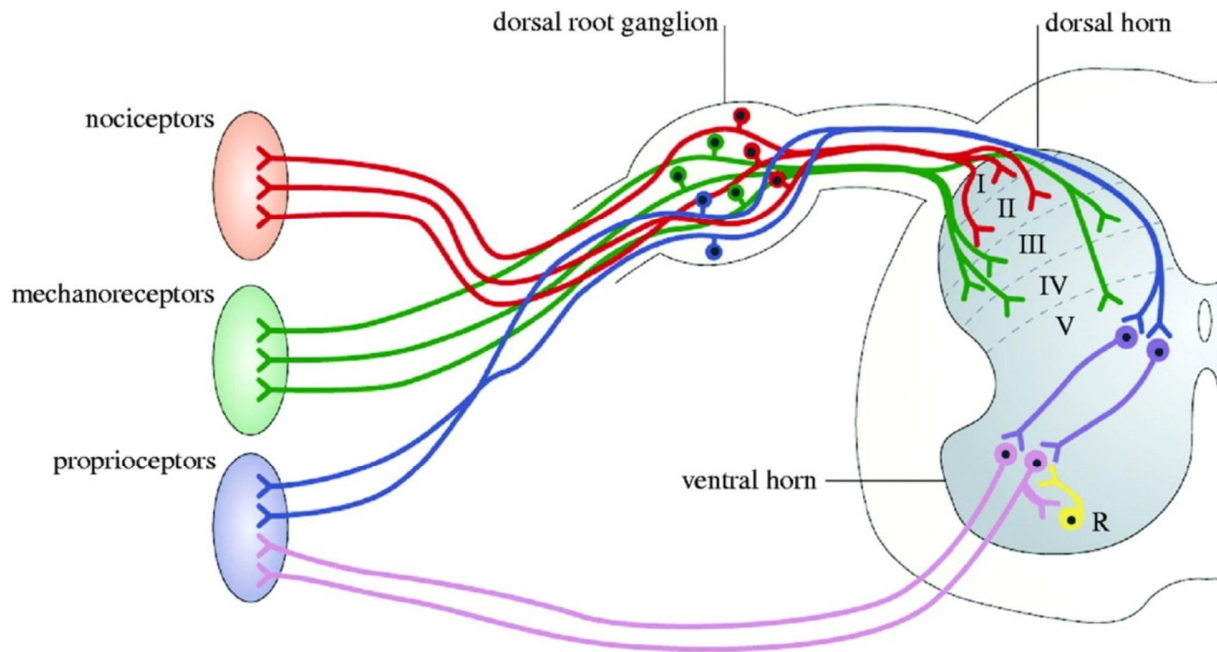
The ability of organisms to detect and respond to the many forces acting on the body is crucial for their interaction with the environment and for survival. Evolutionarily mammals have evolved to differentiate between noxious, such as extreme heat or an injury causing stimuli and innocuous stimuli, such as a mother's nurturing caress, feeling a gentle breeze by the sea or crawling of an insect on the skin. How this assortment of stimuli is perceived by the body has fascinated scientists and philosophers alike for several centuries. The sense of touch was described by Aristotle as one of five basic senses along with sight, hearing, taste and smell. The dawn of the 17th century saw the postulation of four major theories to describe the perception of touch and pain; specificity, intensity, pattern and gate control theories (Perl, 2007, Moayed and Davis, 2013). The specificity theory posits that dedicated pathways carry specific stimuli. For example noxious stimuli were carried to the brain by pain-sensing afferents (later termed nociceptors) while non-noxious stimuli were encoded by mechanoreceptors (Sherrington, 1903). A representation of the connections was provided much earlier by Rene Descartes in his image-concept of pain (Perl, 2007). The specificity theory was further strengthened by the discovery of cutaneous end organs in the skin like the Meissner's and Pacinian corpuscles, Merkel cells etc. This discovery also led to the fall of the intensity theory, which required a sufficient intensity to be reached for a stimulus to feel painful (Dallenbach, 1939). In parallel, the pattern theory was proposed to challenge the specificity theory. According to the pattern theory, response to stimuli is produced by impulses travelling in varied spatio-temporal pattern. The postulate relies on the conduction velocity, adaptation rates and the receptive fields of the primary afferent fibers to generate a sensation in the brain (Lele et al., 1954).

Finally, the Gate Control theory of pain (GCT) combines the above theories to an extent. First proposed by Wall and Melzack in 1965, the GCT is based on the presence of gates in dorsal horn of the spinal cord which is composed mainly of pain-transmission interneurons. According to the theory, noxious stimuli carried by pain transducing fibers open the gate leading to pain perception while an innocuous stimulus closes the gate to pain through a series of feed forward inhibitory networks (Melzack and Wall, 1965). The GCT shed lights on the plasticity of the somatosensory system. Earlier it was assumed that the primary afferents formed a hard-wired circuitry. Under this assumption pathological pain states such as that arising due to neuropathic pain could not be accounted for. The GCT refutes this concept and provides an alternate circuit for conditions of hypersensitivity and also mechanical allodynia.

2.2 The peripheral nervous system

The cell bodies of primary afferent fibers located within the Dorsal Root Ganglia are pseudo-unipolar neurons containing one axon branching into different regions of the hairy and glabrous skin, and a second axon terminating in different laminae of the spinal cord. Cutaneous sensory neurons can be grouped into A β , A δ and C-fibers based on the extent of myelination of the nerves, their conduction velocities, adaptation properties and mechanical thresholds (Brown and Iggo, 1967, Burgess et al., 1968, Zotterman, 1939). A β -fibers are thickly myelinated and have fast conduction velocities (16-100m/s). A δ -fibers are thinly myelinated and have conduction velocities in the range of 5-30m/s and C-fibers are unmyelinated with slow conduction velocities (0.2-2m/s). Furthermore, cutaneous fibers can adapt rapidly (RA) or slowly (SA) to a constant stimuli (Iggo, 1985). Almost all A β -fibers and subsets of A δ and C-fibers exhibit low mechanical threshold to von-Frey filaments suggesting their role in detecting innocuous mechanical stimuli while most A δ and C-fibers have high mechanical thresholds and

are believed to detect noxious mechanical or thermal stimuli (Zotterman, 1939, Koerber and Woodbury, 2002, Zimmermann et al., 2009).



As taken from Caspary & Anderson, Nature reviews neuroscience 2006

Figure 1: Schematic of sensory afferents

A diagram of the somatosensory system showing the heterogeneous group of DRG neurons and their axonal projections in the periphery and the spinal cord.

The stimuli transduced from the skin and deep visceral organs terminate in different laminae of the dorsal horn of spinal cord which acts as the integration port for the signals. The dorsal horn of the spinal cord can be divided into six laminae as described by Rexed using Nissl staining on cross sections of the spinal cord (Light and Perl, 1979). Lamina I, the outermost layer of the dorsal horn receives inputs largely from pain and heat/cold sensing A δ and C-fiber afferents. The lamina II, also referred to as the substantial gelatinosa can be subdivided into two regions; lamina II_o and II_i, and receive inputs from neurons carrying information about pain and

innocuous touch respectively. Laminae III to VI are mainly innervated by hair follicle afferents (mostly A δ and A β) which form flame-shaped arbors and by specialized touch sensing organs in the limbs (Light and Perl, 1979). The different laminae of the dorsal horn are also composed of morphologically distinct, locally projecting interneurons. Nearly 30-40% of interneurons in the dorsal horn is inhibitory and use GABA and/or glycine as neurotransmitters while the remaining interneurons are excitatory and depend on glutamate (Todd, 2010, Zeilhofer et al., 2012). The dorsal horn also contains many projection neurons that are mainly concentrated within lamina I and some as Wide Dynamic Range (WDR) neurons in deep laminae that relay information into different regions of the brainstem and the thalamus (Todd, 2010). While how different innocuous tactile stimuli are integrated within the spinal cord remains unclear, great advancements have been made in understanding how painful stimuli is processed in the dorsal horn, especially under chronic pain conditions and this will be discussed in more detail in later sections of this thesis.

The ability of sensory neurons to detect several distinct sensory modalities is attributed to the heterogeneity of fiber types. During development, DRG neurons undergo a series of diversification events controlled by *neurogenin1* and *neurogenin2* along with a combination of transcription factors (Runx1 and Runx3) (Ma et al., 1999), receptor tyrosine kinases (TrkA, TrkB, TrkC and Ret) (Huang and Reichardt, 2003) and neurotrophic growth factors like Nerve Growth Factor (NGF), Brain Derived Neurotrophic Factor (BDNF), Neurotrophins NT-3, NT-4 and the GDNF family of ligands (Ernsberger, 2009) to form different subsets that can be broadly categorized as nociceptors, thermo-receptors, mechanoreceptors, proprioceptors and pruriceptors (Marmigere and Ernfor, 2007, Liu and Ma, 2011). A more detailed description of mechanoreceptors and to an extent about nociceptors will be provided in the next sections.

2.3 Nociceptors

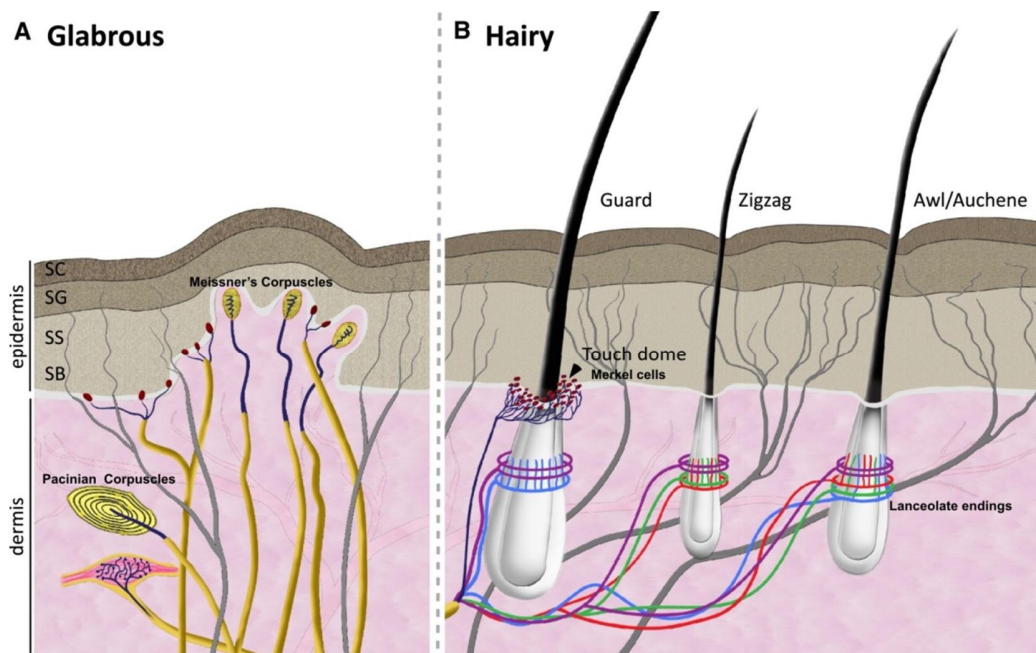
Nociceptors are a class of sensory neurons that are specialized to detect noxious thermal, mechanical or chemical stimuli. They make up a majority of small-to-medium sized neurons in the DRG and can be either thinly myelinated A δ nociceptors (AM fibers) or unmyelinated C-fibers (Woolf and Ma, 2007, Basbaum et al., 2009). Anatomically, nociceptive afferents form extensive free nerve endings in the epidermis of the hairy and the glabrous skin (Zylka et al., 2005) and terminate within lamina I/II_o of the spinal cord dorsal horn. Most nociceptive neurons can detect more than one stimuli (i.e. noxious mechanical and thermal stimuli) making them poly-modal in nature (Basbaum et al., 2009, Woolf and Ma, 2007).

The development of nociceptors depends on a second wave of neurogenesis originating from the neural crest tube driven by *neurogenin1* (*Nng1*) (Ma et al., 1999). All developing nociceptors express receptor tyrosine kinase, TrkA. Following development, some nociceptors lose the expression of TrkA and develop expression of another receptor tyrosine kinase; Ret. At this stage, nociceptors can be further segregated into TrkA⁺ peptidergic or TrkA⁻/Ret⁺ non-peptidergic nociceptors. These two classes of nociceptors can be distinguished by their binding to CGRP and/or substance P and isolectin-B4 respectively (Snider and McMahon, 1998, Molliver et al., 1997). Fully developed nociceptors also express an array of ion channels that is essential for determining the type of noxious stimuli they detect. For example, members of the TRP channel (TRPV1, TRPA1, TRPM8 etc.) have been shown to be activated by noxious thermal and chemical stimuli (Julius and Basbaum, 2001, Caterina et al., 1997). Similarly, nociceptive neurons expressing voltage gated sodium channels like Nav1.7, Nav1.8 (Cox et al., 2006, Zimmermann et al., 2007), ASIC channels (Lingueglia, 2007) and a newly discovered class of Mas-related G protein coupled receptors (MRGPR) have been shown in transducing

harmful mechanical pain (Dong et al., 2001, Cavanaugh et al., 2009). Another interesting class of nociceptors, called the “silent nociceptors” are unmyelinated neurons that are mechanical insensitive under naïve conditions but develop mechanical sensitivity upon injury (Schmidt et al., 1995).

2.4 Mechanoreceptors

Mechanoreceptors constitute a diverse group of neurons that detect innocuous mechanical force acting on the skin. Mechanosensitive neurons can be one of two main types, Low-Threshold Mechanoreceptors (LTMRs) and High Threshold Mechanoreceptors (HTMRs), depending on the strength of mechanical stimuli they detect (Abraira and Ginty, 2013).



As taken from Abraira and Ginty, Neuron 2013

Figure 2: Schematic of cutaneous receptors

Schematic showing the different types of innervations within the skin. Cutaneous mechanoreceptors mainly innervate hair follicles, Merkel cells, Meissner's corpuscles and the Pacinian corpuscles.

One of the hallmark features of mechanoreceptors lies in the diversity of skin structures they innervate. Mammalian skin can be divided into hairy skin, which contributes to nearly 80% of all skin area and the glabrous or non-hairy skin (fig 2).

2.4.1 Hairy skin mechanoreceptors

The hairy skin is composed of 3 major hair follicle subtypes: guard, zig-zag and awl/auchene hairs which are innervated by one or a combination of $A\beta$, $A\delta$ and C-fiber LTMRs in an intricate pattern forming fork-like nerve endings (Hoggan and Hoggan, 1893).

The most abundant fiber type present in the hairy skin are the C-fiber LTMRs which form longitudinal lanceolate endings associated with Zigzag and Awl/Auchene hair follicles which make up 76% and 23% of all hair follicles types in the skin (Li et al., 2011). Although C-fibers were originally thought to transduce noxious stimuli through their free nerve endings, hair follicle C-LTMRs have been shown to be activated by skin indentation and slow movement across the skin associated with tickling or massage-like stimuli (Vrontou et al., 2013). Interestingly, psychophysical studies on C-tactile afferents of human suggest their function in detecting pleasant mechanical stimuli that controls social and emotional aspects of gentle skin to skin contact (McGlone et al., 2014).

The second major type of fiber innervating hair follicles is the $A\delta$ -LTMR or the D-hair receptors. D-hairs get their name from the small down hairs present in cats and rabbit (Brown and Iggo, 1967). D-hairs have unique physiological properties among all fiber types in that they are the most sensitive mechanoreceptor in the skin with the lowest mechanical threshold of activation and the largest receptive field in the skin (Lechner and Lewin, 2013). D-hair receptors form lanceolate endings associated with almost all Zigzag and Awl/Auchene hairs (Li et al.,

2011). Recently, it has been shown that D-hairs receive A δ -fiber innervations in a Caudal-to-Rostral direction suggesting a potential role in detecting movement of hair in one direction (Rutlin et al., 2014).

The third type, A β -fibers are found in two different areas of the hairy skin. RA A β -fibers are found innervating Guard hair follicles which make up only 1-2% of all hair types (Li et al., 2011), while SA A β -fibers form connections with Merkel cells in touch domes of the skin (Iggo and Muir, 1969). Although least abundant in the hairy skin, A β -fibers are predominantly found in the glabrous skin.

2.4.2 Glabrous skin mechanoreceptors

The glabrous skin contains several specialized mechanosensory end organs like the Meissner corpuscles, Pacinian corpuscles, Merkel-cell neurite complexes and Ruffini endings (Iggo and Andres, 1982). Each of these end organs receives primary afferent innervations from different sub-populations of LTMR δ and are tuned to detect different forces like pressure, vibration, skin-indentation, movement of the hair and light touch of the skin.

Meissner δ corpuscles as described by Georg Meissner in 1852 are located in the dermal papillae mainly of the palm and foot (Cauna, 1956). They receive innervations from RA A β -fibers and are termed RAI mechanoreceptors. These afferents fire only at the onset and the offset of the stimuli. Microstimulation studies of the hand show that A β -fibers of the Meissner δ corpuscles have low threshold of activation, are tuned to frequencies of 10-50Hz and have small receptive fields that help detecting flutter δ or similar low frequency vibrations (Talbot et al., 1968, Pare et al., 2001).

Pacinian corpuscles are located in the subcutaneous region of the skin (Zelena, 1978) and are characterized by large receptive fields and firing to high frequency vibrations (200-300Hz). Pacinian corpuscles receive one A β -fiber innervation and are generally termed RAI mechanoreceptors (Wende et al., 2012b, Fleming et al., 2016). Although the function of these corpuscles is not clearly understood, they are believed to sense the texture or dimensions of objects through touch (Brisben et al., 1999).

Merkel cells are specialized keratinocytes that are present in the basal epidermis. They receive inputs from A β -fibers to form Merkel cell-neurite complexes (Halata et al., 2003, Maricich et al., 2009). They are usually present in the basal epidermis or as a cluster of cells called "touch-domes" often associated with guard hairs (Li et al., 2011). In contrast to Meissner's and Pacinian corpuscles, the afferents that form connections with Merkel cells are SAI-type that fire at the onset and remain active throughout the static phase of the stimuli (Carroll, 1998, Maricich et al., 2009). Merkel cell-neurite complex forms a "two-receptor" system with the Merkel cells and the afferents transducing the static and dynamic stimuli respectively contributing to discriminative light touch (Maksimovic et al., 2014, Woo et al., 2014).

Ruffini endings are corpuscular structures that receive one A β -fiber innervation (Chambers et al., 1972). They are characterized by SAII responses that exhibit firing at regular intervals during the static phase as compared to the constant firing of SAI afferents (Zimmermann et al., 2009). The presence of Ruffini endings in most mammals is still unclear. However, physiological recordings place the corpuscles as stretch detectors.

Although electrophysiological properties of cutaneous mechanoreceptors have been extensively characterized in cats, rabbits, monkeys, rodents and humans, very little are known about the molecular identities of the neurons and their composition.

2.5 Diversification of mechanoreceptors

The development of mechanoreceptors is driven by a first wave of neurogenesis controlled by *neurogenin2* (*ngn2*) with the expression of one or a combination TrkB, TrkC and Ret (Ma et al., 1999). This process can be delineated into the early-Ret and the TrkB/TrkC populations (Lallemend and Ernfors, 2012). The early-Ret neurons rely on transcription factor MafA for its diversification between E10.5-E11.5 (Bourane et al., 2009). By E16.5, 3 different subsets of early-Ret can be visualized; Ret⁺/MafA⁺, Ret⁺/MafA⁺/TrkC⁺ and Ret⁺/TrkB⁺/MafA⁺/Shox2⁺ (Abdo et al., 2011, Scott et al., 2011). We now know that the Ret⁺/MafA⁺ neurons are the A β -mechanoreceptors that innervate Meissner's corpuscles and form lanceolate endings on Guard hairs (Bourane et al., 2009) and the Ret⁺/MafA⁺/TrkC⁺ become circumferential A β -field receptors (Bai et al., 2015). It is conceived that the involvement of *Shox2* in the Ret⁺/TrkB⁺/MafA⁺/Shox2⁺ population leads to the development of a TrkB⁺/Ret⁺ population whose function remains unknown (Abdo et al., 2011, Kramer et al., 2006). In parallel, *Shox2* suppresses *Runx3* to form TrkB only population that is believed to form lightly myelinated A δ -fibers (Scott et al., 2011, Li et al., 2011).

On the other hand, C-fiber LTMRs develop through two separate diversification events with the expression of Ret⁺/MrgprB4⁺ and Ret⁺/TH⁺/Vglut3⁺ neurons (Molliver et al., 1997, Liu et al., 2008). The development of Vglut3⁺/TH⁺ neurons is controlled by Transcription factor *Runx1* which diversify into TH⁺ lanceolate endings and Vglut3⁺ free nerve endings (Lou et al., 2013). The Ret⁺/MrgprB4⁺ neurons diversify in later stages of development with the help of

Runx1 which in combination with TrkA controls the segregation of the different Mas related G proteins family (Liu and Ma, 2011). The Ret⁺/MrgprB4⁺ are believed to diversify only in the early postnatal days (Liu et al., 2007).

In spite of our understanding of the development of different subclasses of mechanoreceptors, their role in the behavior of mammals remain poorly understood mainly owing to the lack of genetic tools to manipulate these neurons and the lack of differential touch assays.

2.6 Genetic labelling of mechanoreceptor subtypes

Alongside their role in development, Ret, TrkA, TrkB and TrkC and their ligands have also been used as molecular markers for labelling different sensory neurons. This has been demonstrated in a recent study using unbiased single cell sequencing techniques to classify sensory neurons into four different mechanoreceptor subtypes (Fig 3)(Usoskin et al., 2015).

NF1	NF2	NF3	NF4	NF5	NP1	NP2	NP3	PEP1	PEP2	TH
LDHB CACNA1H TRKB ^{high} NECAB2	LDHB CACNA1H TRKB ^{low} CALB1 RET	LDHB TRKC ^{high} FAM19A1 RET	LDHB TRKC ^{low} PV SPP1 CNTNAP2	LDHB TRKC ^{low} PV SPP1 CNTNAP2	PLXNC1 ^{high} P2X3 GFRA2 MRGPRD	PLXNC1 ^{high} P2X3 TRKA CGRP MRGPRA3	PLXNC1 ^{high} P2X3 SST	TRKA CGRP KIT TAC1 PLXNC1 ^{low}	TRKA CGRP KIT CNTNAP2 FAM19A1	PIEZO2 ^{high} VGLUT3 GFRA2
LTMRs		Proprioceptors			Nonpeptidergic			Peptidergic		C-LTMRs
NEFH		Myelinated			Unmyelinated			Myel.		Unmyel.
RET		RET			RET			TRPV1		RET
		ASIC1			TRPA1					TRPA1
		RUNX3			TRPC3					TRPA1
					NAV1.8/9			NAV1.8/9		NAV1.8/9

As taken from Usoskin *et al.*, Nature neuroscience 2015

Figure 3: Classification of sensory neuron subtypes

Mechanoreceptors can be broadly classified into 4 distinct subtypes as suggested by Usoskin *et al.*, in 2015 using single cell sequencing techniques.

Among these, RA-LTMR δ and their dependence on Ret signaling for forming circuits required for the perception of touch are the best characterized thus far. Using Ret^{CreERT2} knock-in mice, Luo *et al.*, showed that tamoxifen administration at E12.5, marks a population of early-Ret⁺ in adult mice that exhibit features of RA A β -mechanoreceptors as characterized by the expression of NF200, a marker for myelinated sensory neurons and co-receptor GFR α 2 (Luo et al., 2009). They also show that Ret⁺ neurons innervated Meissner δ and Pacinian corpuscles, and formed longitudinal lanceolate endings around hair follicles. Furthermore, using a Wnt^{Cre}::Ret^{f/f} mice, they provide proof that Ret expression and Ret-GFR α 2 signaling is required only for the survival of Pacinian corpuscles and the requirement of TrkB-BDNF signaling for the survival of Meissner δ corpuscles and hair follicle endings (Luo et al., 2009). In parallel, using an in-situ screen Bourane *et al.*, found transcription factor MafA to be expressed in early-Ret⁺ neurons. MafA⁺/Ret⁺/GFR α 2⁺ neurons displayed properties of RA A β -mechanoreceptors and experiments with mutant MafA show that MafA controls the formation of Ret-specific subpopulations. However, the function of RA A β -mechanoreceptors remained unaffected in MafA mutants (Bourane et al., 2009). Another candidate transcription factor found in developing sensory neurons that has been studied in the formation of Ret⁺ neurons is c-Maf. c-Maf is co-expressed with MafA during development and postnatally. A β -fiber conduction velocity and firing properties of the fibers were disrupted in c-Maf^{flox/-} mice. Morphologically, c-Maf^{flox/-} mice displayed reduced NF200⁺ lanceolate endings and a 75% reduction of Meissner δ corpuscles. The strongest effect was a reduction in the quantity of Pacinian corpuscles and a 60% loss of axonal innervation of these corpuscles. Also, the authors found a defect in the detection of vibration in patients carrying a R288P mutation in c-Maf, without any changes in the tactile acuity suggesting a role for c-Maf in maintaining the function of Ret⁺/MafA⁺ neurons

innervating the Pacinian corpuscles (Bourane et al., 2009, Wende et al., 2012a, Wende et al., 2012b). Hair follicle innervating A β -fibers have been found to express Npy2r. Npy2r^{GFP} was found in around 6% of all thoracic DRG neurons and co-expressed NF200 and Ret. Skin-nerve recordings from these mice displayed RA A β -fiber activation properties. GFP positive nerves were found to form lanceolate endings around guard and awl/auchene hair follicles and also innervated Merkel cell touch domes (Li et al., 2011).

C-fiber LTMR δ can be characterized as Vglut3⁺/TH⁺ and MrgprB4⁺ neurons (Li et al., 2011, Lou et al., 2013, Vrontou, 2013). Vglut3-GFP is expressed in 10% of all lumbar DRG neurons almost all of which are unmyelinated. Skin-nerve recordings show that Vglut3⁺ neurons have slow conducting velocities (~0.58m/s) and displayed properties of C-fiber LTMR δ . Behavioral studies on Vglut3^{-/-} mice show significant difference in responses to a tail-clip test and tail withdrawal tests suggesting a role in detecting noxious mechanical stimuli (Seal et al., 2009). However using Vglut3^{Cre} mice, Luo *et al.*, showed that Vglut3 is expressed in 19% of all DRG neurons and those Vglut3⁺ C-fibers can be subdivided into Vglut3⁺/TH⁺ and Vglut3⁺/TH⁻ populations. Vglut3⁺/TH⁺ neurons were found to express Ret and GFR α 2 while they were negative for NF200 and other nociceptive markers like isolectin-B4 or CGRP (Lou et al., 2013). These TH⁺ neurons innervate hair follicles forming lanceolate endings around zigzag and awl/auchene hairs (Li et al., 2011). The Vglut3⁺/TH⁻ neurons form free-nerve endings in the epidermis of the skin. Selective removal of Vglut3⁺/TH⁺ neurons using Vglut3^{Cre}::Runx1^{f/f} showed no impairments in mechanical or thermal sensitivities of mice (Lou et al., 2013).

The second population of C-fibers express Mas related G protein coupled receptor B4 (MrgprB4). MrgprB4 is expressed in 2% of DRG neurons and are present as arborized free nerve endings in the epidermis of the skin along with circular endings around the hair follicles. These

arborizations are believed to resemble CT fibers in humans (Liu et al., 2007). GCaMP imaging using MrgprB4^{Cre} mice showed responses to brushing the skin using a paint-brush and pharmacological activation of MrgprB4⁺ afferents resulted in a positive reinforcement in a conditional place preference test (Vrontou et al., 2013). However electrophysiological proof of MrgprB4⁺ C-LTMR δ is still lacking.

As mentioned earlier, A δ -LTMR δ constitute one of the most sensitive mechanoreceptor subtypes. Although first recorded in cat hindpaw by Iggo and Brown in 1967, the identity of D-hair mechanoreceptors remained unknown until 15 years back (Brown and Iggo, 1967, Stucky et al., 1998). Studies on mice lacking Neurotrophin-4 (NT4^{-/-}) showed reduction in the number of innervated D-hairs upon histological analysis of the skin and a severe loss of A δ -fiber firing in skin-nerve electrophysiology experiments, while over-expression of NT4 lead to an increase in myelinated lanceolate endings (Stucky et al., 1998). Subsequent studies on gene expression in NT4^{-/-} mice led to the discovery of a T-type calcium channel (Ca_v3.2) to be specifically expressed in D-hairs which are also believed to account for the sensitivity of these receptors (Shin et al., 2003, Wang and Lewin, 2011). Similarly, studies on BDNF deficient mice showed reduced mechanical sensitivity of SA-mechanoreceptors (Carroll, 1998). Recently, David Ginty and colleagues studied the expression of TrkB in adult DRG neurons and found that in TrkB^{TauEGFP} knock-in mice; TrkB was expressed in 7% of adult thoracic DRG neurons. In skin-nerve electrophysiology, these medium sized neurons exhibited properties of A δ -LTMR like low mechanical threshold of activation (<0.07mN), Rapidly Adapting nature and medium conduction velocities of approximately 6m/s (Li et al., 2011). They further extrapolated this work to show that lanceolate endings of TrkB^{CreERT2} afferents on zigzag and awl/auchene hairs were concentrated on the caudal side of the hairs that are activated upon deflection of hair in the

Caudal-to-Rostral direction and that this direction selective innervation is driven by the expression of ligand BDNF on the caudal side of the hairs by epithelial cells during development (Rutlin et al., 2014). This suggests a potential role for TrkB⁺ neurons to detect gentle breeze or brushing in a direction specific manner in the hairy skin. Previously, studies using a TrkB^{-/-} mice showed a reduction of medium sized DRG neurons by 32% with a parallel reduction in the innervations of hair follicles, Meissner's corpuscles and Merkel cells suggesting TrkB expression in other end organs alongside D-hairs (Perez-Pinera et al., 2008). However, the exact function of these neurons in the behavior of adult mice remains unknown.

Finally, the least understood of all mechanosensory neuron subpopulation are the TrkC⁺ cells. Although mainly thought to be Proprioceptive neurons that detect spatial positioning and fine limb movement (Marmigere and Ernfors, 2007), a new study showed that TrkC⁺/Ret⁺ expressing neurons form circumferential endings on hair follicles and belong to a class of Field-receptors that detect stroking of a large area of skin but not hair deflection like the lanceolate endings (Bai et al., 2015).

Even though the function of each of these mechanosensory subtypes in the behavior of adult mice has not been directly studied, vast progress has been made in elucidating several ion channels expressed in cutaneous sensory neurons and their involvement in the mechano-transduction apparatus.

2.7 Mechano-transducing channels

2.7.1 Piezo2

Piezo proteins form a major group of mechanically activated transmembrane proteins as shown by in-vitro experiments using *Drosophila* and mammalian Piezo channels (Kim et al.,

2012). In-situ hybridization experiments on mouse DRG neurons showed Piezo2 expression in around 20% of all cells most of which were mechanosensory NF200⁺ with some nociceptors included and also in the periphery and some internal organs (Coste et al., 2010). Whole-cell patch clamp recordings confirmed the requirement of Piezo2 in gating RA mechanical currents. A trio of studies using Piezo2^{GFP} and keratinocyte specific Piezo2-cKO reported a reduction in the static firing of SA-LTMR α and in detection of gentle touch response in mice indicating a role of Piezo2 in Merkel-cell mechanotransduction (Coste et al., 2012, Woo et al., 2014, Maksimovic et al., 2014). Piezo2 has been established as the most prominent mechanotransductive channel in mice (Ranade et al., 2014). Moreover, mice with conditional knock-out of Piezo2 using pvalb^{Cre} and HoxB8^{Cre} show profound defects in proprioceptive behavior like limb position and fine movement (Woo et al., 2015).

2.7.2 Acid Sensing Ion Channels

The ASIC α s form a large family of proton-gated ion channels consisting of 7 isoforms most of which are expressed in mechanosensory and nociceptive neurons (Lingueglia, 2007, Moshourab et al., 2013). ASIC1, ASIC2 and ASIC3 are the best studied in mechanoreceptors (Page et al., 2005, Montano et al., 2009). Histological experiments have shown the expression of both ASIC2 and ASIC3 in lanceolate endings and nerves innervating Meissner α corpuscles and Merkel cells. Gene knockout experiments in rodents show defects in mechanical sensitivities and firing properties of RA-fibers in the skin while the behavioral effects have been very modest in knock-out mice (Price et al., 2001, Mogil et al., 2005), thereby questioning the direct effects of ASIC α s in mechanotransduction.

2.7.3 Transient Receptor Potential channels

The TRP superfamily makes up the most prevalent family of ion channels expressed in sensory neurons of mammals (Damann et al., 2008). Of the six sub-families only 3 (TRPA1, TRPV4 and TRPC1) have been associated with in mechanosensation. Defects in the expression of TRPV4 affect the detection of noxious mechanical stimuli and causes mechanical hypersensitivity to pain (Alessandri-Haber et al., 2004, Suzuki et al., 2003). Studies on TRPA1^{-/-} mice have yielded a mixed phenotype where the disrupted sensitivity to mechanical stimuli in naïve and pathological states has been in addition to defects in thermal and noxious pain sensation (Bautista et al., 2006). TRPC1 deficient mice show reduced action potential firing to low threshold mechanical stimuli in SA-A β and D-hair fibers. Also, TRPC1^{-/-} mice show reduced behavioral responses to brushing of the paw using a cotton-swab (Garrison et al., 2012). However, TRPC1 has also been found to be expressed in nociceptive neurons suggesting a more moderator role for TRP channels in mechanoreceptors rather than a direct gating channel (Christensen and Corey, 2007).

2.7.4 K⁺ channel family

Another family of ion-channels that joins the growing list of mechano-transductory channels is the K⁺ channel family (Medhurst et al., 2001). Behavior studies on KCNK2 and KCNK4 mutant mice exhibited increased mechanical sensitivity to innocuous stimuli while responses to noxious stimuli remained unaffected. KCNK4 has also been shown to be activated by membrane stretch. Furthermore, the two channels have been found to act together to set the threshold for activation and in regulating the excitability of neurons (Noel et al., 2009, Alloui et al., 2006, Bautista et al., 2008).

Another voltage-gated K^+ channel that is expressed in mechanoreceptors, especially $A\beta$ -fibers is KCNQ4. First found in cochlear hair cells and connected to hearing loss, KCNQ4 has been found to be expressed in Meissner's corpuscles and in some lanceolate endings on hair follicles. Using *Kcnq4*^{-/-} mice, Heidenreich et al showed that a loss of KCNQ4 leads to better detection of low frequency vibration acting on the skin similar to people carrying *KCNQ4* mutation whose vibration detection thresholds were lower than healthy siblings, thereby suggesting a role for KCNQ4 in tuning mechanoreceptors to detect different stimuli (Heidenreich et al., 2011).

2.7.5 Stomatin

Stomatin-like protein (SLP3), a mammalian homologue of the *C. elegans MEC2* gene has been shown to be crucial for touch sensation in mice (Huang et al., 1995). SLP3 mRNA is expressed in all DRG neurons and SLP3^{-/-} showed loss of mechanosensitivity in 40% of all myelinated mechanoreceptors in addition to a loss in mechanical currents in these neurons. SLP3 mutant mice also displayed reduced tactile acuity to a two-place texture discrimination test making SLP3 an important unit of myelinated mechanoreceptors (Martinez-Salgado et al., 2007, Wetzel et al., 2007, Lapatsina et al., 2012).

2.7.6 α TAT1

Apart from transmembrane proteins and ion-channels, cytoskeletal proteins have also been implicated in mechanosensation. Initially found in a screen of mutant *C.elegans* insensitive to touch, Mec-17, a α -tubulin acetyltransferase has been shown to be important in touch sensation. More recent studies on the mammalian orthologue of Mec-17, α TAT1, have demonstrated its necessity in transducing mechanical touch and pain (Kalebic et al., 2013).

2.8 Neuropathic pain

To protect the body from tissue damage, it is extremely crucial to detect painful stimuli like extreme heat, harmful chemicals, a sharp object or even fractured bones. An inability to detect and respond to painful stimuli leads to self-destruction and in some cases can also be fatal. This awareness of acute pain is conferred to the body by the action of nociceptors (Woolf and Ma, 2007). However disorders of this system can lead to pain being persistent and chronic. The cause for such malfunction of the somatosensory system can range from a trauma to the nerve or limb, inflammation, spinal cord injury to cancer, diabetes and multiple sclerosis. Neuropathic has been redefined as *pain that arises as a consequence of a lesion or a disease affecting the somatosensory system* (Treede et al., 2008). This persistent pain has no protective features and could manifest as enhanced responses to a normally noxious stimulus (hyperalgesia) or pain perception to an innocuous stimuli (allodynia). Clinically, neuropathic pain has become bothersome with nearly a fifth of the population suffering from different forms of chronic pain (Treede et al., 1992).

Hyperalgesia can be defined as a lowered threshold for pain, an increased sensitivity to pain in response to supra-threshold stimuli and can also occur spontaneously (in the absence of any pain evoking stimuli)(Treede et al., 1992). Hyperalgesia can be classified as primary (occurring at the site of injury) or secondary (occurring in the areas surrounding the injury) (Treede and Magerl, 1995). After nearly 30 years of research it is now generally agreed that primary hyperalgesia occurs as a result of sensitization of nociceptive afferents (Campbell et al., 1988) while secondary hyperalgesia, especially mechanical allodynia is largely associated with central changes in the processing of mechanoreceptor input into the spinal cord (Torebjork et al., 1992).

2.8.1 Primary hyperalgesia

Primary hyperalgesia develops as a result of peripheral sensitization of nociceptive afferents and is generally associated with several inflammatory agents that are released at the site of an inflammation. The compounds that contribute to what is called an "inflammatory soup" can be neurotransmitters, peptides (like CGRP or substance P), neurotrophins, cytokines, chemokines etc. These inflammatory agents are believed to act on the receptors on the nerve terminals of A δ and/or C-fiber nociceptors altering their thermal and mechanical thresholds and activation properties (Basbaum, 1999, Woolf and Ma, 2007, Basbaum et al., 2009). The most extensively studied sensitization of nociceptors in hyperalgesia is to thermal stimuli. In-vivo and in-vitro studies on mice lacking the TRPV1 receptor show absence of heat hyperalgesia after carrageenan induced inflammation models (Davis et al., 2000, Caterina et al., 2000) and that activity of TRPV1 can be modulated by several inflammatory agents (Tominaga et al., 1998). Similarly, TRPA1-deficient mice show deficits in bradykinin or mustard oil- evoked hypersensitivity (Bautista et al., 2006). Though primarily a cold sensor, TRPA1-deficient mice do not show cold hypersensitivity. However, genetic ablation of Nav1.8⁺ cells using a diphtheria toxin receptor results in a loss of cold and mechanical hyperalgesia after inflammation (Abrahamsen et al., 2008). Even though drastic sensitization to mechanical stimuli was not observed in earlier studies, Knockout experiments on Nav1.7, Nav1.8 or double KO mice provide evidence for the requirement of these channels in mechanical and thermal primary hyperalgesia but not in injury driven neuropathic pain or in allodynia (Nassar et al., 2005, Abrahamsen et al., 2008).

2.8.2 Secondary hyperalgesia and mechanical allodynia

Secondary hyperalgesia refers to the hypersensitivity that develops in the areas surrounding an injury. This increased sensitivity occurs upon application of a static punctate or

dynamic mechanical stimulus in a condition termed allodynia but not to heat stimulus (Treede and Magerl, 1995). Mechanical allodynia can be defined as *“pain due to a stimulus that normally does not cause pain”* (Treede et al., 2008). Over the past years, understanding the mechanisms behind light touch feeling painful has progressed through the discovery of the role of myelinated low-threshold mechanoreceptors in allodynia to change in plasticity of pain transmitting neurons within the spinal cord. This evolution has involved elegant intra-neural stimulation studies on human subjects with nerve-injury or using capsaicin patches to mimic hyperalgesia to show that selective blocking of A-fiber nerve conduction eliminated brush evoked allodynia while blocking A δ and C fiber nociceptors did not hyperalgesia (Kilo et al., 1994, LaMotte et al., 1992, Campbell et al., 1988, Torebjork et al., 1992). The short latency for pain and the lack of nociceptor sensitization to mechanical stimuli (LaMotte et al., 1992) confirmed the role of myelinated A-fiber mechanoreceptors in mediating allodynia. This subsequently led to the hypothesis that allodynia is caused as a result of central sensitization. Alongside, various possible mechanisms have been proposed for the development and maintenance of allodynia including ectopic transmission between injured and un-injured afferents in its vicinity, alteration in gene expression patterns, sprouting of myelinated fibers from lamina III/IV of the spinal cord to Lamina I and a disinhibition of inhibitory interneurons in the dorsal horn (Woolf et al., 1992, Lolognier et al., 2015, Bridges et al., 2001).

One of the major challenges in the field has been to identify the neuronal subpopulation that engages in allodynia. With developments in genetic labelling techniques, few possible candidates have been suggested. Delta opioid receptors (DOR) have been found to be co-expressed with TrkA, TrkC and Ret in sensory neurons and DOR-null mice exhibit mechanical allodynia after injury (Scherrer et al., 2009) and agonist of DOR display anti-allodynic properties

in animal models of neuropathic pain (Ossipov et al., 2004). Similarly Mu-opioid receptors (MOR) have also been shown in subpopulations of myelinated sensory neurons (Bardoni et al., 2014). However, both DOR and MOR expression has been found in nociceptors making them heterogeneous thereby limiting the ability to study their role in mechanical allodynia. TLR5, an immune system receptor was newly identified as a marker of A β -LTMR ϕ . Co-application of flagellin (a ligand for TLR5) and QX-314 (a sodium channel blocker) resulted in blockade of sodium currents and evoked action potentials specifically in A β -fibers but not A δ or C-LTMR ϕ in dissociated DRG neurons and also alleviated mechanical allodynia, albeit only for a few hours (Xu et al., 2015). Although this represents an interesting target for treatment of neuropathic pain, better understanding of the cellular mechanisms of allodynia would help develop long lasting recovery.

In parallel, several mechano-transduction channels, like Piezo2, SLP3 etc. have also been associated with mediating allodynia (Wetzel et al., 2007, Ranade et al., 2014, Cox et al., 2006). As stated in earlier sections, cutaneous mechanoreceptors can be myelinated A β , A δ or unmyelinated C-fibers. Despite evidences implicating myelinated A-fibers in allodynia, several studies have focused on testing the role of C-fiber mechanoreceptors in mediating neuropathic pain (Seal et al., 2009, Delfini et al., 2013). This stems from reports suggesting a role for C-fibers LTMR ϕ in gentle touch sensation. Knockout of VGLUT3 significantly reduced mechanical hypersensitivity that accompanies nerve injury (Seal et al., 2009). However, this phenotype was not evident after genetic ablation of Runx1 in VGLUT3 positive neurons, thereby affecting their development (Lou et al., 2013). Instead it was proved that transient expression of VGLUT3 in A fibres during development and/or expression in the spinal cord is required for pain hypersensitivity. Alternatively it has also been shown that genetic ablation of TAF4, a

chemokine like protein that is present in all VGLUT3⁺ C-fibers led to mechanical and chemical hypersensitivity which was reversed upon application of exogenous TFAFA4. This study concluded that TFAFA4 played an inhibitory effect on mechanical nociception that was lost upon its ablation (Delfini et al., 2013).

2.8.3 Central mechanisms of mechanical allodynia

The difficulty in identifying the neurons mediating allodynia has not affected the advancements have been made in understanding the central mechanisms of allodynia. The dorsal horn of the spinal cord processes sensory stimuli arising from the periphery using several inhibitory and excitatory interneurons that subsequently contact the projection neurons for relay into different regions of the brain (Todd, 2010, Prescott et al., 2014). LTMR α detecting innocuous mechanical stimuli terminate onto GABAergic or glycinergic inhibitory interneurons within lamina II_i-III while pain sensing neurons synapse onto excitatory PKC γ or somatostatin interneurons in lamina I-II_o (Braz et al., 2014, Lu et al., 2013, Zeilhofer et al., 2012). A feed forward inhibitory control of A-fiber mechanosensitive neurons comprises a crucial component of the Gate Control Theory (Melzack and Wall, 1965). Several ground-breaking studies on the spinal cord have provided experimental evidence that an injury causes a disinhibition, giving mechanosensitive neurons access to Lamina I pain projecting interneurons through a polysynaptic circuit composed of SOM⁺ and SOM⁺/PKC γ ⁺ excitatory interneurons as a consequence of which, touch feels painful (Duan et al., 2014). The nature of this disinhibition also remains uncertain as of yet with some reports suggesting a demise of GABAergic interneurons (Braz et al., 2012) while others report a diminished inhibition (Foster et al., 2015). Recently, a population of excitatory interneurons expressing Vglut3 was identified in lamina II/III to receive innocuous touch inputs and whose activation leads to persistent mechanical

allodynia while its ablation reduced allodynia suggesting the presence of micro-circuits in the dorsal horn (Peirs et al., 2015). In addition to interneurons, microglia also plays a crucial intermediate role mechanical allodynia. ATP released after nerve injury triggers the activation of microglia through the upregulation of P2X4 receptors and the synthesis of BDNF, which then acts on its native receptor TrkB in the dorsal horn and reduces GABAergic inhibition via a downregulation potassium-chloride exporter (KCC2) (Coull et al., 2003, Coull et al., 2005). This recruitment and proliferation of microglia are mediated by the over-expression of macrophage colony stimulating factor (CSF1) by injured sensory neurons (Guan et al., 2016). The classical scavenger function of microglia also regulates neuropathic pain states. Indeed impairment of microglial phagocytosis in the dorsal horn using TMEM16F cKO mice results in mice not developing allodynia after injury (Batti et al., 2016), suggesting a more complex role for microglia in neuropathic pain states.

2.9 Treatment of Neuropathic pain

Hyperalgesia and allodynia can develop as a consequence of diverse pathological conditions. This variation, along with different levels of pain among individuals has made assessment and diagnosis of pain difficult (Dworkin et al., 2010, Attal and Bouhassira, 2015). A number of improved guidelines for the pharmacological treatment of neuropathic pain are being proposed with time (Finnerup et al., 2015). Currently according to the IASP, there are three lines of medication; the first line of treatment suggests the use of tricyclic antidepressants (TCA), serotonin nor-epinephrine reuptake inhibitors (eg. Duloxetine and venlafaxine) and inhibitors of voltage gated calcium channels (like Gabapentin, Pregabalin etc.) (Dworkin et al., 2007, Li et al., 2006). The second line of treatment recommends opioid analgesics like morphine and oxycodone or mild cannabinoids (Raja et al., 2002). The third line prescribes stronger drugs and is restricted

to patients who are non-responsive to first and second line drugs (Dworkin et al., 2010). However, each of above medications comes with adverse side effects which are worrisome on its own. Studies in rodents and humans have showed elevated levels of NGF upon inflammation and in conditions of arthritis, headaches etc. (Rittner et al., 2008). In parallel, local or systemic application of NGF has been implicated in elevated pain states suggesting a critical role for NGF under inflammatory states (Hefti et al., 2006). This led to the development of therapeutic targets to reduce or block the activation of NGF, the most common of which is Tanezumab (Pfizer), a monoclonal antibody against NGF. The use of anti-NGF in pain pharmacotherapy has proven to be reasonably efficient in many clinical trials (Schnitzer et al., 2015, Chang et al., 2016). Alongside topical application of 5% lidocaine (Wasner et al., 2005) or high-concentration capsaicin patches are currently being tested in Randomized Clinical trials (RCT) (Nolano et al., 1999). The involvement of Nav1.7 and Nav1.8 in enhanced pain states are currently being the basis for the development of antagonists of these voltage-gated sodium channels (Minett et al., 2014, Nassar et al., 2004). Despite the progress, development of better drug targets will be facilitated with a better knowledge on the neurons mediating allodynia.

2.10 Mouse models of neuropathic pain

Taking into consideration different pathological conditions that can lead up to neuropathic pain, different mouse models have been developed to serve as mechanism-based experimental tools. Many of the current models make use of an alteration to the sciatic nerve thereby affecting the hind-paw. Below mentioned are few of the common models of neuropathic pain in mice.

2.10.1 Sciatic nerve transection

This is the oldest model used in the study of neuropathic pain and requires the complete transection of the sciatic nerve near the thigh followed by ligation of the nerves above the area of

transection (Wall et al., 1979). Because of the spontaneous pain that develops upon injury and the frequent self-mutilation observed in many cases, this model is less frequently used.

2.10.2 Partial nerve ligation (PNL)

The PNL model is performed by a tight ligation around 35-50% of the exposed sciatic nerve leaving the rest of the nerve uninjured. This causes spontaneous-pain, hyperalgesia and mechanical allodynia 1 week after the ligation. This model has also been shown to affect a large mixture of L4-L5 DRG neurons (Seltzer et al., 1990).

2.10.3 Chronic constriction injury (CCI)

The CCI model also involves loose ligation of the sciatic nerve at the mid-thigh leading to hyperalgesia to thermal stimuli and allodynia to mechanical stimuli. This model is commonly used for its easy reproducibility and has also been performed on the trigeminal ganglia to produce trigeminal neuralgia. It mainly affects myelinated fibers corresponding to 30% of all DRG neurons. This model however involves an inflammatory component to it (Bennett and Xie, 1988).

2.10.4 Spared nerve injury (SNI)

In the SNI model of neuropathic pain, two (tibial and common peroneal) of the three branches of the sciatic nerve is ligated and axotomized, leaving the third branch (Sural) intact (Decosterd and Woolf, 2000). This results in a hypersensitivity of the sural nerve innervating area of the hind paw. Thermal and mechanical hyperalgesia and allodynia develops three days following the injury and is long lasting. This model is independent to inflammatory pain and is described to be the closest representation of clinically tested neuropathic pain (Pertin et al., 2012).

2.10.5 Spinal nerve ligation

In addition to peripheral nerve ligation, intentional manipulations of the spinal nerves have also been tested. In this model, L5 and L6 spinal nerves are identified and ligated to the distal part of the DRG. This produces allodynia and hyperalgesia that lasts for 10 weeks post injury (Kim and Chung, 1992).

2.10.6 Inflammatory pain

A majority of neuropathic pain is caused by an inflammation to the tissue. Several models of inflammatory pain have thus been developed. This comprises injection of pro-inflammatory agents locally into the paw to facilitate behavioral testing. Such agents can be zymosan, Complete Freund's Agent (CFA), carrageenan, formalin etc (Eliav et al., 1999).

2.10.7 Diabetic neuropathy

Diabetic peripheral neuropathy is one of the many complications of diabetes that is characterized by progressive degeneration of nerves leading to loss of tactile sensation. Even though the mechanism behind diabetic neuropathy remains unclear, mice models to study this condition have been developed. The most common of which is ablation of pancreatic β -cells by injection of streptozotocin (STZ). Administration of a single high dose (SHD) or multiple low doses (MLD) of STZ leads to development of type 1 diabetes and subsequent peripheral neuropathy that manifests as bilateral thermal hyperalgesia and mechanical allodynia (O'Brien et al., 2014, Murakami et al., 2013).

2.10.8 Drug-induced neuropathy

Peripheral neuropathy is also a common side-effect of medication which begins a few weeks after initiation of medication and can last for weeks after thereafter. One such medication

induced neuropathic pain is seen after chemotherapy. Some of the chemotherapeutic agents that can cause dose-dependent neuropathy (as also seen in animal models) are vincristine, paclitaxel and cisplatin (Quasthoff and Hartung, 2002).

These models of neuropathic pain cause diverse types of primary and secondary hyperalgesia and therefore require different types of behavioral test to assay pain. For example the most commonly used method to test punctate primary hyperalgesia and allodynia is using von-Frey filaments (Chaplan et al., 1994). These are fibers of different diameters that can apply a particular force to the skin. Dynamic allodynia are generally tested using paint-brush or cotton swab (Garrison et al., 2012) while thermal hyperalgesia are assayed using a hot/cold plate test, radiant heat test, Randall-Selitto or an acetone drop test (Brenner et al., 2012). Most of these tests will be described in detail in the Methods section.

2.11 TrkB and BDNF: involvement in neuropathic pain

Neurotrophins and their related receptor tyrosine kinases (Trks) are well characterized in the development, diversification and survival of DRG neurons. Most of the neurotrophins and their receptors also play important roles in pain transmission. In the case of BDNF and its cognate receptor TrkB, much of the focus has been confined to the spinal cord and supra-spinal regions. Going in line with evidences of exogenous NGF causing thermal and mechanical hyperalgesia in rats after inflammation or nerve injury (Woolf et al., 1994, Woolf, 1996), intraplantar injections of a high dose of BDNF only produced a marginal thermal hyperalgesia which was short-lived compared to NGF or NT-4 under naïve conditions (Shu et al., 1999). However, repeated injections of BDNF into the DRG caused after injury increased allodynia which was re-attenuated upon injection of anti-BDNF antibodies (Zhou et al., 2000). Interestingly, levels TrkB mRNA is also upregulated following peripheral nerve injury (Ernfors

et al., 1993). Furthermore, TrkB-BDNF signaling within the spinal cord dorsal horn has been implicated in the induction and maintenance of neuropathic pain states (Wang et al., 2009). Whether the pre-synaptic TrkB positive afferents also contribute to this state is yet to be determined.

2.12 General aims

In this study we plan,

1. To elucidate the role of TrkB⁺ neurons in the behavior of mice
2. To test the contribution of TrkB⁺ neurons to mechanical allodynia
3. To develop potential therapeutic strategies to target TrkB afferents in the skin

3 Materials and methods

3.1 Generation of $\text{TrkB}^{\text{CreERT2}}$ mice

A bacterial artificial chromosome (BAC) containing the TrkB mouse locus was obtained from SourceBioscience (RP23-391J8). Individual BAC clones were then screened and electroporated with a plasmid conferring competence for lambda RedET mediated recombineering. A modified $\text{CreERT2-pA-Frt-Ampicillin-Frt}$ cassette was inserted into the ATG of trkB , deleting the entire coding region of exon 2 by homologous recombination using the following primers: homology to CreERT2 : `gacgcctggctcagcgtaggacacgca`
`ctccgactgactggcactggcagctcgggatgtccaatttactga` and homology to FAF: `cccaaacatac`
`acctgcctgattcctgaggtggggacaggagaaaaagtaaaaggaactcacgcctgatagacggttttcgcctttgacgttg`. The identity of the clones were confirmed by PCR and full length sequencing of the inserted cassette, and the ampicillin cassette was removed using bacterial Flp. Purified BAC DNA was then dissolved into Endotoxin-free TE and injected into pronuclei derived from the hybrid B6D2F1/N strain (Charles River Laboratories) or prepared for intracytoplasmic sperm injection (ICSI) as previously described. Both methods were successful and produced offspring. The genotype of mice was determined by performing PCR using the following primers: `gcactgattcgcaccagtt` (fwd) and `gagtcattcttagcgccgta` (rev), yielding products of 408bp.

3.2 Generation of $\text{Avil}^{\text{mCherry}}$ mice

The $\text{Avil}^{\text{hM3Dq-mCherry}}$ line was obtained by a knock-in of a $\text{Lox-STOP-Lox-hM3Dq-mCherry}$ cassette into the Avilin locus, to replace exon 2 and 66bp upstream. The targeting construct was transfected into A9 ESCs. Individual ESC clones were screened to identify homologous recombination. Southern blots were performed as described previously (Stantcheva et al., 2016). DNA was digested with PstI and HindIII and hybridized with 5 ϕ or 3 ϕ probe,

respectively. We obtained 9600bp (wild-type)- and 6300bp (targeted) DNA fragments by using the 5 ϕ probe and 7100bp (wild-type)- and 6100bp (targeted) DNA fragments by using the 3 ϕ probe. Positive clones were injected into 8-cell stage embryos to generate heterozygous mice for the targeted allele. To determine the genotype, PCR were performed using the following primer pairs: gccccgtaatgcagaagaag (fwd), gtgtagtcctcgttgggga (rev).

3.3 Avil^{iDTR} mice

For diphtheria toxin mediated ablation, Avil^{iDTR} mice as described previously (Stantcheva et al., 2016) were crossed to TrkB^{CreERT2} to generate TrkB^{CreERT2}::Avil^{iDTR} heterozygous mice. Littermates lacking the Cre (referred to as Avil^{iDTR}) were used as controls. For optogenetic activation using channelrhodopsin, TrkB^{CreERT2} were crossed to Rosa26^{ChR2-YFP} mice to generate TrkB^{CreERT2}::Rosa26^{ChR2-YFP} mice.

All mice were housed in the EMBL, Mouse Biology Unit, Monterotondo according to the Italian legislation (Art. 9, 27. Jan 1992, no 116) under license from the Italian Ministry of Health, and in compliance with the ARRIVE guidelines. (*Note: the above mentioned mouse lines were generated by the Heppenstall lab before my arrival at EMBL, Monterotondo*).

3.4 Tamoxifen treatment

To induce efficient Cre recombination, adult TrkB^{CreERT2} mice (6-8 weeks of age) were injected intraperitoneally with 75mg/kg of body weight of Tamoxifen (Sigma Aldrich, T5648) in sunflower seed oil (Sigma Aldrich, S5007) for 5 consecutive days. Mice were then used for experiments 5 days after the final injection.

3.5 Immunofluorescence

DRG were extracted from adult mice and fixed with 4% PFA for 2 hours or overnight at 4°C. Tissues were embedded in 12% bovine gelatin (Sigma Aldrich, G9391) and sectioned at 50µm. Sections were then treated with cold 50% ethanol for 30 minutes and incubated with blocking solution containing 5% Serum (goat or donkey) and 0.01% Tween-20 in PBS for 30 minutes and subsequently with one or more primary antibodies in blocking solution overnight at 4°C. Secondary antibodies were added in blocking solution for 1-2 hours and the slides were mounted with prolong gold (Invitrogen, P36930).

To determine the central projections of TrkB⁺ neurons, lumbar spinal cord was dissected from mice and fixed with 4% PFA for 2 hours or overnight at 4°C. Small pieces of the spinal cord were then cryopreserved in 30% sucrose (in PBS) overnight and embedded in Tissue-Tek O.C.T compound. 40µm cross sections of the tissue were cut using a cryostat (Leica, CM3050S) and stained as described above. In certain cases, an extra signal enhancement step was used by incubating sections with a biotinylated anti-rabbit or anti-goat antibody overnight at 4°C followed by incubation with streptavidin-conjugated secondary antibody for 1 hour at 4°C.

For SNAP-tag labeling of the peripheral afferents, the back skin and the paw of TrkB^{CreERT2}::Rosa26^{SnapCaaX} mice were injected intradermally with 10µM of Snap Cell TMR-Star (New England Biolabs, S9105S) (Yang et al., 2015). The skin was dissected after 6 hours and fixed with 4% PFA overnight. The tissues were then cryoprotected in 30% sucrose overnight at 4°C and embedded in Tissue-Tek O.C.T compound. 40µm thick sections of the hairy skin and 20µm sections of the glabrous skin were cut using a cryostat (Leica, CM3050S) and stained with one or more antibodies as described above.

For human DRG/skin staining, frozen DRG δ s were obtained from the National Disease Research Interchange (NDRI, USA). Tissue was sectioned at 20 μ m using a cryostat. Sections were then dried, post-fixed with 4% PFA and immunostained as mentioned above. Primary and secondary antibodies were incubated in a solution containing 2% BSA (wt/vol) and 0.01% Tween-20 in PBS. Fresh skin from the palm was SNAP frozen in Tissue Tek O.C.T compound, sectioned at 20 μ m. Sections were then dried and post-fixed. Protocols similar to DRG were used for Meissner δ corpuscles staining.

The following primary antibodies were used:

Table 1: List of antibodies used

Antibody	Concentration	Supplier/catalog.
Rabbit anti-RFP	1:200	Rockland, 600-401-379
Mouse anti-NF200	1:500	Sigma Aldrich, N0142
Mouse anti-CGRP	1:500	Rockland, 200-301-D15
Isolectin GS-B4-biotin XX- conjugate	1:100	Invitrogen I21414
Rabbit anti-TH	1:1000	Millipore, AB152
Rabbit anti-PGP9.5	1:200	Dako, Z5116
Rabbit anti-S100	1:200	Dako, Z0311
Goat anti-Human HB-EGF	1:50	R&D systems, AF-259-NA
Rabbit anti-cFos	1:1000	Santa Cruz, Sc-52
Rabbit anti-TrkB	1:200	ThermoFisher PA5-34026
Rabbit anti-Ret	1:100	Abcam ab134100
Mouse anti-TrkA	1:100	ThermoFisher MA5-15509

All Alexa conjugated secondary antibodies were used at 1:1000 concentration and streptavidin conjugated antibodies were used at 1:600 concentration. All images were taken with a Leica SP5 Confocal microscope and analyzed in ImageJ.

3.6 In-situ Hybridization

DRG were dissected from $\text{TrkB}^{\text{CreERT2}}$ mice and postfixed overnight in 4% PFA at 4°C and cryoprotected in 30% sucrose solution overnight at 4°C. Tissues were then embedded in tissue Tek O.C.T compound and 10µm sections were cut using a cryostat. *In-situ* hybridization was performed as previously described (Mirabeau et al., 2007) using a riboprobe generated from a cDNA template (Klein et al., 1989). Briefly, sections were digested for 6 minutes with proteinase K, acetylated, and hybridized with the either sense or antisense probes in a solution containing 50% formamide, 5X SSC, 5x Denhardt's solution, 500 µg/ml salmon sperm DNA and 250 µg/ml tRNA overnight at 56°C. Tissues were then washed post-hybridization with 50% formamide, 2X SSC, then with 0.5X SSC at 56°C and finally with 2X SSC at ambient temperature. Sections were blocked and incubated overnight with anti-digoxigenin-AP (Roche; at 1:1000). Signal detection was done using NBT/BCIP substrate.

3.7 Ex-vivo skin nerve preparation

The skin-nerve electrophysiology was performed in collaboration with Francisco Taberner at the University of Heidelberg using a preparation previously described (Zimmermann et al., 2009). In brief 8-16 weeks old mice were euthanatized with CO₂. The skin of the hind limb was dissected and placed corium side up in a bath chamber filled with 32°C-warm synthetic interstitial fluid (108 mM NaCl, 3.5 mM KCl, 0.7mM MgSO₄, 26mM NaHCO₃, 1.7mM NaH₂PO₄, 1.5mM CaCl₂, 9.5mM sodium gluconate, 5.5mM glucose and 7.5mM sucrose at a pH of 7.4). The nerves were teased into thin bundles and laid on the recording electrode connected to

a Neurolog extracellular recording amplifier (Digitimer, modules NL104, NL125/NL126). Different regions of the skin were stimulated mechanically using a glass rod to locate single fiber units. A Powerlab 2 4SP system and Labchart 7.1 software (AD Instruments) was used to analyse the data and the units were classified according to their conduction velocity, von Frey hair thresholds and adaptation properties to suprathreshold stimuli. Further characterization with ramp-and-hold mechanical stimulation was achieved with a computer-controlled nanomotor® (Kleindieck) which allowed for simultaneous recording of electrophysiological and stimulation data. For light stimulation of ChR2 expressing nerve fibers, blue-light pulses from a laser (at 470nm) were focused on discrete spots by coupling the light guide (FG910UEC, Thorlabs) to a 20x microscope objective using a custom-made adapter. The different light-pulse durations and frequencies were generated by the built-in stimulator function of LabChart 7.1 and simultaneously recorded. The light intensities were assessed with a powermeter (PM100D, Thorlabs).

3.8 Diphtheria toxin injection

$\text{TrkB}^{\text{CreERT2}}::\text{Avil}^{\text{idTR}}$ mice were injected intraperitoneally with 40µg/kg of diphtheria toxin (Sigma, D0564) twice separated by a gap of 72 hours between the two injections. Behavioral tests were performed 7 days after the final DTX injection. All mice received diphtheria toxin injections. The weight and the condition of mice were monitored during the injection period.

3.9 Behavioral testing

All behavior experiments were performed on adult male mice (>6 weeks of age). For controls, littermates without the Cre were used. The experimenter was always blind to the genotype of the mice.

3.9.1 Acetone drop test

The acetone drop test was used for testing the effect of evaporative cooling on the glabrous skin. Mice were habituated for 30 minutes on an elevated platform with mesh flooring. A single drop of cold acetone was sprayed onto to the plantar side of the hindpaw of mice using a blunt syringe without touching the paw of the mice (Choi et al., 1994). The behavioral responses were scored according to the following scheme: 0=no response, 1=paw withdrawal or a single flick, 2=repeated flicking of the paw and 3=licking of the paw. The test was repeated 5 times by alternating the paw and mice between trials.

3.9.2 Hot plate test

To measure responses to noxious heat, a hot plate (Ugo Basile, 35150) was preset to 52°C. Mice were placed on top of the plate individually and the latency to response as observed by flicking or licking of the hindpaw was noted. A cutoff of 30 seconds was set in order to avoid injury to the mice. All experiments were video recorded.

3.9.3 Grip strength test

The grip strength test was performed to test the ability of mice to grip a metal grid (Bioseb; BIO-GS3). Mice were placed on a metal grid with all 4 paws touching the grid. The tail of the mice was gently pulled and the force at which the mice first let go of the grid was measured. The test was repeated 5 times with a 30 second interval between trials.

3.9.4 Pin-prick test

The plantar side of the hindpaw was gently poked using an insect pin glued onto a 1g von-Frey filament without penetrating the skin. The responses, as observed by either an immediate flicking or licking of the paw were noted for 10 trials with an interval of 1 minute between the trials.

3.9.5 Tape-test

Mice were habituated to a plexiglass chamber for 15 minutes. A 3cm by 1cm piece of adhesive tape (Identi tape) was applied along the back of the mice. Responses were quantified as an attempt to remove the tape by shaking, scratching or biting of the tape over a 5 minute period (Woo et al., 2014).

3.9.6 Cotton swab test

Mice were placed on an elevated platform with a mesh floor and habituated for 30 minutes. A cotton bud was puffed-out to about 3 times its original size. The hindpaw of mice were then brushed using this cotton swab in the heel-to-toe direction and the frequency of responses were noted (Garrison et al., 2012). The trials were repeated 10 times alternating between paws with an interval of 1 minute between trials.

3.9.7 Von Frey test

For the von Frey test, mice were habituated on an elevated platform with a mesh floor for 30 minutes. The plantar side of the hindpaw was stimulated with calibrated von-Frey filaments (North coast medical, NC12775-99). The 50% paw withdrawal thresholds were calculated using the Up-Down method (Chaplan et al., 1994). In this method, the paw of mice was stimulated by

a particular filament. A positive response to the filament lead to testing using a lower filament while a negative response to a filament lead to using a higher filament.

Post SNI, von Frey testing was confined to the sural nerve innervating region of the paw.

3.9.8 Dynamic brush test

To measure dynamic allodynia, the plantar hindpaw was stimulated by stroking using a paintbrush in the heel-to-toe direction. The responses were scored as described by Duan *et.,al* (Duan et al., 2014). For each test under baseline conditions, 0= no response, 1= paw withdrawal, 2= flicking of the paw and 3 =licking of the paw. After injury responses were quantified: 0=brief withdrawal, 1=prolonged paw withdrawal toward the body, 2=repeated flicking or flinching of the affected leg, 3= licking of the paw.

3.10 Models of neuropathic pain

3.10.1 Spared nerve injury model

The spared nerve injury (SNI) was performed as described by *Pertin et al* (Pertin et al., 2012). Adult mice were anesthetized using 2.5% isoflurane. The sciatic nerve near the thigh region was exposed; the common peroneal and tibial nerves were ligated using a suture thread and cut, leaving the sural nerve intact leading to hypersensitivity of the sural nerve innervating region of the paw. Behavioral testing was performed starting from 3 days after injury.

3.10.2 CFA model

For the inflammatory model of neuropathic pain, the hindpaw of mice was injected with 20ul of CFA (Sigma Aldrich, F5881). Behavioral tests were performed 24 hours and 48 hours after inflammation.

3.10.3 Chemotherapy induced neuropathic pain

To mimic chemotherapy induced neuropathic pain, wildtype C57BL6 mice were injected with 1mg/kg of Paclitaxel (Sigma Aldrich, T7191) intraperitoneally for 4 alternate days. Mice develop bilateral mechanical allodynia 1 week after the final injection.

3.10.4 Diabetes induced peripheral neuropathy

To induce diabetic neuropathy, wildtype C57BL6 mice were injected systemically with 180mg/kg of Streptozotocin (STZ, Sigma Aldrich S0130) in 0.05M citrate buffer (pH 4.5). This single high dose of STZ leads to the development of Type 1 diabetes mellitus within 3 days of administration. Mice with blood-glucose levels greater than 350mg/dL were considered diabetic. The health of the mice especially the blood-glucose levels were monitored regularly using the ACCU-CHEK glucose sticks (Aviva) and maintained between 350-400mg/dL by administration of insulin (Caninsulin 40U/ml MSD animal health) as per Table 2. 4 weeks after the onset of diabetes, mice develop mechanical hypersensitivity. Behavior experiments to test allodynia were carried out as mentioned earlier.

Table 2: Insulin dosage to maintain blood-glucose levels

Blood-glucose levels (mg/dL)	Insulin dosage (Units)
375-425	2U
425-500	3U
500-600	4U
>600	5U

3.11 Light activation using channelrhodopsin

Optogenetic stimulation of the paw was performed using 470nm Blue DPSS laser (SLOC CO., Ltd; BL473T8) coupled to a powerlab source (Powerlab 4SP) to generate light pulses. A fiber optic cable (0.93NA, SLOC CO., Ltd; FC-200-10-PC) was used to deliver 5-10ms pulses of blue light (15Hz) onto the plantar hindpaw of mice. Paw withdrawal to light application was considered as a positive response. In all experiments, ipsilateral and contralateral paws of $\text{TrkB}^{\text{CreERT2}}::\text{Rosa26}^{\text{ChR2-YFP}}$ were tested along with littermate controls (referred to as $\text{Rosa26}^{\text{ChR2-YFP}}$).

3.12 C-fos labelling of the spinal cord

For c-Fos labelling of the spinal cord, $\text{TrkB}^{\text{CreERT2}}::\text{Rosa26}^{\text{ChR2}}$ mice were exposed to optogenetic stimulation of the injured (ipsilateral) and contralateral paw with a 15Hz blue laser light (473nm) for 1 minute. Mice were sacrificed and the lumbar spinal cord was removed and fixed with 4% PFA overnight at 4°C. Tissues were then cryoprotected in 30% sucrose and embedded in Tissue-Tek O.C.T compound. 40µm sections of the spinal cord were cut using a cryostat. The sections were then treated with cold 50% EtOH for 30 minutes followed by blocking in a solution containing 10% normal goat serum in PBS with 0.01% Tween20 for 30 minutes. Sections were then incubated with primary antibodies in blocking solution overnight at 4°C followed by incubation with secondary antibody for 1 hour in the blocking solution.

All sections were imaged using Leica SP5 Confocal microscope. The numbers of C-fos positive cells in each lamina of the ipsilateral and contralateral sides of the dorsal horn were counted using imaris software.

3.13 Production of recombinant BDNF^{SNAP}

cDNAs encoding for the murine BDNF and SNAP proteins including a C-terminal poly-Histidine Tag (His₆) inserted for purification purposes were cloned into the pMP-PB vector as a fusion protein (Matasci et al., 2011). Protein expression was carried out using Chinese hamster ovary (CHO) cells as described by Balasubramanian *et al.*, (Balasubramanian et al., 2015). Secreted BDNF^{SNAP} was purified from cell medium using a Ni-NTA resin (Qiagen, #30210) and eluted with an excess of imidazole. Eluted fractions were then pooled, concentrated and stored for further analysis. (*Produced by David Hacker, Laurance Durrer and Soraya Quinche of the Protein expression facility at the EPFL, Lausanne.*)

3.14 Synthesis of BG-IR700

3mg of IRDye®700DX N-hydroxysuccinimide ester fluorophore (LI-COR Biosciences GmbH, Bad Homburg, Germany) were dissolved in 150ul DMSO and treated with 1.5mg BG-PEG11-NH₂[add reference below] and 5ul diisopropylethylamine. After 1h, the product BG-PEG11-IRDye®700DX was purified by HPLC using a Waters Sunfire Prep C18 OBD 5uM; 19 x 150 mm column using 0.1M triethylammonium acetate (TEAA) (pH 7.0) and 0.1M TEAA in water/acetonitrile 3:7 (pH 7.0) as mobile phases A and B, respectively. A linear gradient from 100% A to 100% B within 30 minutes was used. The fractions containing the product were lyophilized (Brun et al., 2009). (*Produced by Ahmad Fawzi Hussain, Stefan Barth at Aachen and Luc Reymond at EPFL, Lausanne.*)

3.15 In-vitro labeling of BDNF^{SNAP}

3.15.1 HEK293T labeling

HEK293T cells were transfected with a combination of 0.125µg trkB/trkA/trkC in pcDNA plasmid and 0.125µg p75NTR (all gifts from Moses Chao, Addgene plasmid #24088,

#24089, #24093 and #24091 respectively) using Lipofectamine 2000 (Invitrogen, 11668-019) in a medium containing DMEM (Gibco, 41966-029), 10% FBS, 1% penicillin/streptomycin. Cells were incubated in serum-free medium for 1 hour before labelling. 0.1 μ M BDNF^{SNAP} was coupled to 0.3 μ M of Snap-surface 647 (New England Biolabs, S9136S) for 1 hour at 37°C and applied onto cells for 15 minutes at 4°C. The cells were imaged using a Zeiss AxioObserver A1 microscope.

3.15.2 DRG labelling

DRG from TrkB^{CreERT2}::Rosa26^{tdRFP} mice were dissected in PBS and treated with 1mg/ml collagenase IV (Sigma Aldrich, C5138) and 0,05% Trypsin (Gibco, 25300-054) for 25 minutes each at 37°C. Cells were then filtered through 100 μ m cup filters (BD biosciences, 340629) and suspended in medium containing DMEM (Gibco, 41966-029), 10% heat inactivated Fetal Bovine Serum (PAA, A15101), 0.8% Glucose and 100U of Penicillin/Streptomycin (Gibco, 15140-122). Dissociated cells were plated onto glass coverslips treated with Poly-L-lysine and stored at 37°C (Stantcheva et al., 2016). An equimolar concentration of BDNF^{SNAP} was coupled to a mixture of Snap-Biotin (New England Biolabs, S9110S) and QD655 quantum dots (Invitrogen, Q10121MP) at 37°C for 30 minutes. The above mixture was applied onto cells for 5 minutes at 37°C and imaged using a Zeiss AxioObserver A1 microscope.

3.16 In-vitro photo-ablation

HEK293T cells transfected with TrkB (as described above) were incubated with a mixture of 1 μ M BDNF^{SNAP} and 3 μ M BG-IR700 for 30 minutes at 37°C. Cells were then exposed to near infra-red light (680nm) illuminated at 40J/cm² for 2 minutes. Cells were stained with Propidium iodide (eBioscience; 00-6990-50) 24 hours after light exposure to assess cellular apoptosis. Non-

transfected HEK293T cells with BDNF^{SNAP}-IR700 and transfected cells with IR700 alone were used as controls.

3.17 In-vivo photo-ablation

The left hindpaw of non-transgenic C57BL6 mice were injected with BDNF^{SNAP} coupled to BG-IR700 in a 1:3 ratio. 15-20 minutes after the injection, near infra-red laser light (650nm) at 120-150J/cm² or 550-600J/cm² was applied onto the paw of the mice for different time periods. This regime was repeated for 3 consecutive days. Behavioral tests were performed 1-3 days after the final treatment. For rescue experiments, neuropathic pain was first induced in C57BL6 mice using one of the models described above. Photo-treatment with BDNF^{SNAP}-IR700 was performed on the 5th, 6th and 7th days after SNI.

3.18 Statistical analysis

All statistical data are presented as Standard error of the mean (SEM) along with the number of samples analysed (n). Student's *t*-test and/or 2-way Repeated measures ANOVA were used and $p < 0.05$ was considered statistically significant.

4 Results

4.1 Molecular characterization of TrkB⁺ sensory neurons in adult mice

4.1.1 TrkB expression in the DRG

In order to visualize the expression pattern of TrkB in the DRG, we generated TrkB^{CreERT2}::Rosa26^{RFP} reporter mice. Upon administration of 75mg/kg of tamoxifen for 5 consecutive days, we found robust RFP expression in approximately 10% of all DRG neurons which corresponded to the ~8% of cells which expressed TrkB mRNA (Fig 4).

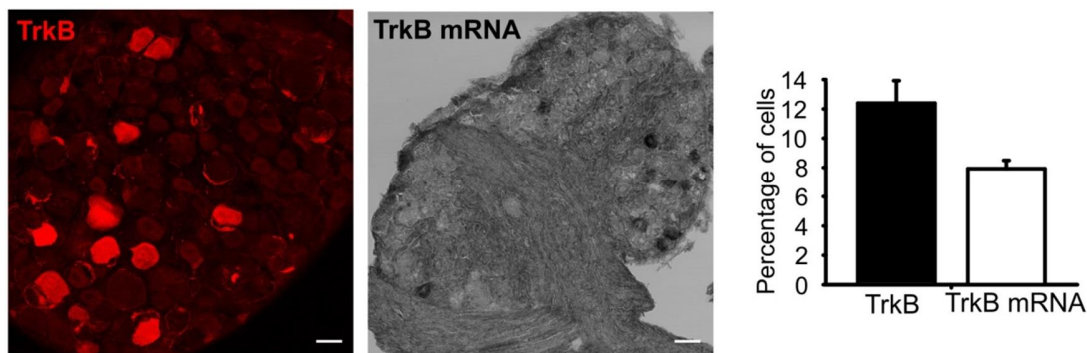
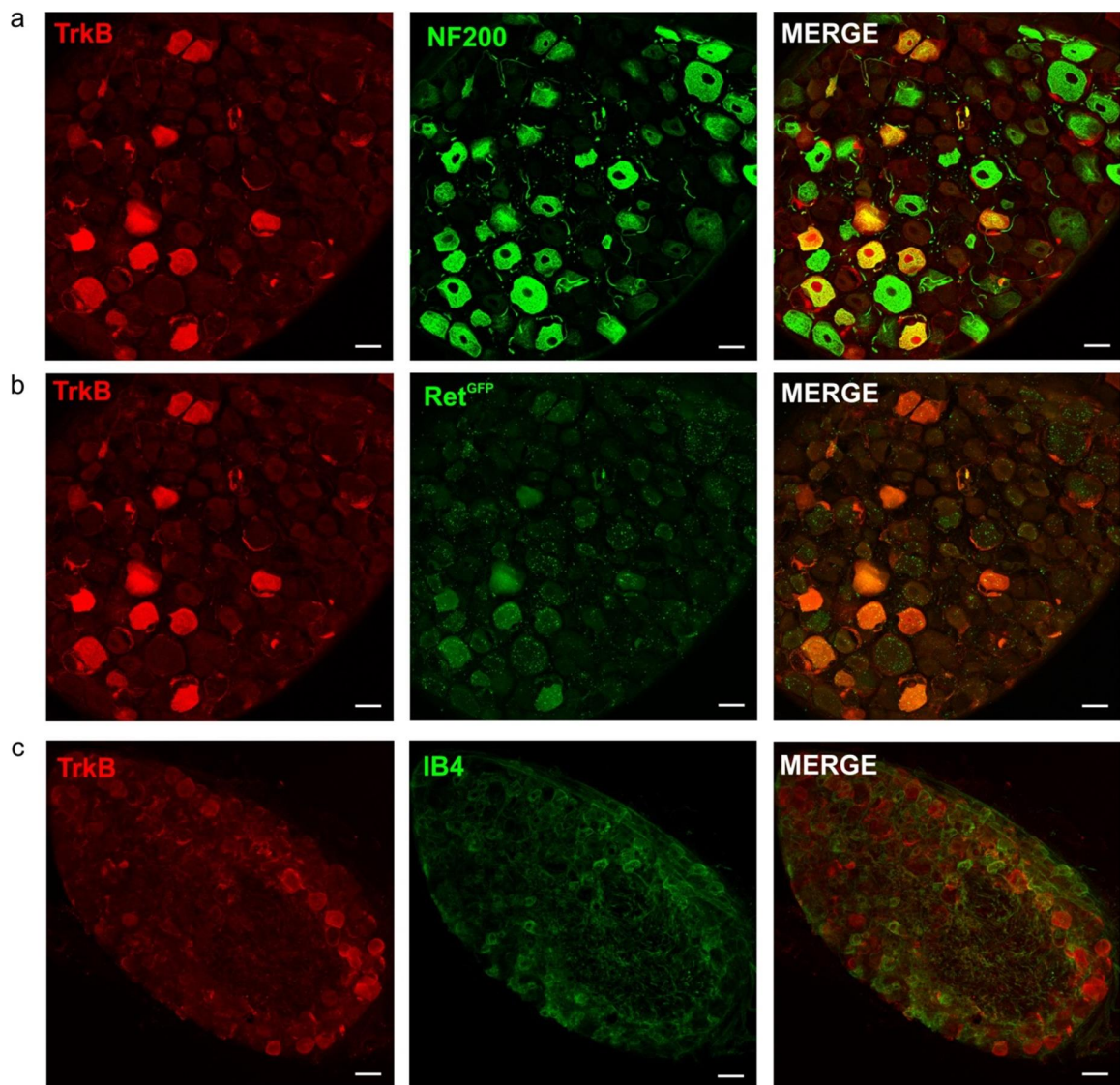


Figure 4: Expression of TrkB in DRG

Expression of RFP and TrkB-mRNA in DRG sections and quantification of the number of TrkB⁺ DRG

We next co-labelled neurons with known markers of sensory neurons and found that majority of TrkB⁺ neurons co-expressed NF200, a marker for myelinated sensory neurons (Fig 5a). We also found a small proportion of TrkB⁺ neurons (~40%) to co-expresses Ret, a marker for a subset of rapidly adapting LTMR δ (Fig 5b).



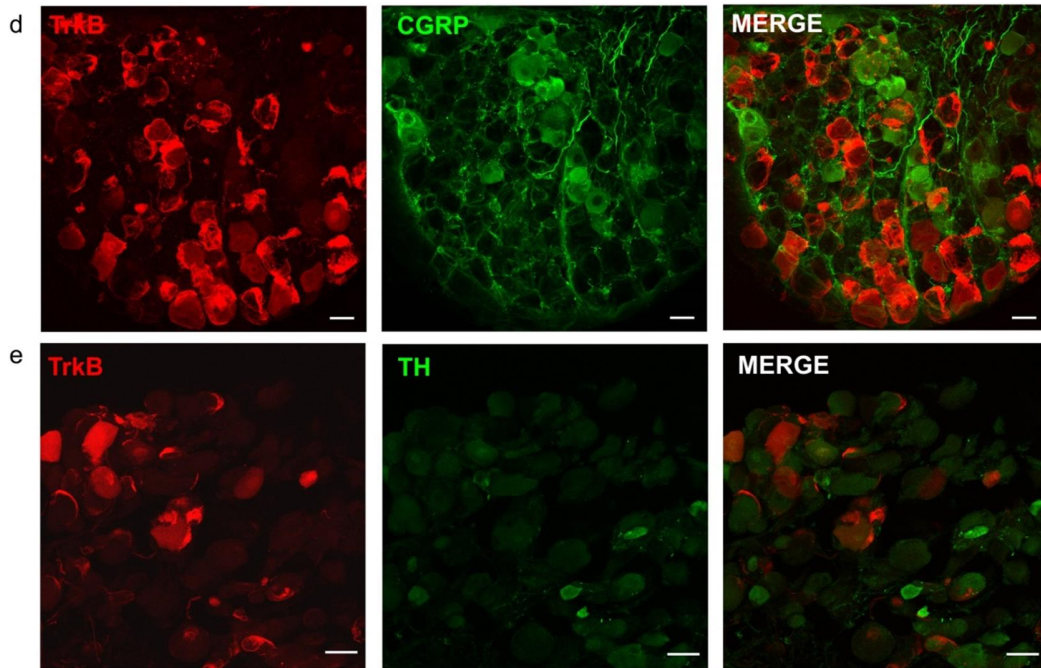


Figure 5: Co-localization of TrkB with known molecular markers

Double immunofluorescence of sections of DRG from $\text{TrkB}^{\text{CreERT2}}::\text{Rosa26}^{\text{RFP}}$ mice with markers (a) NF200, (b) Ret, visualized using $\text{TrkB}^{\text{CreERT2}}::\text{Rosa26}^{\text{RFP}}::\text{Ret}^{\text{EGFP}}$ triple transgenic mice, (c) IB4, (d) CGRP, and (e) TH. Scale bar $50\mu\text{m}$

However, all TrkB^+ neurons were negative for Isolectin B4; a marker for non-peptidergic nociceptors, CGRP; a marker for peptidergic nociceptors and TH, a marker for C-fiber LTMRs (Fig 5c-e, 11a).

4.1.2 TrkB expression in the skin

The peripheral afferents of TrkB^+ neurons in the skin were labelled by generating $\text{TrkB}^{\text{CreERT2}}::\text{Rosa26}^{\text{SnapCaaX}}$ mice, making use of the Snap-tag technology which uses a site specific binding of O(6)-benzylguanine (BG)-modified molecules to a Snap-tag protein (Yang et al., 2015). Using this line, we found TrkB^+ afferents in the hairy skin where they formed lanceolate endings on hair follicles (Fig 6).

Interestingly, we also found TrkB expressing afferents in the glabrous skin where they innervated specialized end organs called Meissner's corpuscles which detect gentle pressure applied to the surface of the skin (Fig 7).

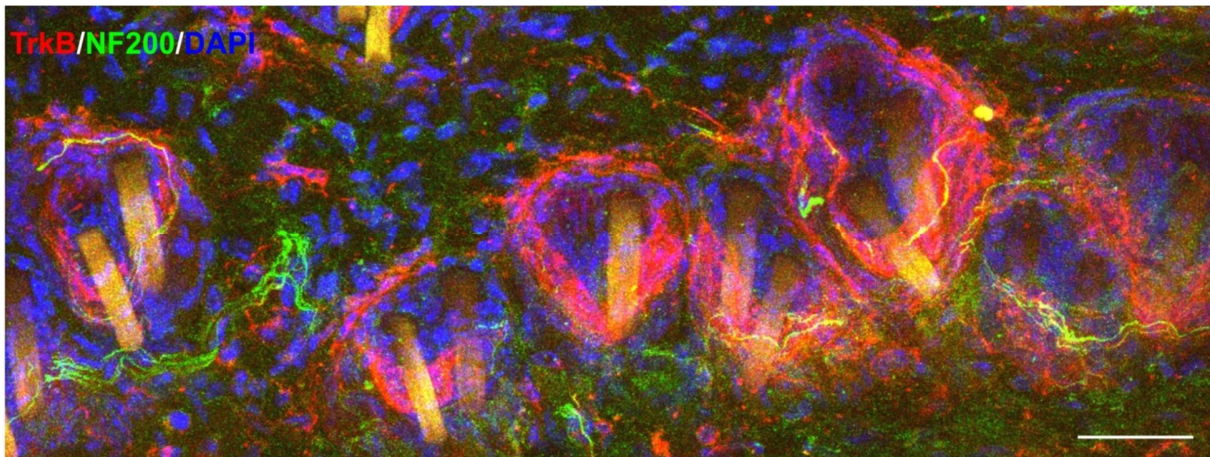


Figure 6: TrkB innervates hair follicles in the skin

Cross-section of the back hairy skin showing TrkB⁺ lanceolate endings of TrkB^{CreERT2}::Rosa26^{SnapCaaX} mice labeled with Snap Cell TMRstar (red), NF200 (green) and DAPI (blue). Scale bar 40µm.

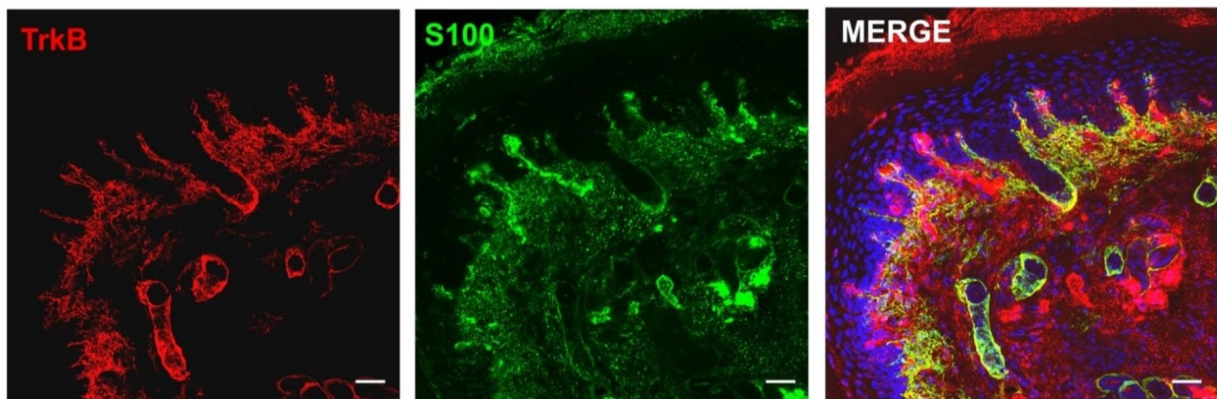


Figure 7: TrkB innervates Meissner's corpuscles in glabrous skin

Section from the hind-paw of TrkB^{CreERT2}::Rosa26^{Chr2YFP} (red) stained with anti-S100 a marker for Meissner's corpuscles (green) and DAPI (blue). Scale bar 40µm.

4.1.3 TrkB expression in the spinal cord

We next examined the central projections of TrkB neurons in the spinal cord by generating a reporter line in which Cre dependent expression of mCherry was driven from the sensory neuron specific Avil locus (Supplementary Fig.). TrkB^{CreERT2}::Avil^{mCherry} positive afferents were present in laminae III/IV of the dorsal horn of the spinal cord where they formed columnar structures extending dorsally (Fig 8).

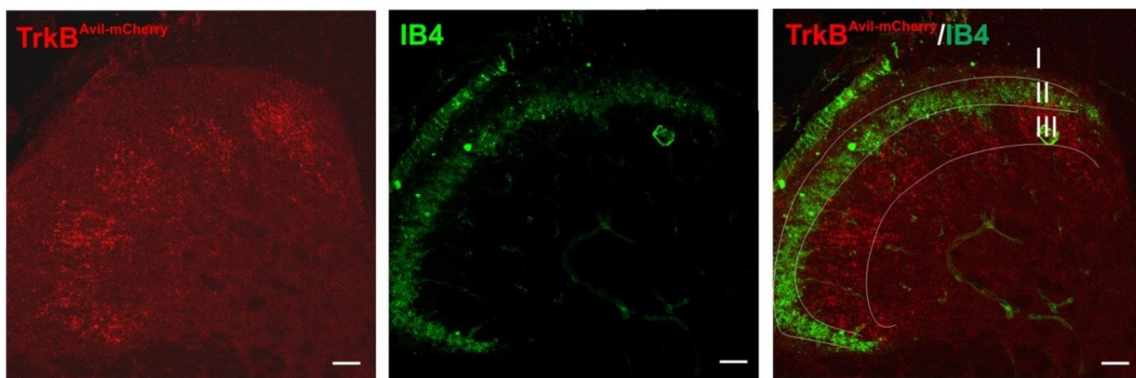


Figure 8: TrkB terminates in laminae III/IV of the dorsal horn

Section through the dorsal horn of the lumbar spinal cord of TrkB^{CreERT2}::Avil^{mCherry} mice stained with IB4, a marker for lamina II shows TrkB⁺ afferents in laminae III/IV. Scale bar 50 μ m.

4.1.4 TrkB expression in human DRG and skin

We also examined the expression of TrkB in human tissues using an antibody against TrkB (TrkB-IR). In DRG δ s, all TrkB-IR observed were NF200⁺ (Fig 9a), with some TrkB-IR being Ret⁺ (Fig 9b). All TrkB-IR cells were negative for TrkA (Fig 9c) which was used as a marker for nociceptors. In accordance with the mouse data, TrkB-IR was also found innervating the Meissner δ corpuscles in the palmar skin (Fig 10). Together, these results suggest that TrkB marks a population of mechanoreceptors.

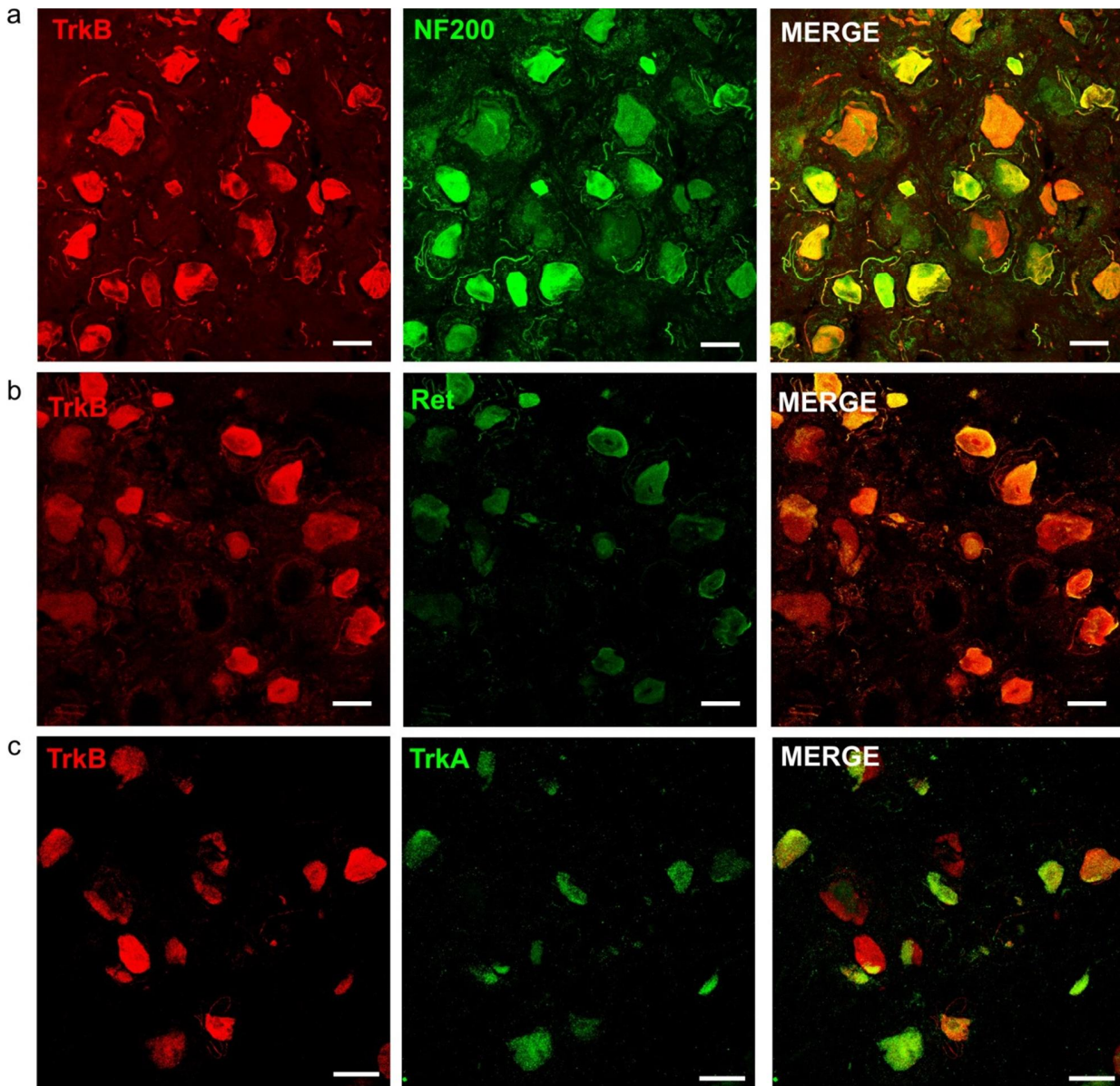


Figure 9: TrkB-IR in human DRG marks mechanoreceptors

Double immunofluorescence of human DRG sections stained with antibodies against TrkB and (a) NF200, (b) Ret and (c) TrkA showing TrkB-IR colocalization with NF200 and Ret but not TrkA. Scale bar 40 μ m.

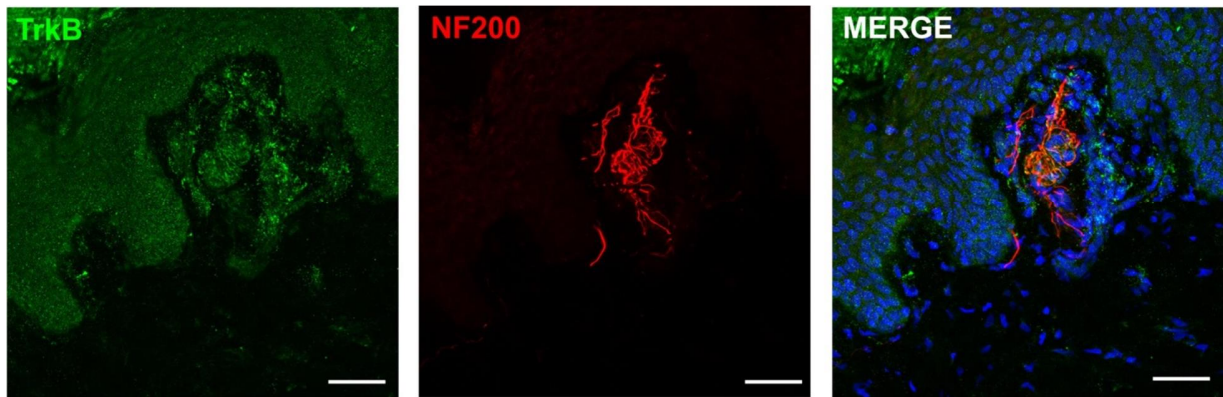


Figure 10: TrkB-IR in Meissner δ corpuscles of human palmar skin

Cross-section of the human glabrous skin from the palmar region stained with antibodies against TrkB (red) and NF200 (green), and DAPI (blue). Scale bar 40 μ m.

4.1.5 Ex-vivo skin nerve electrophysiology

To establish the identity of TrkB⁺ sensory neurons, we characterized their response properties by combining skin-nerve electrophysiology and optogenetic activation. Mice expressing the light-gated ion channel channelrhodopsin (Rosa26^{ChR2}) in TrkB⁺ neurons were generated (TrkB^{CreERT2::Rosa26^{ChR2}}) and functionally characterized based on the conduction velocities, firing patterns and the lowest force required to generate action potentials (Fig 11b-c). Photostimulation of the skin of the TrkB^{CreERT2::Rosa26^{ChR2-EYFP}} mice with blue light (470nm) evoked action potentials in two different fiber types; D-hairs (as characterized by conduction velocities in the range of 2-10 m/s) and RA A β -LTMR δ or RAM δ (>15 m/s) while other populations were unresponsive to light (Fig 11d). These fibers also exhibited very fine mechanical thresholds (<0.1g) upon probing the skin with graded von-Frey filaments (fig 8j).

These experiments taken together with the histological characterization confirm that TrkB is expressed in myelinated neurons that innervate hair follicles and are tuned to detect gentle mechanical stimuli.

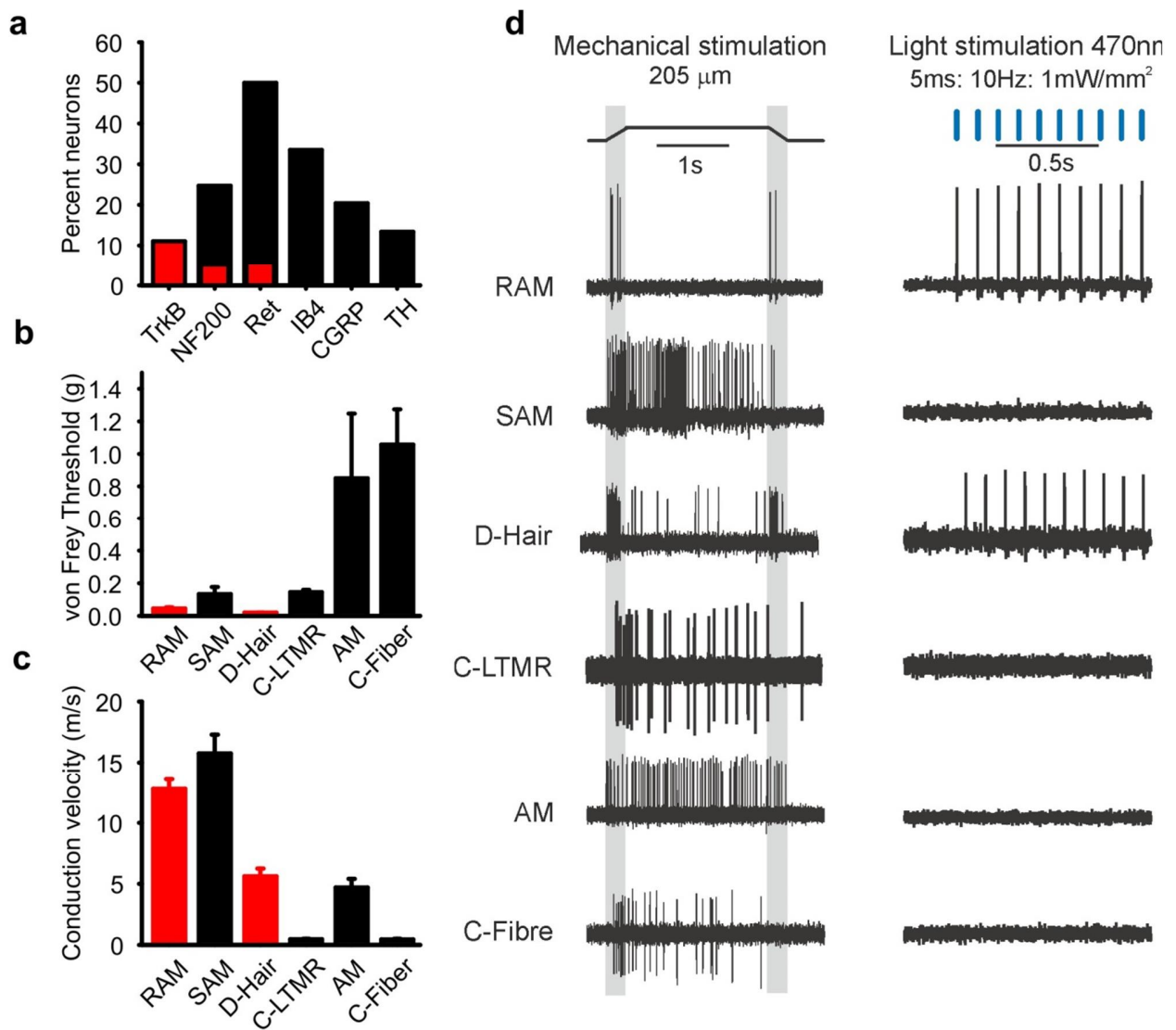


Figure 11: Skin-nerve electrophysiology of TrkB⁺ afferents

Quantification of staining on mouse DRG sections (a). In-vitro skin nerve preparation from TrkB^{CreERT2}::Rosa26^{ChR2} mice showing (b) the minimum force required to activate the indicated fiber type, (c) the conduction velocities of the fiber types and (d) responses to 10Hz stimulation with blue light. Red bar represents TrkB⁺ afferents (n=10). Error bars represent SEM. Data generated by Dr. Francisco Taberner.

4.2 Functional characterization of TrkB⁺ neurons

4.2.1 Ablation of TrkB⁺ neurons leads to reduction in responses to gentle touch

Next, to determine the function of TrkB⁺ D-hairs and RAM ϕ in the behavior of adult mice, we genetically ablated TrkB neurons in the peripheral nervous system using a Cre-dependent diphtheria toxin receptor (iDTR), knocked-in to the sensory neuron specific Advilin locus. This line facilitates the deletion of TrkB⁺ neurons only within the DRG without affecting other tissues (Stantcheva et al., 2016). Upon systemic injection of diphtheria toxin in TrkB^{CreERT2}::Avil^{iDTR} mice, we achieved a >90% ablation of TrkB⁺ neurons (Fig 12a-c). Also, we noticed a reduction in the number of NF200⁺ neurons by ~40% with no change in the expression of other markers such as Isolectin B4, CGRP or TH (Fig 12c).

TrkB^{CreERT2}::Avil^{iDTR} mice were then subjected to a series of behavioral tests to examine their sensory deficits. Ablated mice showed normal responses to evaporative cooling of the hind-paw evoked by acetone (Fig 12d), or in latency to respond to noxious heat (Fig 12e). Similarly, responses to noxious pinprick remained unaltered by ablation (Fig 12g). We also noticed that the grip strength (Fig 12f) and the ability to detect and remove a small piece of tape stuck to the back (Fig 12h) remained unaffected after ablation of TrkB⁺ neurons.

We tested responses to dynamic mechanical stimulation of the skin by brushing the plantar surface of paw using a puffed out cotton swab which exerts forces in the range 0.7-1.6mN. We observed a significant reduction in responsiveness upon ablation of TrkB⁺ neurons (Fig 12i). These differences, however, were not apparent upon brushing using a stronger force elicited by a paint brush (>4mN, Fig). These results suggest that under baseline conditions, TrkB⁺ sensory neurons are required for detecting the lightest of mechanical stimuli acting on the skin.

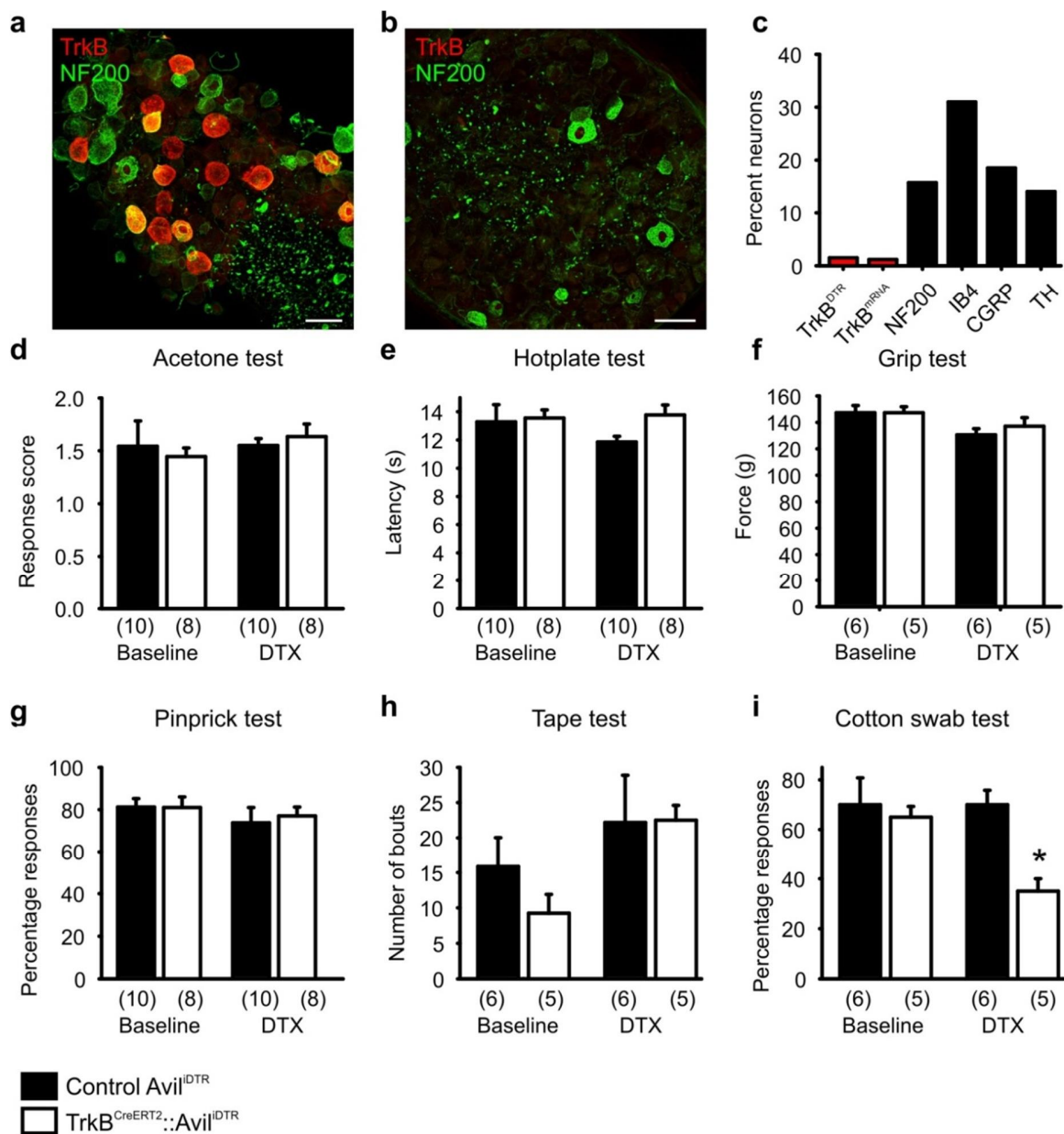


Figure 12: Diphtheria toxin mediated ablation of TrkB⁺ neurons

Immunofluorescence of DRG sections from TrkB^{CreERT2::}Avil^{iDTR} mice with an antibody against the diphtheria toxin receptor (red) in (a) untreated mice and (b) after ablation. (c) Quantification of DRG sections indicating a ~90% decrease in TrkB^{DTR} and TrkB^{mRNA} cells after ablation and ~40% reduction in NF200⁺ neurons without affecting other subpopulations. Behavioral responses in littermate control mice (Avil^{iDTR}, black bars) and TrkB^{CreERT2::}Avil^{iDTR} mice (white bars); no differences in responses upon ablation in (d) acetone drop test (t-test; $p > 0.05$), (e) hot plate test (t-test; $p > 0.05$), (f) grip test (t-test; $p > 0.05$), (g) pin-prick test (t-test; $p > 0.05$), (h) tape test (t-test; $p > 0.05$). (i) Ablated mice shows reduction in responses to cotton swab (t-test, $p < 0.001$). Scale bars in A, B 50 μ m, error bars indicate SEM.

4.3 Role in mechanical allodynia

As mentioned earlier, previous studies have implicated myelinated LTMRs in mechanical allodynia. However, the identities of neurons that drive this condition have remained poorly understood. Taking into account, the sensitivity of TrkB⁺ neurons, we next asked whether they contribute to mechanical hypersensitivity in mouse models of neuropathic pain. To this end, we took both a loss of function and a gain of function approach using genetic ablation and optogenetic activation of TrkB neurons respectively.

4.3.1 Inflammatory pain unaffected in TrkB ablated mice

Neuropathic pain can manifest as mechanical hypersensitivity to inflammation of the skin or to a nerve injury. We first considered the inflammatory model of neuropathic pain by injecting Complete Freund's Adjuvant (CFA) into the plantar surface of the hind-paw and recording responses to punctate von-Frey filaments and dynamic brush stimuli. Ablation of TrkB⁺ neurons in TrkB^{CreERT2}::Avil^{idTR} mice had no effect on the mechanical hypersensitivity after inflammation (Fig 13a-b). We next examined whether optogenetic activation of TrkB neurons could evoke pain under inflammatory conditions. Using stimulation parameters which evoked robust firing in the ex-vivo skin nerve preparation, we observed no differences in behavioral response to light application to the hind-paw either in basal conditions or after inflammation in TrkB^{CreERT2}::Rosa26^{ChR2} mice (Fig 13c).

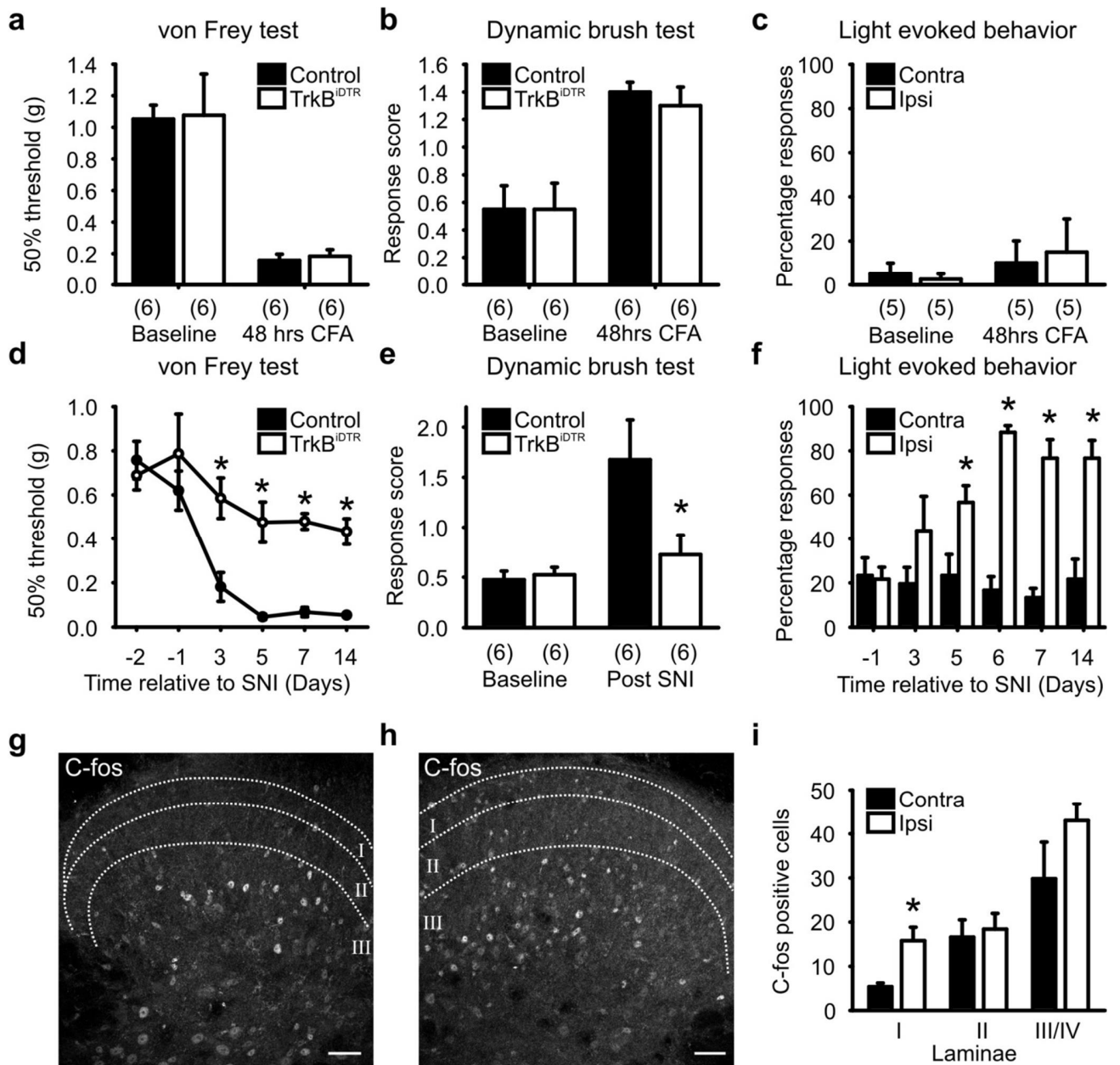


Figure 13: TrkB⁺ neurons drive mechanical allodynia

Mechanical allodynia in both control Avil^{iDTR} (black bar) and TrkB^{CreERT2}::Avil^{iDTR} (white bar) mice 48 hours after CFA injections as measured by (a) von Frey filaments (t-test; $p > 0.05$) and (b) dynamic brush stimuli (t-test; $p > 0.05$). All mice received diphtheria toxin injections. (c) Paw withdrawal frequencies in contralateral (black bar) and CFA injected ipsilateral (white bar) paw of TrkB^{CreERT2}::Rosa26^{Chr2} mice upon stimulation with 473nm blue light shows no significant difference under baseline conditions and 48 hours after CFA injection (Mann-Whitney test; $p > 0.05$). (d) Mechanical thresholds to von Frey filaments indicating that ablation of TrkB⁺ neurons abolished the development of mechanical allodynia after SNI in TrkB^{CreERT2}::Avil^{iDTR} mice (white circles) in comparison to Avil^{iDTR} controls (black circles) ($n=7$ for both sets, Two-way RM ANOVA; $p < 0.001$ followed by a Bonferroni post-hoc test). (e)

Reduced dynamic brush allodynia in ablated $\text{TrkB}^{\text{CreERT2}}::\text{Avil}^{\text{iDTR}}$ mice (white bar) as compared to littermate controls (black bar; t-test $p < 0.05$). **(f)** Nocifensive behavior evoked by optogenetic stimulation of ipsilateral (black bars) and contralateral (white bar) paw of $\text{TrkB}^{\text{CreERT2}}::\text{Rosa26}^{\text{Chr2}}$ mice after SNI (Two-way RM ANOVA; $p < 0.001$). **(g-h)** Cross section of the lumbar spinal cord from $\text{TrkB}^{\text{CreERT2}}::\text{Rosa26}^{\text{Chr2}}$ mice labelled for c-fos after 1 minute exposure to a 15Hz blue light 7 days post SNI **(g)** Represents the contralateral uninjured and **(h)** the injured ipsilateral dorsal horn. **(i)** Shows quantification of the number of c-fos positive cells in each lamina of the lumbar spinal cord within a 40 μm section (black bar contralateral, white bar ipsilateral). Scale bars in G and H, 40 μm . Error bars indicate SEM.

4.3.2 TrkB^+ neurons contribute to allodynia after nerve injury

We next induced neuropathic pain in mice using the Spared Nerve Injury (SNI) model wherein two of the three branches of the sciatic nerve are ligated together and cut leaving the sural nerve intact. This allows for testing the hypersensitivity of the intact sural nerve innervating areas of the hind paw. Using this well-established model, we found that control mice developed a strong mechanical hypersensitivity in the sural nerve territory of the hind-paw to both von-Frey filaments and dynamic brush stimuli after injury. Strikingly however, upon ablation of TrkB^+ sensory neurons, mice failed to develop mechanical allodynia to both punctate and dynamic stimuli, and mechanical thresholds remained at preinjury levels throughout the experimental period (Fig 13d-e).

We subsequently activated TrkB^+ afferents in $\text{TrkB}^{\text{CreERT2}}::\text{Rosa26}^{\text{Chr2-EYFP}}$ mice using optogenetics and found that photostimulation of the hind-paw induced prolonged paw withdrawal and pain-like behavior (flicking and licking) of the injured ipsilateral paw starting from 3 days after injury and persisted throughout the testing period (Fig 13f). This behavior was not observed in the uninjured contralateral paw or in control littermates.

Taken together these results suggest that TrkB^+ neurons are required for the induction and maintenance of nerve injury driven mechanical allodynia.

4.3.3 c-fos induction increases in lamina I after SNI

Much of the new evidence links the mechanism of neuropathic pain to a disinhibition of interneurons in the spinal cord dorsal horn thereby granting LTMR afferents direct access to pain circuits. To test this idea we looked into induction of the immediate early gene C-fos in the dorsal horn of the spinal cord. Optogenetic stimulation of the paw of naïve $\text{TrkB}^{\text{CreERT2}}::\text{Rosa26}^{\text{ChR2}}$ mice resulted in C-fos immunoreactivity primarily in laminae III and IV of the spinal cord, the region where TrkB afferents terminate (Fig 13g,i). However, upon nerve injury, identical stimulation of the paw induced an increased C-fos staining in lamina I of the dorsal horn, an area associated with nociceptive processing (Fig 13h,i).

Thus, TrkB^+ sensory neurons are necessary and sufficient to transmit gentle touch signals that evoke pain under pathological conditions.

4.4 BDNF^{SNAP} as a target for TrkB^+ neurons

Treatment of allodynia has been clinically challenging with current treatment, involving the use of conventional analgesics and opioids like morphine, being often ineffective. This has been largely attributed to the lack of understanding of the circuitry involved in neuropathic pain. In light of the clinical importance of mechanical allodynia in neuropathic pain patients, we developed a pharmacological strategy to target TrkB^+ neurons which provoke this pain state. TrkB receptor signals through binding to ligands, Brain Derived Neurotrophic Factor (BDNF) or Neurotrophin-4 (NT4). With bulk of the evidence pointing to BDNF being the most common ligand of TrkB, we produced a recombinant BDNF protein with a Snap-Tag fused to its c-terminus. The recombinant protein was produced in CHO cells and purified by the Protein expression facility in EPFL, Lausanne.

4.4.1 BDNF^{SNAP} labels TrkB⁺ neurons in-vitro

BDNF^{SNAP} was coupled to a fluorescent Snap-Surface647 substrate and applied in-vitro to HEK293T cells expressing neurotrophin receptors (TrkA, TrkB or TrkC along with p75NTR). Fluorescently labelled BDNF^{SNAP} displayed strong co-localization with TrkB/p75 (Fig 14a), and did not bind to cells expressing other neurotrophin receptors TrkA/p75 (Fig 14b) or TrkC/p75 (Fig 14c).

Next to test whether BDNF^{SNAP} recognizes TrkB receptors in DRG neurons, we conjugated 7nM of BDNF^{SNAP} to Qdot 655 quantum dots in an equimolar ratio and applied the mixture on to dissociated DRG neurons from TrkB^{CreERT2}::Rosa26^{RFP} mice. We observed a >95% overlap between BDNF^{SNAP} and TrkB⁺ neurons (Fig 14d) indicating that recombinant BDNF^{SNAP} is highly selective to TrkB neurons.

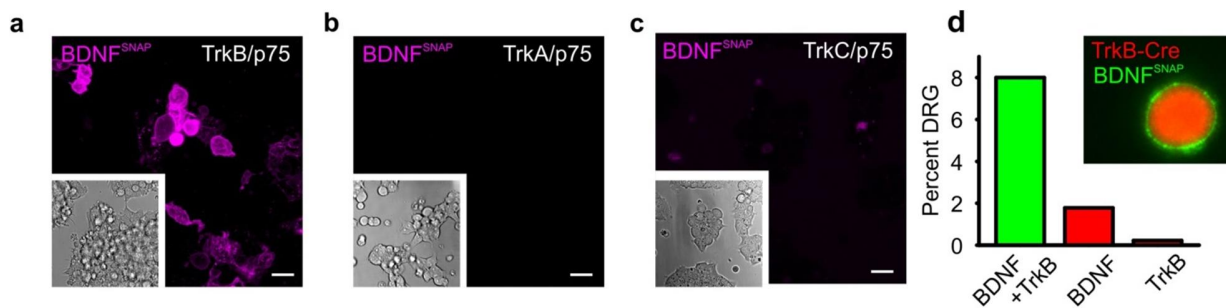


Figure 14: BDNF^{SNAP} labelling on cells in-vitro

HEK293T cells labelled with BDNF^{SNAP} upon transfection with (a) TrkB/p75NTR, (b) TrkA/p75NTR, or (c) TrkC/p75NTR. (d) Labeling and quantification of dissociated DRG (inset) from TrkB^{CreERT2}::Rosa26^{RFP} mice with BDNF^{SNAP} shows significant overlap of BDNF^{SNAP} binding to TrkB⁺ cells. Scale bars 20μm.

4.4.2 BDNF^{SNAP} mediated ablation in-vitro

In order to manipulate TrkB neurons, BDNF^{SNAP} was conjugated to a benzylguanine modified derivative of the highly potent near-infrared photosensitizer IRDye@700DX

phthalocyanine (IR700). In the first set of experiments, BDNF^{SNAP}-IR700 coupled mixture was applied on to HEK293T cells expressing TrkB/p75 and cell death was assayed following near infrared illumination. Cells expressing TrkB/p75 showed substantial cell death 24 hours after light exposure (Fig 15a) that was not evident upon mock transfection or treatment with IR700 alone (Fig 15b,c).

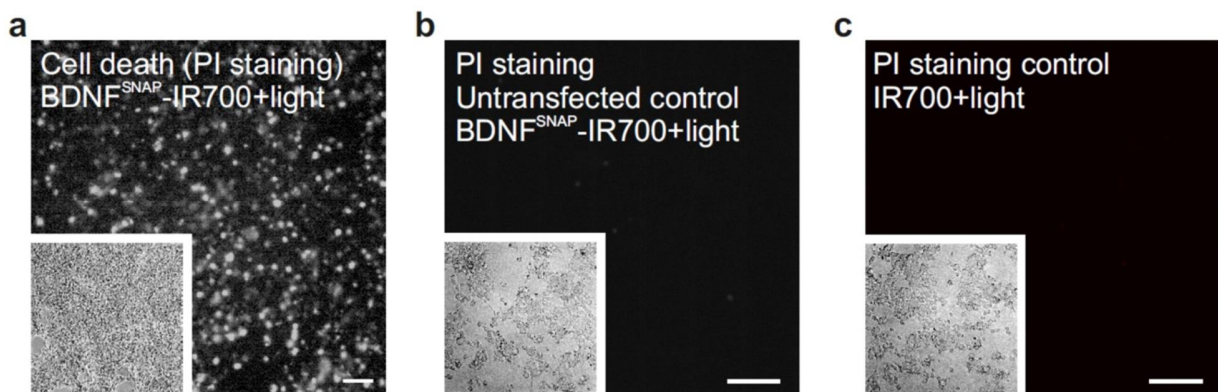


Figure 15: BDNF^{SNAP} mediated ablation in-vitro

HEK293T cells transfected with TrkB/p75NTR and stained with propidium iodide 24 hours after treatment with BDNF^{SNAP}-IR700 and near infrared exposure (a). BDNF^{SNAP} mock transfected HEK293T cells stained with propidium iodide 24 hours after photoablation (b). Staining of HEK293T cells transfected with TrkB/p75NTR with propidium iodide 24 hours after treatment with IR700 alone and near infrared illumination (c). Scale bars 50μm.

4.4.3 BDNF^{SNAP} mediated ablation in-vivo

We next injected 5μM BDNF^{SNAP}-IR700 into the paw of TrkB^{CreERT2}::Rosa26^{SnapCaaX} mice followed by exposure to near infrared laser at 120-150J/cm², 15-20 minutes after injection. This procedure was performed for 3 consecutive days. Sections of the skin from these mice displayed extensive loss of TrkB⁺ lanceolate endings around hair follicles and fibers innervating Meissner's corpuscles in the Glabrous skin (Fig 19a), while no reduction in innervation was seen in control skin sections injected with unconjugated IR700 and exposure to light (Fig 19b).

We further investigated whether this loss of TrkB⁺ afferents was a result of death of TrkB⁺ neurons in the DRG. We observed no difference in the proportion of TrkB⁺ neurons 7 days after photoablation (Fig 16a-b) indicating that the loss of fibers in the skin reflects local retraction from their peripheral targets.

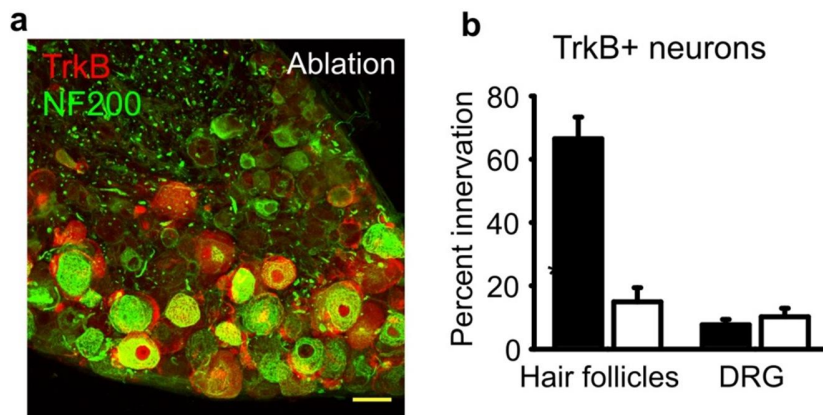


Figure 16: BDNF^{SNAP} mediated ablation in DRG sections

Quantification of the proportion of hair follicle innervation and DRG neurons positive for TrkB following photoablation in the paw of TrkB^{CreERT2}::Rosa26^{RFP} mice. Scale bar 40 μ m.

We also subjected mice to a series of behavioral tests and found no differences in their responses to noxious stimuli such as heat, cold and pin-prick after BDNF^{SNAP}-IR700 mediated ablation (Fig 17a-c). Surprisingly, the sensitivity of mice to cotton swab also remained unaffected (Fig 17d) probably due to the small area of ablation and the compensatory effects of intact TrkB afferents.

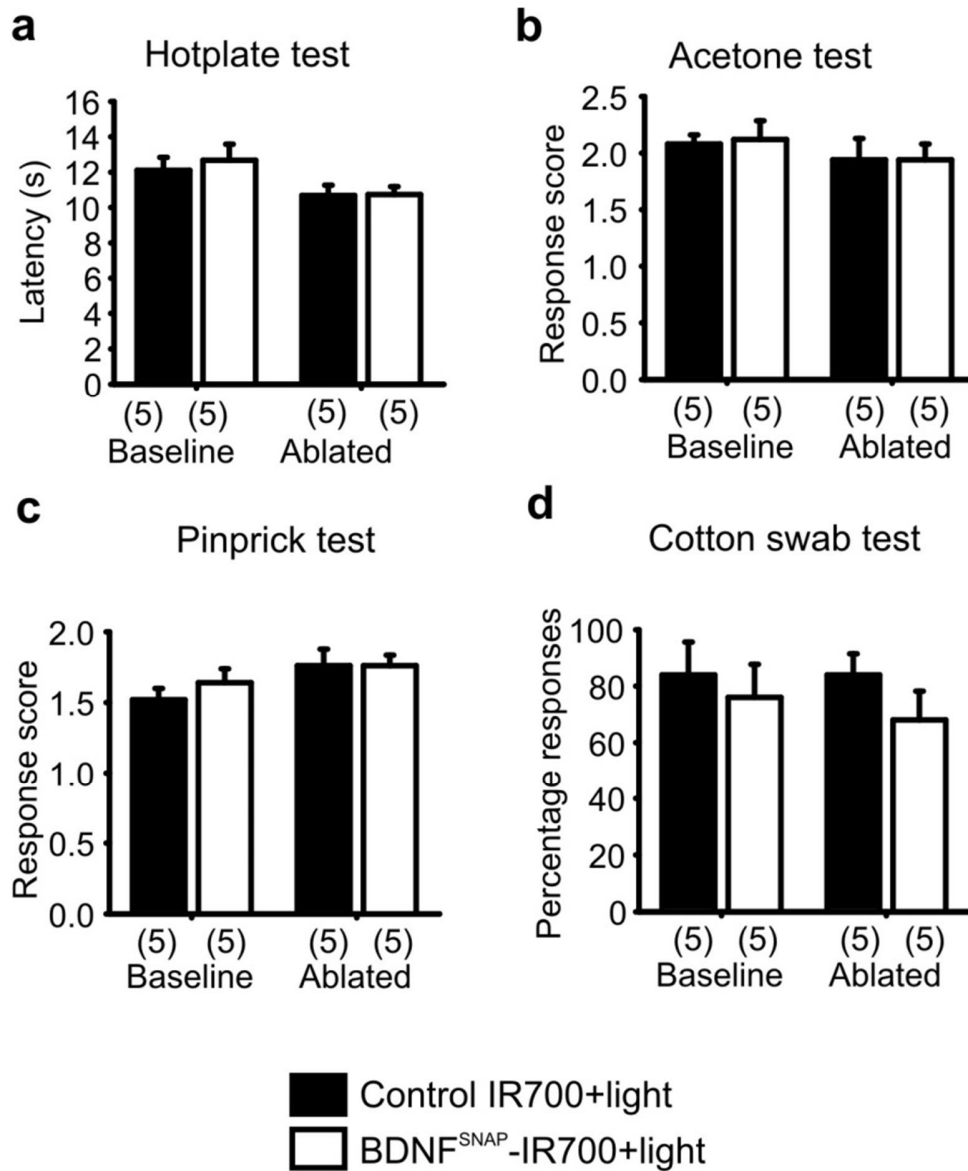


Figure 17: BDNF^{SNAP} mediated ablation in-vivo
 BDNF^{SNAP}-IR700 mediated photoablation in the paw does not affect baseline sensory behavior responses to (a) hot plate test (t-test; $p > 0.05$), (b) acetone drop test (t-test; $p > 0.05$), (c) pin-prick test (t-test; $p > 0.05$) and (d) cotton swab test (t-test; $p > 0.05$). Error bars indicate SEM

4.4.4 BDNF^{SNAP} mediated rescue of mechanical allodynia

Having confirmed the specificity of BDNF^{SNAP} to TrkB⁺ neurons, we assessed the behavioral effects of BDNF^{SNAP}-IR700 mediated photoablation on injury induced hypersensitivity. To do this, we first induced neuropathic pain in wildtype C57BL6 mice using the SNI model.

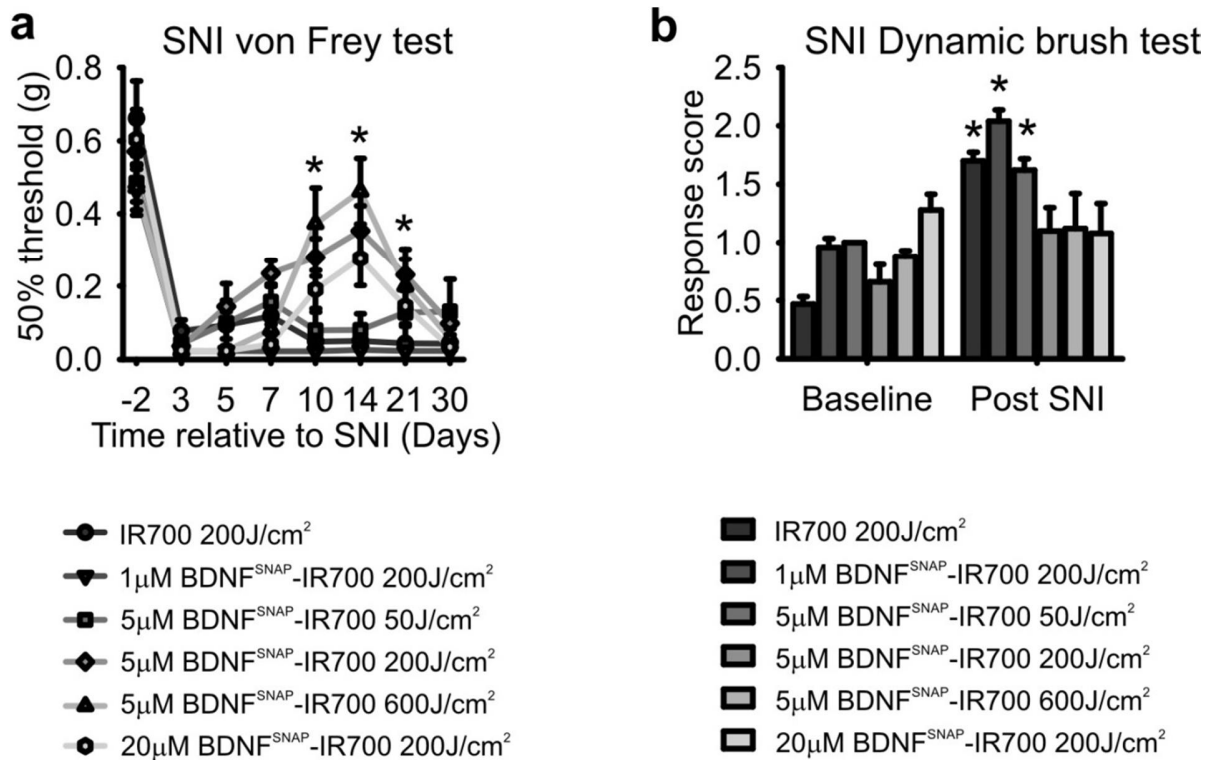


Figure 18: Photoablation using BDNF^{SNAP} rescues mechanical allodynia

BDNF^{SNAP}-IR700 mediated photoablation of the hind-paw of SNI mice results in a dose specific reversal of mechanical allodynia, tested with von Frey filaments (**a**) (n=10 or 5, two-way RM ANOVA; p<0.05 followed by a Bonferroni post-hoc test) and dynamic brush stimuli (**b**) (t-test; p<0.05).

Upon development of robust mechanical allodynia, the injured paw of mice was injected with BDNF^{SNAP}-IR700 and illuminated with near infrared light for 3 consecutive days and we

observed that starting from 3 days after final photo-ablation, mice showed a significant increase in pain thresholds to both punctate von-Frey filaments and to dynamic brush compared to control mice leading to recovery from mechanical allodynia (Fig 18a-b) which lasted for 2 weeks before reappearance of allodynia. This recovery trend was observed under various different concentrations of BDNF^{SNAP}-IR700 coupling and light dosage conditions satisfying robustness of the system (Fig 18a-b).

To ask if the recovery from allodynia and its subsequent reappearance is due to the retraction and re-innervation of TrkB⁺ afferents in the skin, photo-ablated hindpaws of TrkB^{CreERT2}::Rosa26^{SnapCaaX} mice were labelled with TMR-star BG substrate at different time points in the course of the experiment. 7 days after photo-ablation, when the recovery from allodynia was at its peak, we observed no TrkB⁺ afferents in the skin, which reappeared after 25 days of photo-ablation (Fig 19a-c) corresponding to the behavioral results.

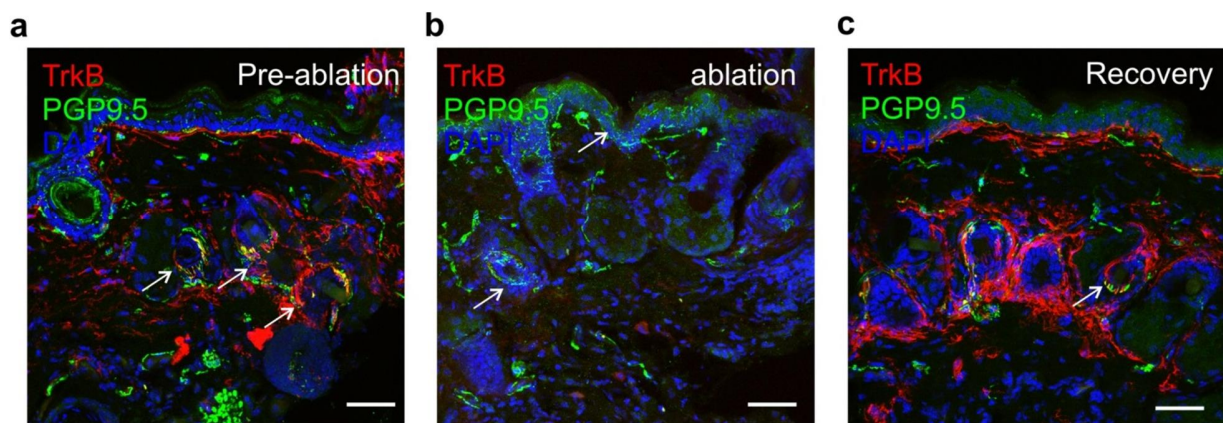


Figure 19: Visualization of BDNF^{SNAP} mediated ablation in-vivo

Loss of TrkB⁺ afferents (red), but presence of other fibers (green) upon BDNF^{SNAP}-IR700 mediated photoablation. (a) Innervation of paw hairy skin before ablation, arrows shows lanceolate endings. (b) Loss of TrkB⁺ afferents after ablation, arrows shows PGP9.5 fibers. Note the absence of TrkB⁺ fibers (red) but PGP9.5 positive circumferential and longitudinal lanceolate endings (green). (c) Reinnervation of skin by TrkB⁺ afferents at 24 days post ablation.

To test the efficiency of BDNF^{SNAP} mediated photoablation to reduce mechanical allodynia and to increase its translational research potential, we followed up with 2 independent models of neuropathic pain; Diabetic neuropathy and chemotherapy induced neuropathic pain.

4.4.5 BDNF^{SNAP} mediated rescue of diabetic peripheral neuropathy

In the first model, mice were induced with diabetes by systemic injection of a single high dose (SHD) of Streptozotocin (STZ, 180mg/kg). 1 week after STZ injection, mice developed hyperglycemia which was frequently monitored by measuring blood-glucose levels using ACCU-CHEK glucose sticks and a conventional glucometer. Mice with blood-glucose levels above 300mg/dL were considered diabetic. The blood-glucose levels were maintained between 350-400mg/dL by administration of insulin once a week. The SHD-STZ model is well known to produce early neuropathic pain and indeed 3-4 weeks after STZ injection, mice developed robust bilateral mechanical allodynia as measured by von-Frey filaments. The left hindpaw of diabetic mice were then injected with BDNF^{SNAP}-IR700 and illuminated with near infrared light following the same protocol as before. 3 days following the photo-ablation paradigm, mice started showing signs of rescue from allodynia which lasted 17 days before allodynia phenotype reemerged (Fig 20a).

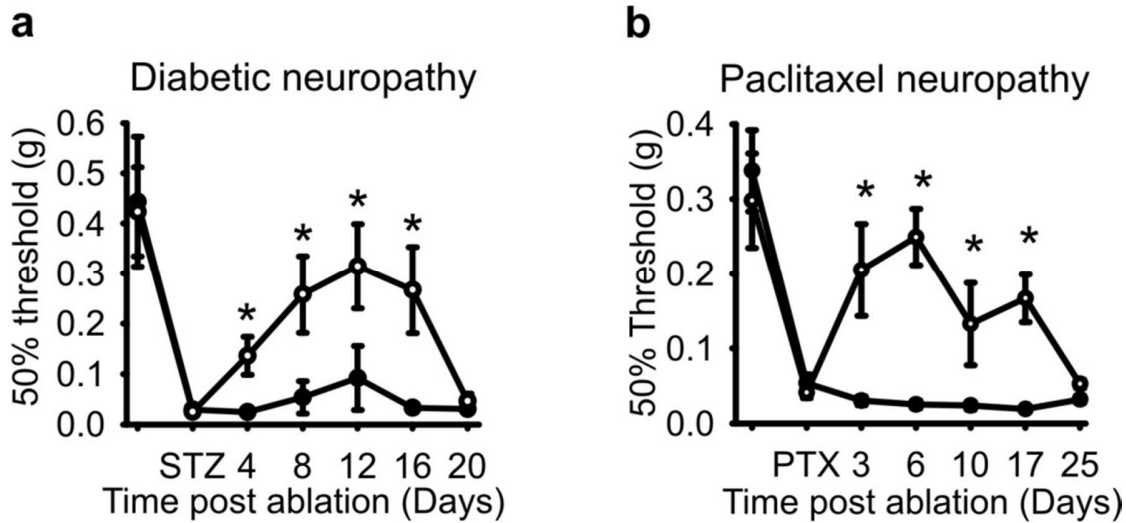


Figure 20: BDNF^{SNAP} mediated rescue of diabetic and chemotherapy induced neuropathy
 BDNF^{SNAP}-IR700 mediated photoablation rescues mechanical allodynia in (a) streptozotocin (STZ) model of diabetic neuropathy (n=5, two-way RM ANOVA; p<0.05 followed by a Bonferroni post-hoc test. Open circles; 5μM BDNF^{SNAP}-IR700 at 200J/cm², closed circles, 5μM IR700 at 200J/cm²) and (b) paclitaxel (PTX) model of chemotherapy induced neuropathy (n=5, two-way RM ANOVA; p<0.05 followed by a Bonferroni post-hoc test. Open circles; 5μM BDNF^{SNAP}-IR700 at 200J/cm², closed circles, 5μM IR700 at 200J/cm²).

4.4.6 BDNF^{SNAP} mediated rescue of chemotherapy induced neuropathic pain

In the second model, to mimic chemotherapy induced neuropathic pain, wildtype C57BL6 mice were injected systemically with Paclitaxel for 4 alternate days. As reported by earlier studies, mice develop long lasting bilateral allodynia 1 week after the final injection. Upon development of allodynia, the left hindpaw was photo-ablated using BDNF^{SNAP}-IR700 as mentioned before. Similar to the previous models, this treatment led to the recovery from allodynia starting from 3 days after photo-ablation and lasted for 22 days (Fig 20b).

5 Discussion

The sensory neurons of the DRG form a complex circuit between end organs in the skin and different laminae of the spinal cord where the signals are processed and transmitted to different brain regions (Abraira and Ginty, 2013). Injury or nerve damage causes an imbalance in this circuitry leading to neuropathic pain. Our knowledge on how the signals are processed under conditions of injury have been very limited owing to the heterogeneity of sensory afferents and the lack of molecular tools to investigate this condition. In this study, using an inducible Cre line (Feil et al., 2009) to mark a population of mechanoreceptors (TrkB) we show that, TrkB⁺ neurons mark D-hairs and A β -RA LTMR ϕ s in mice and histologically exhibit similar features in humans. We also show that DRG specific ablation of TrkB abolishes the development of mechanical allodynia after injury while specific activation of this subpopulation using channelrhodopsin produces nocifensive behavior after injury. Furthermore, we develop a novel technology to deliver phototoxic dye to TrkB afferents in the skin to reverse mechanical allodynia in different neuropathic pain states.

5.1 TrkB is expressed in LTMR subsets

The sensory neurons within the DRG form a heterogeneous mixture with different physiological properties. Developmental studies have shown that almost all DRG neurons express one or a combination of receptor tyrosine kinases, mainly TrkA, TrkB, TrkC and Ret (Lallemend and Ernfors, 2012). The advent of genetic manipulation techniques has facilitated the study of the molecular and functional characteristics of these neurons individually (Li et al., 2011). In this aspect, one of the least understood subset is the TrkB⁺ neurons in the DRG. So in order to elucidate the stimulus-response properties of these neurons, the Heppenstall lab had generated a TrkB^{CreERT2} mouse line. TrkB^{CreERT2} was found to be expressed in ~10% of all DRG

neurons and co-labelled a common marker of myelinated mechanoreceptors; NF200 and interestingly 40% of all TrkB⁺ neurons also co-expressed Ret, a marker for a subset of myelinated A β -mechanoreceptor (Luo et al., 2009). Analysis on the peripheral and central projections of TrkB afferents revealed features of mechanoreceptors including labelling of lanceolate endings on hair follicles, innervations of Meissner δ corpuscles on the glabrous skin and terminations within laminae III/IV of the dorsal horn of the spinal cord. Moreover, using an ex-vivo skin nerve preparation coupled to optogenetic activation of TrkB afferents, we show that TrkB marks all A δ -LTMR δ (also known as D-hairs) and RA A β -LTMR δ . Our results in accordance with previous studies (Li et al., 2011, Wende et al., 2012b) establish that TrkB⁺ neurons are indeed myelinated LTMR δ .

We also extrapolated on these results to test the expression of TrkB in human tissues. Staining human DRG sections with an antibody against TrkB and other neurochemical markers revealed that all TrkB neurons also co-expressed NF200 and a reasonable fraction of cells were also Ret⁺. Similarly, staining of TrkB on the glabrous skin obtained from the palm labelled Meissner δ corpuscles. Since very little co-localization was seen with nociceptive markers in the DRG and skin, we can deduce that the histological profile of TrkB⁺ neurons is the same in mice and humans. But due to inaccessibility to hairy skin, the labeling of TrkB in human hair follicles remains elusive.

5.2 TrkB⁺ neurons are required to detect gentle mechanical stimuli

Microneurography and electrophysiological experiments in rodents, primates and humans show mechanoreceptors innervating different end organs in the skin to perform varied functions. While hairy skin mechanoreceptors detect movement of hair by brushing or a gentle breeze across the skin, glabrous skin mechanoreceptors perform more unique tactile functions

depending on the end-organs (Brown and Iggo, 1967). In contrast to testing pain in mice, inadequate methods to assay gentle touch have hampered progress in understanding tactile acuity of these structures in the skin. In our study, using established behavior tests, evaluation of the sensory deficits in $\text{TrkB}^{\text{CreERT2}}$ mice upon DRG specific ablation of TrkB neurons using Diphtheria toxin receptor driven from the Advilin locus (Stantcheva et al., 2016), revealed no differences in responses to noxious heat or cold and pricking of the paw using a pin. Our results also show that ablated mice exhibited no difference in awareness to a tape stuck on the back of the neck or in their ability to grip onto a grid. However, a reduction in the ability of ablated mice to respond to brushing of the hind-paw with a puffed-out cotton swab suggested the role of TrkB^+ neurons in detecting light mechanical force. This was in agreement with the electrophysiological recordings from the skin which required very low von Frey filaments to activate TrkB^+ afferents. The cotton-swab test however is considered arbitrary in many cases as the exact force acting on the skin can vary between trials. Since using a heavier set of bristles produced a paw withdrawal response in both sets of mice, we are forced to hypothesize that the force applied by the cotton-swab are fine enough to not be recognized in TrkB ablated mice. In the above mentioned experiments, most of the behavior tests (barring the tape-test) have been limited to the plantar side of the hind-paw. One question that pertains is the role of TrkB^+ neurons innervating the hair. It was suggested as early as the 1940s that the slightest movement using a cotton-bristle which represents sensations of tickle or gentle blowing of air within a receptive field were enough to activate D-hairs (Zotterman, 1939). Recently, using in-vivo electrophysiology and single hair manipulation techniques, Ginty and colleagues showed that D-hairs are sensitive to deflection in the caudal-to-rostral direction due to the concentration of TrkB^+ innervations in the caudal side of the hair (Rutlin et al., 2014). In lieu of these

experiments, we performed optogenetic stimulation of the back skin. Blue-light stimulation of the nape of the neck or the border of the ear using excitation parameters that produced robust action potential firing in skin-nerve experiments elicited a flicking of the ears or the head. This behavior was different from previously described wiping or itching in response to pain (Wilson et al., 2011). More detailed investigation into this behavior and better tests would be necessary to dissect out the exact role of TrkB⁺ neurons in behaving mice under naïve conditions.

5.3 TrkB⁺ neurons drive mechanical allodynia after injury

The molecular and functional characteristics of TrkB⁺ neurons along with several lines of evidence indicating a role for myelinated mechanoreceptors in mediating allodynia, makes this subset of neurons a key candidate in neuropathic pain. In the first set of experiments, using CFA induced inflammation of the skin we found that ablation of TrkB⁺ neurons had no effect on the development of allodynia or primary hyperalgesia. Similarly, channelrhodopsin mediated activation of the injured hind-paw did not result in any pain like behavior in mice. Detailed studies on different models of neuropathic pain (as mentioned in 2.8.5) place the SNI model as the closest reflection of clinical states as the inflammatory component left behind after injury is bare minimal (Pertin et al., 2012). So utilizing the SNI model, in a second approach we show that ablation of TrkB⁺ neurons abolished the development of mechanical allodynia to both punctate and dynamic mechanical stimuli after injury. This suggests a role for TrkB⁺ neurons in maintaining allodynia states. In an attempt to understand if these neurons are solely required to maintain allodynia or can directly transmit pain after injury, we tested optogenetic activation of the hind-paw of TrkB^{CreERT2}::Rosa26^{Chr2} mice. Surprisingly, blue-light activation of the injured hind-paw resulted in strong nocifensive behavior as visualized by prolonged paw withdrawal,

flicking and licking of the paw. Taken together our results confirm that TrkB⁺ neurons are necessary and sufficient to drive allodynia after nerve injury.

Two key questions arise from our findings:

1. What is the mechanism behind touch sensing neurons transmitting pain after an injury?
Or in other words what is the mechanism of mechanical allodynia?
2. Having found the population of mechano-sensory neurons mediating allodynia, would selective targeting of these neurons hold the key to the rescue of pain?

There is general acceptance in the field that allodynia is a result of changes within the dorsal horn of the spinal cord in which myelinated LTMRs which terminate in Lamina III/IV gain access to pain projection neurons in lamina I. It was initially proposed that this phenomenon was due to sprouting of A β and A δ -LTMR afferents from lamina III into lamina II two weeks after peripheral nerve injury (Woolf et al., 1992). This was contradicted by others claiming that the method used by Woolf *et al.*, also labels C-fibers following nerve damage (Mannion et al., 1996). It is now believed to materialize through a complex disinhibition of interneurons within laminae III/IV (Duan et al., 2014, Foster et al., 2015, Peirs et al., 2015). Therefore using c-fos labelling in the spinal cord we followed up on this theory. Optogenetic activation of TrkB⁺ afferents in the hind-paw of naïve mice induced c-fos activity in lamina III/IV. Interestingly, similar activation of injured hind-paw produced increased c-fos labeling within lamina I. Understanding the mechanism of inhibition and the interneurons involved would require further investigation.

5.4 BDNF^{SNAP} as a therapeutic molecule for allodynia in mice

One of the common approaches to reduce neuropathic pain is the use of anti-inflammatory drugs such as aspirin or ibuprofen. More complex neuropathic pain states have heavily relied on the analgesic effects of opioids (like morphine and oxycodone), cannabinoids and tricyclic antidepressants (TCA) (Attal and Bouhassira, 2015, Dworkin et al., 2010). These drugs have limited effectiveness and larger side-effects with less than 50% of patients benefitting from medication. The cutaneous receptors in the skin have been the testing ground for several therapeutic targets. Three particularly interesting studies influenced our next approach of blocking pain at the periphery.

1. Development of monoclonal anti-NGF antibodies (Tanezumab) on the basis that NGF and its receptor TrkA play important roles in several chronic pain states such as osteoarthritis, lower back pain etc., supported by evidence of pain insensitivity in patients with specific mutations in genes encoding for TrkA (Hefti et al., 2006, Rittner et al., 2008).
2. Targeting inhibitory opsins to nociceptive neurons via viral injections to block pain in mice upon exposure to light (Iyer et al., 2014, Daou et al., 2016)
3. A potential cancer therapy using near infrared photosensitizers (IR700) conjugated to monoclonal antibodies to human epidermal growth factor receptors (HER1/HER2) (Mitsunaga et al., 2011).

Having previously found a paradoxical role for TrkB⁺ neurons in mechanical allodynia, we asked if depleting TrkB⁺ afferents in the skin would help in blocking mechanical allodynia. And to answer this question, we designed a photo-therapeutic method based on BDNF to perform ligand mediated laser ablation. Primary to the approach was the production of BDNF^{SNAP}. With the help

of collaborators at the Protein expression facility at EPFL, Lausanne, we designed a recombinant BDNF tagged with a Snap-tag protein (BDNF^{SNAP}) in an attempt to target neurons expressing TrkB.

We first validated the specificity of BDNF^{SNAP} by labelling HEK293T cells and DRG δ in-vitro. BDNF^{SNAP} bound to HEK293T cells transfected with TrkB/p75 while there was no evident labelling in cells transfected with TrkA/p75 or TrkC/p75. Similarly in dissociated DRG neurons from TrkB^{CreERT2}::Rosa26^{RFP} mice, BDNF^{SNAP} labelling was mainly restricted to RFP⁺ cells. Second, we made use of a modified version of a phototoxic dye (IRDye®700DX) containing a benzyl guanine moiety (BG-PEG11-NH₂) which was made by Kai Johnsson at EPFL, Lausanne. BDNF^{SNAP} was coupled to BG-IR700 and applied the mixture onto HEK293T cells and exposed the cells to near-infrared light. Staining the cells for propidium iodide (PI), a marker of cellular apoptosis, we were able to deduce that BDNF^{SNAP}-IR700 mixture is capable of causing cellular death specifically in HEK293T cells over-expressing TrkB receptors.

We were also able to achieve ablation of TrkB⁺ afferents in the skin following local photo-ablation as seen by the loss of fibers in the TrkB^{CreERT2}::Rosa26^{SnapCaaX} mice. A deeper look into the skin revealed that photo-ablation causes a site specific retraction of TrkB⁺ fibers that reappear after 20-25 days. Behavior testing of mice upon photo-ablation of TrkB⁺ afferents revealed no differences in responses to noxious thermal and mechanical stimuli in comparison with un-ablated controls. Surprisingly, in contrast to genetic ablation using diphtheria toxin, we did not see a reduction in responses to brushing of the skin with a cotton swab. One plausible explanation to this could be the area of ablation being smaller than the region brushed resulting in activation of intact afferents.

5.5 BDNF^{SNAP} mediated photo-ablation reverses mechanical allodynia

The specificity of BDNF^{SNAP} to TrkB receptors and the above established photo-ablation paradigm prompted us use to this technique in an attempt to alleviate mechanical allodynia. Once again using the SNI model of neuropathic pain, we show that photo-ablation of the injured paw of mice resulted in increased mechanical thresholds to both punctate and dynamic mechanical stimuli in a concentration and illumination specific manner. This rescue from allodynia lasted for two weeks before allodynia reappeared correlating with the histological findings of re-innervations of the skin. This intrigued us to take a step forward and test the efficacy of this technology other clinically important models of neuropathic pain. Remarkably, we also show that this technology can be used to rescue allodynia arising from pain diabetic neuropathy and chemotherapy induced neuropathic pain. These results taken together not only identify the neurons that relay mechanical allodynia, but also describe a novel site specific approach to treat allodynia arising from different pathological conditions.

5.6 Future perspectives

Previously, we established that genetic ablation of TrkB⁺ neurons using diphtheria toxin affected the ability of mice to detect gentle mechanical stimulation of the paw using a cotton swab correlating with our electrophysiology data that the force required to activate TrkB⁺ afferents in a skin-nerve preparation is extremely low. Studies in humans and mice suggest that the light mechanical stimulation of the skin causes a type of itch referred to as mechanical itch. This behavior is seen particularly upon stimulation of vellus hairs (Fukuoka et al., 2013, Bourane et al., 2015). Considering the similarities between vellus hairs and D-hairs, and encouraged by the fluttering-like responses to optogenetic stimulation of the back skin, we are currently designing a behavior paradigm to test touch evoked itching as a functional correlate of light

touch. A role for TrkB⁺ neurons in mechanical itch could potentially help preventing ~~alloknesis~~ a form of mechanical itch that accompanies chronic itch conditions and lasts much after its treatment.

The molecular characterization of TrkB⁺ sensory neurons revealed expression in D-hairs and RA-A β fibers. One of the many questions that rise from the mechanical allodynia phenotype is; do both the subpopulations (D-hairs and A β -LTMR \emptyset) contribute to allodynia? To address this question we plan to take two approaches to selectively ablate one of the two populations. In the first set of experiments we will use a NT-4^{-/-} mice (obtained from Gary Lewin, MDC Berlin) in which all D-hairs are lost in adults (Stucky et al., 1998). Behavior testing for mechanical allodynia in these mice before and after the loss of D-hairs would help clarifying the role of A δ -LTMR \emptyset in neuropathic pain. In the second set of experiments, we will cross TrkB^{CreERT2}::Rosa26^{SnapCaaX} mice to Ret^{EGFP/EGFP} homozygous mice (Jain et al., 2006) to generate (TrkB^{CreERT2}::Rosa26^{SnapCaaX}::Ret^{EGFP/EGFP}) triple transgenic mice under the hypothesis that TrkB⁺/Ret⁺ neurons form A β -LTMR \emptyset (Luo et al., 2009, Bourane et al., 2009). Administration of tamoxifen to this line should result in condition knock-out of the Ret locus resulting in selective ablation of TrkB⁺/Ret⁺ neurons enabling us to evaluate the role of A β -LTMR \emptyset in mechanical allodynia.

Throughout the thesis, the mention of central sensitization has been repeated under different contexts. Electrophysiological recordings by several labs across the globe using in-vivo and in-vitro techniques constantly find presynaptic currents from A-fiber mechanoreceptors in dorsal horn inhibitory interneurons. A loss in the inhibitory control following nerve injury results in primary afferent fibers accessing nociceptive pathways. Markers for many inhibitory

interneurons subtypes have been identified in recent years (Braz et al., 2012, Foster et al., 2015, Duan et al., 2014, Peirs et al., 2015). It is now evident from these studies that touch sensing neurons can synapse onto GABAergic or glycinergic inhibitory interneurons some of which can be marked by Dynorphin or to VGlut3⁺ excitatory interneurons which are under inhibitory control under basal conditions or to PKC γ neurons. But to what extent the A-fibers regulate different interneurons and the identity of all interneurons that participate in allodynia is still uncertain. We strongly believe this can be solved using our TrkB^{CreERT2} mouse line. Monosynaptic virus tracing techniques or C-fos labelling can be used to identify the interneurons that receive A δ and A β -LTMR terminations on activation of TrkB using TrkB^{CreERT2}::Rosa26^{ChR2-YFP} mice. Electrophysiological recordings on spinal cord interneurons or projection neurons after injury upon ablation and optogenetic/pharmaco-genetic activation of TrkB⁺ afferents would help resolve the mechanism underlying allodynia. This in combination with behavioral tests would help map the central circuits involved in different pathological pain conditions.

Apart from spinal cord mechanisms, alteration in gene expression in injured neurons could be the cause for long lasting neuropathic pain. Our TrkB^{CreERT2} mouse line gives us a good tool to study the changes in gene expression in TrkB⁺ neurons following nerve injury. To this end we have setup a RNA sequencing protocol in which a small number of TrkB⁺ cells (5-10) are manually picked using a patch pipette (Fig 21), snap frozen and sent to the Genomics core facility in EMBL, Heidelberg for RNA sequencing. Analysis of the results from this experiment could shed light onto some of the peripheral and presynaptic mechanisms underlying mechanical allodynia.

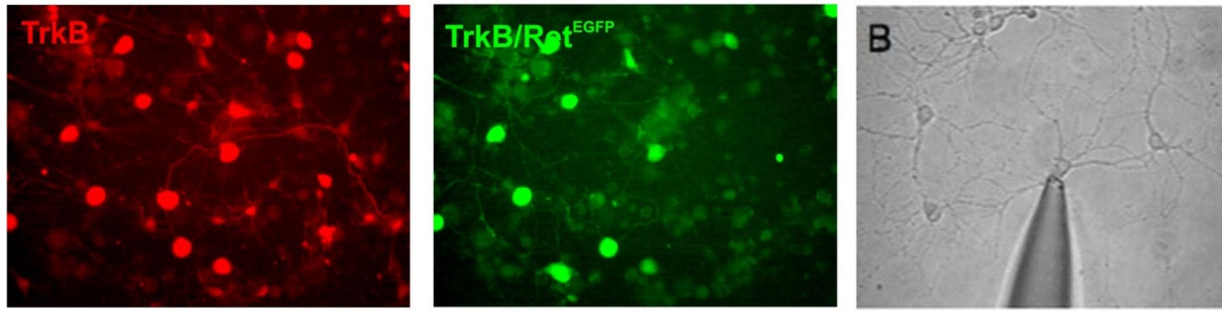


Figure 21: Manual picking of cells for sequencing

Manual picking of dissociated DRG ϕ s from TrkB^{CreERT2}::Rosa26^{SnapCaaX}::Ret^{EGFP} triple transgenic mice.

Additionally, we would also like to focus our attention in understanding the mechanism behind ablation using BDNF^{SNAP}-IR700. We have shown proof of retraction and re-innervation of fibers following photo-ablation in TrkB^{CreERT2}::Rosa26^{SnapCaaX} mice. Expression of TrkB and BDNF has been found in non-neuronal cells including keratinocytes, mast cells, immune system cells etc. (Shibayama and Koizumi, 1996) and in macrophages that accompanies nerve injury or inflammation. Even though we do not observe dramatic behavior deficit upon ablation, it will be of importance to study the impact of photo-ablation of other cell types in the skin and their contribution to the observed phenotype especially considering the pharmaco-therapeutic prospects of our approach. One interesting idea to answer this issue would be to undertake *in-vivo* high speed deep tissue imaging of photoablation in live skin tissues from BG-substrate labelled TrkB^{CreERT2}::Rosa26^{SnapCaaX} mice. The re-innervation of nerves after ablation posts potentially interesting questions: Do the nerves innervate the correct end-organs? What directs them into the same location? And are these afferents physiologically the same as before? We plan to conduct detailed histological analysis of the re-innervation and skin-nerve recordings to answer these questions.

6 Conclusion

We have managed to find a crucial element of the somatosensory circuit involved in neuropathic pain and developed a new technology based on ligand mediated ablation of nerve fibers to rescue this pain state.

In conclusion,

1. TrkB is expressed in 10% of all DRG neurons and exhibit characteristics of low threshold mechanoreceptors, specifically D-hairs and RA A β -fibers.
2. DRG specific ablation of TrkB⁺ neurons reduces responses to gentle touch
3. TrkB ablated mice fail to develop mechanical allodynia while activating the same induces pain after injury.
4. Local photo-ablation of TrkB⁺ afferents using a combination of BDNF^{SNAP}-IR700 rescues allodynia in several neuropathic pain states

Finally, I hope the contribution made through this work will serve useful to the scientific community in understanding and developing new drugs to treat some aspects of the disease of neuropathic pain.

7 References

- ABDO, H., LI, L., LALLEMEND, F., BACHY, I., XU, X. J., RICE, F. L. & ERNFORS, P. 2011. Dependence on the transcription factor Shox2 for specification of sensory neurons conveying discriminative touch. *Eur J Neurosci*, 34, 1529-41.
- ABRAHAMSEN, B., ZHAO, J., ASANTE, C. O., CENDAN, C. M., MARSH, S., MARTINEZ-BARBERA, J. P., NASSAR, M. A., DICKENSON, A. H. & WOOD, J. N. 2008. The cell and molecular basis of mechanical, cold, and inflammatory pain. *Science*, 321, 702-5.
- ABRAIRA, V. E. & GINTY, D. D. 2013. The sensory neurons of touch. *Neuron*, 79, 618-39.
- ALESSANDRI-HABER, N., DINA, O. A., YEH, J. J., PARADA, C. A., REICHLING, D. B. & LEVINE, J. D. 2004. Transient receptor potential vanilloid 4 is essential in chemotherapy-induced neuropathic pain in the rat. *J Neurosci*, 24, 4444-52.
- ALLOUI, A., ZIMMERMANN, K., MAMET, J., DUPRAT, F., NOEL, J., CHEMIN, J., GUY, N., BLONDEAU, N., VOILLEY, N., RUBAT-COUDERT, C., BORSOTTO, M., ROMÉY, G., HEURTEAUX, C., REEH, P., ESCHALIER, A. & LAZDUNSKI, M. 2006. TREK-1, a K⁺ channel involved in polymodal pain perception. *Embo j*, 25, 2368-76.
- ATTAL, N. & BOUHASSIRA, D. 2015. Pharmacotherapy of neuropathic pain: which drugs, which treatment algorithms? *PAIN*, 156, S104-S114.
- BAI, L., LEHNERT, B. P., LIU, J., NEUBARTH, N. L., DICKENDESHER, T. L., NWE, P. H., CASSIDY, C., WOODBURY, C. J. & GINTY, D. D. 2015. Genetic Identification of an Expansive Mechanoreceptor Sensitive to Skin Stroking. *Cell*, 163, 1783-95.
- BALASUBRAMANIAN, S., MATASCI, M., KADLECOVA, Z., BALDI, L., HACKER, D. L. & WURM, F. M. 2015. Rapid recombinant protein production from piggyBac transposon-mediated stable CHO cell pools. *J Biotechnol*, 200, 61-9.
- BARDONI, R., TAWFIK, V. L., WANG, D., FRANCOIS, A., SOLORZANO, C., SHUSTER, S. A., CHOUDHURY, P., BETELLI, C., CASSIDY, C., SMITH, K., DE NOOIJ, J. C., MENNICKEN, F., O'DONNELL, D., KIEFFER, B. L., WOODBURY, C. J., BASBAUM, A. I., MACDERMOTT, A. B. & SCHERRER, G. 2014. Delta opioid receptors presynaptically regulate cutaneous mechanosensory neuron input to the spinal cord dorsal horn. *Neuron*, 81, 1312-27.
- BASBAUM, A. I. 1999. Distinct neurochemical features of acute and persistent pain. *Proc Natl Acad Sci U S A*, 96, 7739-43.
- BASBAUM, A. I., BAUTISTA, D. M., SCHERRER, G. & JULIUS, D. 2009. Cellular and molecular mechanisms of pain. *Cell*, 139, 267-84.
- BATTI, L., SUNDUKOVA, M., MURANA, E., PIMPINELLA, S., DE CASTRO REIS, F., PAGANI, F., WANG, H., PELLEGRINO, E., PERLAS, E., DI ANGELANTONIO, S., RAGOZZINO, D. & HEPPESTALL, P. A. 2016. TMEM16F Regulates Spinal Microglial Function in Neuropathic Pain States. *Cell Rep*, 15, 2608-15.
- BAUTISTA, D. M., JORDT, S. E., NIKAI, T., TSURUDA, P. R., READ, A. J., POBLETE, J., YAMOA, E. N., BASBAUM, A. I. & JULIUS, D. 2006. TRPA1 mediates the inflammatory actions of environmental irritants and proalgesic agents. *Cell*, 124, 1269-82.
- BAUTISTA, D. M., SIGAL, Y. M., MILSTEIN, A. D., GARRISON, J. L., ZORN, J. A., TSURUDA, P. R., NICOLL, R. A. & JULIUS, D. 2008. Pungent agents from Szechuan

- peppers excite sensory neurons by inhibiting two-pore potassium channels. *Nat Neurosci*, 11, 772-9.
- BENNETT, G. J. & XIE, Y. K. 1988. A peripheral mononeuropathy in rat that produces disorders of pain sensation like those seen in man. *Pain*, 33, 87-107.
- BOURANE, S., DUAN, B., KOCH, S. C., DALET, A., BRITZ, O., GARCIA-CAMPMANY, L., KIM, E., CHENG, L., GHOSH, A., MA, Q. & GOULDING, M. 2015. Gate control of mechanical itch by a subpopulation of spinal cord interneurons. *Science*, 350, 550-4.
- BOURANE, S., GARCES, A., VENTEO, S., PATTYN, A., HUBERT, T., FICHARD, A., PUECH, S., BOUKHADDAOUI, H., BAUDET, C., TAKAHASHI, S., VALMIER, J. & CARROLL, P. 2009. Low-threshold mechanoreceptor subtypes selectively express MafA and are specified by Ret signaling. *Neuron*, 64, 857-70.
- BRAZ, J., SOLORZANO, C., WANG, X. & BASBAUM, A. I. 2014. Transmitting pain and itch messages: a contemporary view of the spinal cord circuits that generate gate control. *Neuron*, 82, 522-36.
- BRAZ, J. M., SHARIF-NAEINI, R., VOGT, D., KRIEGSTEIN, A., ALVAREZ-BUYLLA, A., RUBENSTEIN, J. L. & BASBAUM, A. I. 2012. Forebrain GABAergic neuron precursors integrate into adult spinal cord and reduce injury-induced neuropathic pain. *Neuron*, 74, 663-75.
- BRENNER, D. S., GOLDEN, J. P. & GEREAU, R. W. T. 2012. A novel behavioral assay for measuring cold sensation in mice. *PLoS One*, 7, e39765.
- BRIDGES, D., THOMPSON, S. W. & RICE, A. S. 2001. Mechanisms of neuropathic pain. *Br J Anaesth*, 87, 12-26.
- BRISBEN, A. J., HSIAO, S. S. & JOHNSON, K. O. 1999. Detection of vibration transmitted through an object grasped in the hand. *J Neurophysiol*, 81, 1548-58.
- BROWN, A. G. & IGGO, A. 1967. A quantitative study of cutaneous receptors and afferent fibres in the cat and rabbit. *J Physiol*, 193, 707-33.
- BRUN, M. A., TAN, K. T., NAKATA, E., HINNER, M. J. & JOHNSON, K. 2009. Semisynthetic fluorescent sensor proteins based on self-labeling protein tags. *J Am Chem Soc*, 131, 5873-84.
- BURGESS, P. R., PETIT, D. & WARREN, R. M. 1968. Receptor types in cat hairy skin supplied by myelinated fibers. *J Neurophysiol*, 31, 833-48.
- CAMPBELL, J. N., RAJA, S. N., MEYER, R. A. & MACKINNON, S. E. 1988. Myelinated afferents signal the hyperalgesia associated with nerve injury. *Pain*, 32, 89-94.
- CARROLL, P. 1998. Role for BDNF in mechanosensation.pdf. *Nature*, volume 1.
- CATERINA, M. J., LEFFLER, A., MALMBERG, A. B., MARTIN, W. J., TRAFTON, J., PETERSEN-ZEITZ, K. R., KOLTZENBURG, M., BASBAUM, A. I. & JULIUS, D. 2000. Impaired nociception and pain sensation in mice lacking the capsaicin receptor. *Science*, 288, 306-13.
- CATERINA, M. J., SCHUMACHER, M. A., TOMINAGA, M., ROSEN, T. A., LEVINE, J. D. & JULIUS, D. 1997. The capsaicin receptor: a heat-activated ion channel in the pain pathway. *Nature*, 389, 816-24.
- CAUNA, N. 1956. Nerve supply and nerve endings in Meissner's corpuscles. *Am J Anat*, 99, 315-50.
- CAVANAUGH, D. J., LEE, H., LO, L., SHIELDS, S. D., ZYLKA, M. J., BASBAUM, A. I. & ANDERSON, D. J. 2009. Distinct subsets of unmyelinated primary sensory fibers

- mediate behavioral responses to noxious thermal and mechanical stimuli. *Proc Natl Acad Sci U S A*, 106, 9075-80.
- CHAMBERS, M. R., ANDRES, K. H., VON DUERING, M. & IGGO, A. 1972. The structure and function of the slowly adapting type II mechanoreceptor in hairy skin. *Q J Exp Physiol Cogn Med Sci*, 57, 417-45.
- CHANG, D. S., HSU, E., HOTTINGER, D. G. & COHEN, S. P. 2016. Anti-nerve growth factor in pain management: current evidence. *J Pain Res*, 9, 373-83.
- CHAPLAN, S. R., BACH, F. W., POGREL, J. W., CHUNG, J. M. & YAKSH, T. L. 1994. Quantitative assessment of tactile allodynia in the rat paw. *J Neurosci Methods*, 53, 55-63.
- CHOI, Y., YOON, Y. W., NA, H. S., KIM, S. H. & CHUNG, J. M. 1994. Behavioral signs of ongoing pain and cold allodynia in a rat model of neuropathic pain. *Pain*, 59, 369-76.
- CHRISTENSEN, A. P. & COREY, D. P. 2007. TRP channels in mechanosensation: direct or indirect activation? *Nat Rev Neurosci*, 8, 510-21.
- COSTE, B., MATHUR, J., SCHMIDT, M., EARLEY, T. J., RANADE, S., PETRUS, M. J., DUBIN, A. E. & PATAPOUTIAN, A. 2010. Piezo1 and Piezo2 are essential components of distinct mechanically activated cation channels. *Science*, 330, 55-60.
- COSTE, B., XIAO, B., SANTOS, J. S., SYEDA, R., GRANDL, J., SPENCER, K. S., KIM, S. E., SCHMIDT, M., MATHUR, J., DUBIN, A. E., MONTAL, M. & PATAPOUTIAN, A. 2012. Piezo proteins are pore-forming subunits of mechanically activated channels. *Nature*, 483, 176-81.
- COULL, J. A., BEGGS, S., BOUDREAU, D., BOIVIN, D., TSUDA, M., INOUE, K., GRAVEL, C., SALTER, M. W. & DE KONINCK, Y. 2005. BDNF from microglia causes the shift in neuronal anion gradient underlying neuropathic pain. *Nature*, 438, 1017-21.
- COULL, J. A., BOUDREAU, D., BACHAND, K., PRESCOTT, S. A., NAULT, F., SIK, A., DE KONINCK, P. & DE KONINCK, Y. 2003. Trans-synaptic shift in anion gradient in spinal lamina I neurons as a mechanism of neuropathic pain. *Nature*, 424, 938-42.
- COX, J. J., REIMANN, F., NICHOLAS, A. K., THORNTON, G., ROBERTS, E., SPRINGELL, K., KARBANI, G., JAFRI, H., MANNAN, J., RAASHID, Y., AL-GAZALI, L., HAMAMY, H., VALENTE, E. M., GORMAN, S., WILLIAMS, R., MCHALE, D. P., WOOD, J. N., GRIBBLE, F. M. & WOODS, C. G. 2006. An SCN9A channelopathy causes congenital inability to experience pain. *Nature*, 444, 894-8.
- DALLENBACH, K. M. 1939. Pain: History and Present Status.
- DAMANN, N., VOETS, T. & NILIUS, B. 2008. TRPs in our senses. *Curr Biol*, 18, R880-9.
- DAOU, I., BEAUDRY, H., ASE, A. R., WIESKOPF, J. S., RIBEIRO-DA-SILVA, A., MOGIL, J. S. & SEGUELA, P. 2016. Optogenetic Silencing of Nav1.8-Positive Afferents Alleviates Inflammatory and Neuropathic Pain. *eNeuro*, 3.
- DAVIS, J. B., GRAY, J., GUNTHORPE, M. J., HATCHER, J. P., DAVEY, P. T., OVEREND, P., HARRIES, M. H., LATCHAM, J., CLAPHAM, C., ATKINSON, K., HUGHES, S. A., RANCE, K., GRAU, E., HARPER, A. J., PUGH, P. L., ROGERS, D. C., BINGHAM, S., RANDALL, A. & SHEARDOWN, S. A. 2000. Vanilloid receptor-1 is essential for inflammatory thermal hyperalgesia. *Nature*, 405, 183-7.
- DECOSTERD, I. & WOOLF, C. J. 2000. Spared nerve injury: an animal model of persistent peripheral neuropathic pain. *Pain*, 87, 149-58.

- DELFINI, M. C., MANTILLERI, A., GAILLARD, S., HAO, J., REYNDERS, A., MALAPERT, P., ALONSO, S., FRANCOIS, A., BARRERE, C., SEAL, R., LANDRY, M., ESCHALLIER, A., ALLOUI, A., BOURINET, E., DELMAS, P., LE FEUVRE, Y. & MOQRICH, A. 2013. TFAFA4, a chemokine-like protein, modulates injury-induced mechanical and chemical pain hypersensitivity in mice. *Cell Rep*, 5, 378-88.
- DONG, X., HAN, S., ZYLKA, M. J., SIMON, M. I. & ANDERSON, D. J. 2001. A diverse family of GPCRs expressed in specific subsets of nociceptive sensory neurons. *Cell*, 106, 619-32.
- DUAN, B., CHENG, L., BOURANE, S., BRITZ, O., PADILLA, C., GARCIA-CAMPMANY, L., KRASHES, M., KNOWLTON, W., VELASQUEZ, T., REN, X., ROSS, S. E., LOWELL, B. B., WANG, Y., GOULDING, M. & MA, Q. 2014. Identification of spinal circuits transmitting and gating mechanical pain. *Cell*, 159, 1417-32.
- DWORKIN, R. H., O'CONNOR, A. B., AUDETTE, J., BARON, R., GOURLAY, G. K., HAANPÄÄ, M. L., KENT, J. L., KRANE, E. J., LEBEL, A. A., LEVY, R. M., MACKAY, S. C., MAYER, J., MIASKOWSKI, C., RAJA, S. N., RICE, A. S. C., SCHMADER, K. E., STACEY, B., STANOS, S., TREEDE, R. D., TURK, D. C., WALCO, G. A. & WELLS, C. D. 2010. Recommendations for the Pharmacological Management of Neuropathic Pain: An Overview and Literature Update. *Mayo Clin Proc*, 85, S3-s14.
- DWORKIN, R. H., O'CONNOR, A. B., BACKONJA, M., FARRAR, J. T., FINNERUP, N. B., JENSEN, T. S., KALSO, E. A., LOESER, J. D., MIASKOWSKI, C., NURMIKKO, T. J., PORTENOY, R. K., RICE, A. S., STACEY, B. R., TREEDE, R. D., TURK, D. C. & WALLACE, M. S. 2007. Pharmacologic management of neuropathic pain: evidence-based recommendations. *Pain*, 132, 237-51.
- ELIAV, E., HERZBERG, U., RUDA, M. A. & BENNETT, G. J. 1999. Neuropathic pain from an experimental neuritis of the rat sciatic nerve. *Pain*, 83, 169-82.
- ERNFORS, P., ROSARIO, C. M., MERLIO, J. P., GRANT, G., ALDSKOGIUS, H. & PERSSON, H. 1993. Expression of mRNAs for neurotrophin receptors in the dorsal root ganglion and spinal cord during development and following peripheral or central axotomy. *Molecular Brain Research*, 17, 217-226.
- ERNSBERGER, U. 2009. Role of neurotrophin signalling in the differentiation of neurons from dorsal root ganglia and sympathetic ganglia. *Cell Tissue Res*, 336, 349-84.
- FEIL, S., VALTCHEVA, N. & FEIL, R. 2009. Inducible Cre mice. *Methods Mol Biol*, 530, 343-63.
- FINNERUP, N. B., ATTAL, N., HAROUTOUNIAN, S., MCNICOL, E., BARON, R., DWORKIN, R. H., GILRON, I., HAANPAA, M., HANSSON, P., JENSEN, T. S., KAMERMAN, P. R., LUND, K., MOORE, A., RAJA, S. N., RICE, A. S., ROWBOTHAM, M., SENA, E., SIDDALL, P., SMITH, B. H. & WALLACE, M. 2015. Pharmacotherapy for neuropathic pain in adults: a systematic review and meta-analysis. *Lancet Neurol*, 14, 162-73.
- FLEMING, M. S., LI, J. J., RAMOS, D., LI, T., TALMAGE, D. A., ABE, S. I., ARBER, S. & LUO, W. 2016. A RET-ER81-NRG1 Signaling Pathway Drives the Development of Pacinian Corpuscles. *J Neurosci*, 36, 10337-10355.
- FOSTER, E., WILDNER, H., TUDEAU, L., HAUETER, S., RALVENIUS, W. T., JEGEN, M., JOHANNSEN, H., HOSLI, L., HAENRAETS, K., GHANEM, A., CONZELMANN, K. K., BOSL, M. & ZEILHOFER, H. U. 2015. Targeted ablation, silencing, and activation

- establish glycinergic dorsal horn neurons as key components of a spinal gate for pain and itch. *Neuron*, 85, 1289-304.
- FUKUOKA, M., MIYACHI, Y. & IKOMA, A. 2013. Mechanically evoked itch in humans. *Pain*, 154, 897-904.
- GARRISON, S. R., DIETRICH, A. & STUCKY, C. L. 2012. TRPC1 contributes to light-touch sensation and mechanical responses in low-threshold cutaneous sensory neurons. *J Neurophysiol*, 107, 913-22.
- GUAN, Z., KUHN, J. A., WANG, X., COLQUITT, B., SOLORZANO, C., VAMAN, S., GUAN, A. K., EVANS-REINSCH, Z., BRAZ, J., DEVOR, M., ABBOUD-WERNER, S. L. & LANIER, L. L. 2016. Injured sensory neuron-derived CSF1 induces microglial proliferation and DAP12-dependent pain. 19, 94-101.
- HALATA, Z., GRIM, M. & BAUMAN, K. I. 2003. Friedrich Sigmund Merkel and his "Merkel cell", morphology, development, and physiology: review and new results. *Anat Rec A Discov Mol Cell Evol Biol*, 271, 225-39.
- HEFTI, F. F., ROSENTHAL, A., WALICKE, P. A., WYATT, S., VERGARA, G., SHELTON, D. L. & DAVIES, A. M. 2006. Novel class of pain drugs based on antagonism of NGF. *Trends Pharmacol Sci*, 27, 85-91.
- HEIDENREICH, M., LECHNER, S. G., VARDANYAN, V., WETZEL, C., CREMERS, C. W., DE LEENHEER, E. M., ARANGUEZ, G., MORENO-PELAYO, M. A., JENTSCH, T. J. & LEWIN, G. R. 2011. KCNQ4 K(+) channels tune mechanoreceptors for normal touch sensation in mouse and man. *Nat Neurosci*, 15, 138-45.
- HOGGAN, G. & HOGGAN, F. E. 1893. Forked Nerve Endings on Hairs. *J Anat Physiol*, 27, 224-31.
- HUANG, E. J. & REICHARDT, L. F. 2003. Trk receptors: roles in neuronal signal transduction. *Annu Rev Biochem*, 72, 609-42.
- HUANG, M., GU, G., FERGUSON, E. L. & CHALFIE, M. 1995. A stomatin-like protein necessary for mechanosensation in *C. elegans*. *Nature*, 378, 292-5.
- IGGO, A. 1985. Sensory receptors in the skin of mammals and their sensory functions. *Rev Neurol (Paris)*, 141, 599-613.
- IGGO, A. & ANDRES, K. H. 1982. Morphology of cutaneous receptors. *Annu Rev Neurosci*, 5, 1-31.
- IGGO, A. & MUIR, A. R. 1969. The structure and function of a slowly adapting touch corpuscle in hairy skin. *J Physiol*, 200, 763-96.
- IYER, S. M., MONTGOMERY, K. L., TOWNE, C., LEE, S. Y., RAMAKRISHNAN, C., DEISSEROTH, K. & DELP, S. L. 2014. Virally mediated optogenetic excitation and inhibition of pain in freely moving nontransgenic mice. *Nat Biotechnol*, 32, 274-8.
- JAIN, S., GOLDEN, J. P., WOZNIAK, D., PEHEK, E., JOHNSON, E. M., JR. & MILBRANDT, J. 2006. RET is dispensable for maintenance of midbrain dopaminergic neurons in adult mice. *J Neurosci*, 26, 11230-8.
- JULIUS, D. & BASBAUM, A. I. 2001. Molecular mechanisms of nociception. *Nature*, 413, 203-10.
- KALEBIC, N., SORRENTINO, S., PERLAS, E., BOLASCO, G., MARTINEZ, C. & HEPPENSTALL, P. A. 2013. alphaTAT1 is the major alpha-tubulin acetyltransferase in mice. *Nat Commun*, 4, 1962.

- KILO, S., SCHMELZ, M., KOLTZENBURG, M. & HANDWERKER, H. O. 1994. Different patterns of hyperalgesia induced by experimental inflammation in human skin. *Brain*, 117 (Pt 2), 385-96.
- KIM, S. E., COSTE, B., CHADHA, A., COOK, B. & PATAPOUTIAN, A. 2012. The role of Drosophila Piezo in mechanical nociception. *Nature*, 483, 209-12.
- KIM, S. H. & CHUNG, J. M. 1992. An experimental model for peripheral neuropathy produced by segmental spinal nerve ligation in the rat. *Pain*, 50, 355-63.
- KLEIN, R., PARADA, L. F., COULIER, F. & BARBACID, M. 1989. trkB, a novel tyrosine protein kinase receptor expressed during mouse neural development. *Embo j*, 8, 3701-9.
- KOERBER, H. R. & WOODBURY, C. J. 2002. Comprehensive phenotyping of sensory neurons using an ex vivo somatosensory system. *Physiol Behav*, 77, 589-94.
- KRAMER, I., SIGRIST, M., DE NOOIJ, J. C., TANIUCHI, I., JESSELL, T. M. & ARBER, S. 2006. A role for Runx transcription factor signaling in dorsal root ganglion sensory neuron diversification. *Neuron*, 49, 379-93.
- LALLEMEND, F. & ERNFORS, P. 2012. Molecular interactions underlying the specification of sensory neurons. *Trends Neurosci*, 35, 373-81.
- LAMOTTE, R. H., LUNDBERG, L. E. & TOREBJORK, H. E. 1992. Pain, hyperalgesia and activity in nociceptive C units in humans after intradermal injection of capsaicin. *J Physiol*, 448, 749-64.
- LAPATSINA, L., JIRA, J. A., SMITH, E. S. J., POOLE, K., KOZLENKOV, A., BILBAO, D., LEWIN, G. R. & HEPPENSTALL, P. A. 2012. Regulation of ASIC channels by a stomatin/STOML3 complex located in a mobile vesicle pool in sensory neurons. *Open Biol*, 2.
- LECHNER, S. G. & LEWIN, G. R. 2013. Hairy sensation. *Physiology (Bethesda)*, 28, 142-50.
- LELE, P. P., SINCLAIR, D. C. & WEDDELL, G. 1954. The reaction time to touch. *J Physiol*, 123, 187-203.
- LI, C. Y., ZHANG, X. L., MATTHEWS, E. A., LI, K. W., KURWA, A., BOROUJERDI, A., GROSS, J., GOLD, M. S., DICKENSON, A. H., FENG, G. & LUO, Z. D. 2006. Calcium channel alpha2delta1 subunit mediates spinal hyperexcitability in pain modulation. *Pain*, 125, 20-34.
- LI, L., RUTLIN, M., ABRAIRA, V. E., CASSIDY, C., KUS, L., GONG, S., JANKOWSKI, M. P., LUO, W., HEINTZ, N., KOERBER, H. R., WOODBURY, C. J. & GINTY, D. D. 2011. The functional organization of cutaneous low-threshold mechanosensory neurons. *Cell*, 147, 1615-27.
- LIGHT, A. R. & PERL, E. R. 1979. Spinal termination of functionally identified primary afferent neurons with slowly conducting myelinated fibers. *J Comp Neurol*, 186, 133-50.
- LINGUEGLIA, E. 2007. Acid-sensing ion channels in sensory perception. *J Biol Chem*, 282, 17325-9.
- LIU, Q., VRONTOU, S., RICE, F. L., ZYLKA, M. J., DONG, X. & ANDERSON, D. J. 2007. Molecular genetic visualization of a rare subset of unmyelinated sensory neurons that may detect gentle touch. *Nat Neurosci*, 10, 946-8.
- LIU, Y. & MA, Q. 2011. Generation of somatic sensory neuron diversity and implications on sensory coding. *Curr Opin Neurobiol*, 21, 52-60.
- LIU, Y., YANG, F.-C., OKUDA, T., DONG, X., ZYLKA, M. J., CHEN, C.-L., ANDERSON, D. J., KUNER, R. & MA, Q. 2008. Mechanisms of Compartmentalized Expression of

- Mrg Class G-Protein-Coupled Sensory Receptors. *The Journal of Neuroscience*, 28, 125-132.
- LOLIGNIER, S., EIJKELKAMP, N. & WOOD, J. N. 2015. Mechanical allodynia. *Pflugers Arch*, 467, 133-9.
- LOU, S., DUAN, B., VONG, L., LOWELL, B. B. & MA, Q. 2013. Runx1 controls terminal morphology and mechanosensitivity of VGLUT3-expressing C-mechanoreceptors. *J Neurosci*, 33, 870-82.
- LU, Y., DONG, H., GAO, Y., GONG, Y., REN, Y., GU, N., ZHOU, S., XIA, N., SUN, Y. Y., JI, R. R. & XIONG, L. 2013. A feed-forward spinal cord glycinergic neural circuit gates mechanical allodynia. *J Clin Invest*, 123, 4050-62.
- LUO, W., ENOMOTO, H., RICE, F. L., MILBRANDT, J. & GINTY, D. D. 2009. Molecular identification of rapidly adapting mechanoreceptors and their developmental dependence on ret signaling. *Neuron*, 64, 841-56.
- MA, Q., FODE, C., GUILLEMOT, F. & ANDERSON, D. J. 1999. NEUROGENIN1 and NEUROGENIN2 control two distinct waves of neurogenesis in developing dorsal root ganglia. *Genes Dev*, 13, 1717-28.
- MAKSIMOVIC, S., NAKATANI, M., BABA, Y., NELSON, A. M., MARSHALL, K. L., WELLNITZ, S. A., FIROZI, P., WOO, S. H., RANADE, S., PATAPOUTIAN, A. & LUMPKIN, E. A. 2014. Epidermal Merkel cells are mechanosensory cells that tune mammalian touch receptors. *Nature*, 509, 617-21.
- MANNION, R. J., DOUBELL, T. P., COGGESHALL, R. E. & WOOLF, C. J. 1996. Collateral sprouting of uninjured primary afferent A-fibers into the superficial dorsal horn of the adult rat spinal cord after topical capsaicin treatment to the sciatic nerve. *J Neurosci*, 16, 5189-95.
- MARICICH, S. M., WELLNITZ, S. A., NELSON, A. M., LESNIAK, D. R., GERLING, G. J., LUMPKIN, E. A. & ZOGHBI, H. Y. 2009. Merkel cells are essential for light-touch responses. *Science*, 324, 1580-2.
- MARMIGERE, F. & ERNFORS, P. 2007. Specification and connectivity of neuronal subtypes in the sensory lineage. *Nat Rev Neurosci*, 8, 114-27.
- MARTINEZ-SALGADO, C., BENCKENDORFF, A. G., CHIANG, L. Y., WANG, R., MILENKOVIC, N., WETZEL, C., HU, J., STUCKY, C. L., PARRA, M. G., MOHANDAS, N. & LEWIN, G. R. 2007. Stomatin and sensory neuron mechanotransduction. *J Neurophysiol*, 98, 3802-8.
- MATASCI, M., BALDI, L., HACKER, D. L. & WURM, F. M. 2011. The PiggyBac transposon enhances the frequency of CHO stable cell line generation and yields recombinant lines with superior productivity and stability. *Biotechnol Bioeng*, 108, 2141-50.
- MCGLONE, F., WESSBERG, J. & OLAUSSON, H. 2014. Discriminative and affective touch: sensing and feeling. *Neuron*, 82, 737-55.
- MEDHURST, A. D., RENNIE, G., CHAPMAN, C. G., MEADOWS, H., DUCKWORTH, M. D., KELSELL, R. E., GLOGER, II & PANGALOS, M. N. 2001. Distribution analysis of human two pore domain potassium channels in tissues of the central nervous system and periphery. *Brain Res Mol Brain Res*, 86, 101-14.
- MELZACK, R. & WALL, P. D. 1965. Pain mechanisms: a new theory. *Science*, 150, 971-9.
- MINETT, M. S., FALK, S., SANTANA-VARELA, S., BOGDANOV, Y. D., NASSAR, M. A., HEEGAARD, A. M. & WOOD, J. N. 2014. Pain without nociceptors? Nav1.7-independent pain mechanisms. *Cell Rep*, 6, 301-12.

- MIRABEAU, O., PERLAS, E., SEVERINI, C., AUDERO, E., GASCUEL, O., POSSENTI, R., BIRNEY, E., ROSENTHAL, N. & GROSS, C. 2007. Identification of novel peptide hormones in the human proteome by hidden Markov model screening. *Genome Res*, 17, 320-7.
- MITSUMAGA, M., OGAWA, M., KOSAKA, N., ROSENBLUM, L. T., CHOYKE, P. L. & KOBAYASHI, H. 2011. Cancer cell-selective in vivo near infrared photoimmunotherapy targeting specific membrane molecules. *Nat Med*, 17, 1685-91.
- MOAYEDI, M. & DAVIS, K. D. 2013. Theories of pain: from specificity to gate control. *J Neurophysiol*, 109, 5-12.
- MOGIL, J. S., BREESE, N. M., WITTY, M. F., RITCHIE, J., RAINVILLE, M. L., ASE, A., ABBADI, N., STUCKY, C. L. & SEGUELA, P. 2005. Transgenic expression of a dominant-negative ASIC3 subunit leads to increased sensitivity to mechanical and inflammatory stimuli. *J Neurosci*, 25, 9893-901.
- MOLLIVER, D. C., WRIGHT, D. E., LEITNER, M. L., PARSADANIAN, A. S., DOSTER, K., WEN, D., YAN, Q. & SNIDER, W. D. 1997. IB4-binding DRG neurons switch from NGF to GDNF dependence in early postnatal life. *Neuron*, 19, 849-61.
- MONTANO, J. A., CALAVIA, M. G., GARCIA-SUAREZ, O., SUAREZ-QUINTANILLA, J. A., GALVEZ, A., PEREZ-PINERA, P., COBO, J. & VEGA, J. A. 2009. The expression of ENa(+)C and ASIC2 proteins in Pacinian corpuscles is differently regulated by TrkB and its ligands BDNF and NT-4. *Neurosci Lett*, 463, 114-8.
- MOSHOURAB, R. A., WETZEL, C., MARTINEZ-SALGADO, C. & LEWIN, G. R. 2013. Stomatin-domain protein interactions with acid-sensing ion channels modulate nociceptor mechanosensitivity. *J Physiol*, 591, 5555-74.
- MURAKAMI, T., IWANAGA, T., OGAWA, Y., FUJITA, Y., SATO, E., YOSHITOMI, H., SUNADA, Y. & NAKAMURA, A. 2013. Development of sensory neuropathy in streptozotocin-induced diabetic mice. *Brain Behav*, 3, 35-41.
- NASSAR, M. A., LEVATO, A., STIRLING, L. C. & WOOD, J. N. 2005. Neuropathic pain develops normally in mice lacking both Na(v)1.7 and Na(v)1.8. *Mol Pain*, 1, 24.
- NASSAR, M. A., STIRLING, L. C., FORLANI, G., BAKER, M. D., MATTHEWS, E. A., DICKENSON, A. H. & WOOD, J. N. 2004. Nociceptor-specific gene deletion reveals a major role for Nav1.7 (PN1) in acute and inflammatory pain. *Proceedings of the National Academy of Sciences of the United States of America*, 101, 12706-12711.
- NOEL, J., ZIMMERMANN, K., BUSSEROLLES, J., DEVAL, E., ALLOUI, A., DIOCHOT, S., GUY, N., BORSOTTO, M., REEH, P., ESCHALIER, A. & LAZDUNSKI, M. 2009. The mechano-activated K⁺ channels TRAAK and TREK-1 control both warm and cold perception. *Embo j*, 28, 1308-18.
- NOLANO, M., SIMONE, D. A., WENDELSCHAFFER-CRABB, G., JOHNSON, T., HAZEN, E. & KENNEDY, W. R. 1999. Topical capsaicin in humans: parallel loss of epidermal nerve fibers and pain sensation. *Pain*, 81, 135-45.
- O'BRIEN, P. D., SAKOWSKI, S. A. & FELDMAN, E. L. 2014. Mouse models of diabetic neuropathy. *ILAR J*, 54, 259-72.
- OSSIPOV, M. H., LAI, J., KING, T., VANDERAH, T. W., MALAN, T. P., JR., HRUBY, V. J. & PORRECA, F. 2004. Antinociceptive and nociceptive actions of opioids. *J Neurobiol*, 61, 126-48.

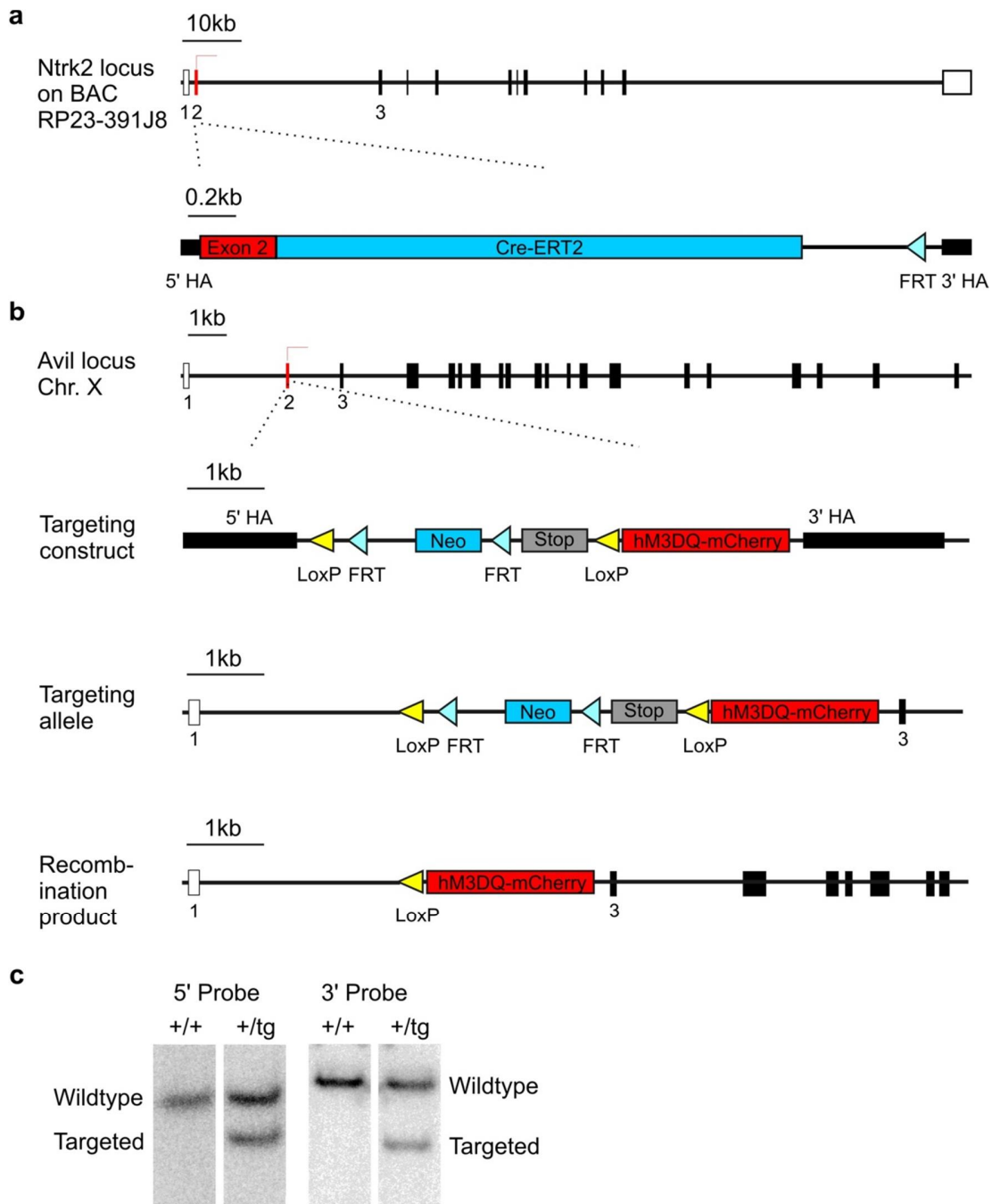
- PAGE, A. J., BRIERLEY, S. M., MARTIN, C. M., PRICE, M. P., SYMONDS, E., BUTLER, R., WEMMIE, J. A. & BLACKSHAW, L. A. 2005. Different contributions of ASIC channels 1a, 2, and 3 in gastrointestinal mechanosensory function. *Gut*, 54, 1408-15.
- PARE, M., ELDE, R., MAZURKIEWICZ, J. E., SMITH, A. M. & RICE, F. L. 2001. The Meissner corpuscle revised: a multiafferented mechanoreceptor with nociceptor immunochemical properties. *J Neurosci*, 21, 7236-46.
- PEIRS, C., WILLIAMS, S. P., ZHAO, X., WALSH, C. E., GEDEON, J. Y., CAGLE, N. E., GOLDRING, A. C., HIOKI, H., LIU, Z., MARELL, P. S. & SEAL, R. P. 2015. Dorsal Horn Circuits for Persistent Mechanical Pain. *Neuron*, 87, 797-812.
- PEREZ-PINERA, P., GARCIA-SUAREZ, O., GERMANA, A., DIAZ-ESNAL, B., DE CARLOS, F., SILOS-SANTIAGO, I., DEL VALLE, M. E., COBO, J. & VEGA, J. A. 2008. Characterization of sensory deficits in TrkB knockout mice. *Neurosci Lett*, 433, 43-7.
- PERL, E. R. 2007. Ideas about pain, a historical view. *Nat Rev Neurosci*, 8, 71-80.
- PERTIN, M., GOSSELIN, R. D. & DECOSTERD, I. 2012. The spared nerve injury model of neuropathic pain. *Methods Mol Biol*, 851, 205-12.
- PRESCOTT, S. A., MA, Q. & DE KONINCK, Y. 2014. Normal and abnormal coding of somatosensory stimuli causing pain. *Nat Neurosci*, 17, 183-91.
- PRICE, M. P., MCILWRATH, S. L., XIE, J., CHENG, C., QIAO, J., TARR, D. E., SLUKA, K. A., BRENNAN, T. J., LEWIN, G. R. & WELSH, M. J. 2001. The DRASIC cation channel contributes to the detection of cutaneous touch and acid stimuli in mice. *Neuron*, 32, 1071-83.
- QUASTHOFF, S. & HARTUNG, H. P. 2002. Chemotherapy-induced peripheral neuropathy. *J Neurol*, 249, 9-17.
- RAJA, S. N., HAYTHORNTHWAITTE, J. A., PAPPAGALLO, M., CLARK, M. R., TRAVISON, T. G., SABEEN, S., ROYALL, R. M. & MAX, M. B. 2002. Opioids versus antidepressants in postherpetic neuralgia: a randomized, placebo-controlled trial. *Neurology*, 59, 1015-21.
- RANADE, S. S., WOO, S. H., DUBIN, A. E., MOSHOURAB, R. A., WETZEL, C., PETRUS, M., MATHUR, J., BEGAY, V., COSTE, B., MAINQUIST, J., WILSON, A. J., FRANCISCO, A. G., REDDY, K., QIU, Z., WOOD, J. N., LEWIN, G. R. & PATAPOUTIAN, A. 2014. Piezo2 is the major transducer of mechanical forces for touch sensation in mice. *Nature*, 516, 121-5.
- RITTNER, H. L., BRACK, A. & STEIN, C. 2008. Pain and the immune system. *Br J Anaesth*, 101, 40-4.
- RUTLIN, M., HO, C. Y., ABRAIRA, V. E., CASSIDY, C., BAI, L., WOODBURY, C. J. & GINTY, D. D. 2014. The cellular and molecular basis of direction selectivity of Adelta-LTMRs. *Cell*, 159, 1640-51.
- SCHERRER, G., IMAMACHI, N., CAO, Y. Q., CONTET, C., MENNICKEN, F., O'DONNELL, D., KIEFFER, B. L. & BASBAUM, A. I. 2009. Dissociation of the opioid receptor mechanisms that control mechanical and heat pain. *Cell*, 137, 1148-59.
- SCHMIDT, R., SCHMELZ, M., FORSTER, C., RINGKAMP, M., TOREBJORK, E. & HANDWERKER, H. 1995. Novel classes of responsive and unresponsive C nociceptors in human skin. *J Neurosci*, 15, 333-41.
- SCHNITZER, T. J., EKMAN, E. F., SPIERINGS, E. L., GREENBERG, H. S., SMITH, M. D., BROWN, M. T., WEST, C. R. & VERBURG, K. M. 2015. Efficacy and safety of

- tanezumab monotherapy or combined with non-steroidal anti-inflammatory drugs in the treatment of knee or hip osteoarthritis pain. *Ann Rheum Dis*, 74, 1202-11.
- SCOTT, A., HASEGAWA, H., SAKURAI, K., YARON, A., COBB, J. & WANG, F. 2011. Transcription factor short stature homeobox 2 is required for proper development of tropomyosin-related kinase B-expressing mechanosensory neurons. *J Neurosci*, 31, 6741-9.
- SEAL, R. P., WANG, X., GUAN, Y., RAJA, S. N., WOODBURY, C. J., BASBAUM, A. I. & EDWARDS, R. H. 2009. Injury-induced mechanical hypersensitivity requires C-low threshold mechanoreceptors. *Nature*, 462, 651-5.
- SELTZER, Z., DUBNER, R. & SHIR, Y. 1990. A novel behavioral model of neuropathic pain disorders produced in rats by partial sciatic nerve injury. *Pain*, 43, 205-18.
- SHERRINGTON, C. S. 1903. Qualitative difference of spinal reflex corresponding with qualitative difference of cutaneous stimulus. *J Physiol*, 30, 39-46.
- SHIBAYAMA, E. & KOIZUMI, H. 1996. Cellular localization of the Trk neurotrophin receptor family in human non-neuronal tissues. *Am J Pathol*, 148, 1807-18.
- SHIN, J. B., MARTINEZ-SALGADO, C., HEPPENSTALL, P. A. & LEWIN, G. R. 2003. A T-type calcium channel required for normal function of a mammalian mechanoreceptor. *Nat Neurosci*, 6, 724-30.
- SHU, X. Q., LLINAS, A. & MENDELL, L. M. 1999. Effects of trkB and trkC neurotrophin receptor agonists on thermal nociception: a behavioral and electrophysiological study. *Pain*, 80, 463-70.
- SNIDER, W. D. & MCMAHON, S. B. 1998. Tackling pain at the source: new ideas about nociceptors. *Neuron*, 20, 629-32.
- STANTCHEVA, K. K., IOVINO, L., DHANDAPANI, R., MARTINEZ, C., CASTALDI, L., NOCCHI, L., PERLAS, E., PORTULANO, C., PESARESI, M., SHIRLEKAR, K. S., DE CASTRO REIS, F., PAPAROUTAS, T., BILBAO, D. & HEPPENSTALL, P. A. 2016. A subpopulation of itch-sensing neurons marked by Ret and somatostatin expression. *EMBO Rep*, 17, 585-600.
- STUCKY, C. L., DECHIARA, T., LINDSAY, R. M., YANCOPOULOS, G. D. & KOLTZENBURG, M. 1998. Neurotrophin 4 is required for the survival of a subclass of hair follicle receptors. *J Neurosci*, 18, 7040-6.
- SUZUKI, M., MIZUNO, A., KODAIRA, K. & IMAI, M. 2003. Impaired pressure sensation in mice lacking TRPV4. *J Biol Chem*, 278, 22664-8.
- TALBOT, W. H., DARIAN-SMITH, I., KORNHUBER, H. H. & MOUNTCASTLE, V. B. 1968. The sense of flutter-vibration: comparison of the human capacity with response patterns of mechanoreceptive afferents from the monkey hand. *J Neurophysiol*, 31, 301-34.
- TODD, A. J. 2010. Neuronal circuitry for pain processing in the dorsal horn. *Nat Rev Neurosci*, 11, 823-36.
- TOMINAGA, M., CATERINA, M. J., MALMBERG, A. B., ROSEN, T. A., GILBERT, H., SKINNER, K., RAUMANN, B. E., BASBAUM, A. I. & JULIUS, D. 1998. The cloned capsaicin receptor integrates multiple pain-producing stimuli. *Neuron*, 21, 531-43.
- TORBORK, H. E., LUNDBERG, L. E. & LAMOTTE, R. H. 1992. Central changes in processing of mechanoreceptive input in capsaicin-induced secondary hyperalgesia in humans. *J Physiol*, 448, 765-80.

- TREEDE, R.-D. & MAGERL, W. 1995. Modern Concepts of Pain and Hyperalgesia: Beyond the Polymodal C-Nociceptor. *Physiology*, 10, 216-228.
- TREEDE, R. D., JENSEN, T. S., CAMPBELL, J. N., CRUCCU, G., DOSTROVSKY, J. O., GRIFFIN, J. W., HANSSON, P., HUGHES, R., NURMIKKO, T. & SERRA, J. 2008. Neuropathic pain: redefinition and a grading system for clinical and research purposes. *Neurology*, 70, 1630-5.
- TREEDE, R. D., MEYER, R. A., RAJA, S. N. & CAMPBELL, J. N. 1992. Peripheral and central mechanisms of cutaneous hyperalgesia. *Prog Neurobiol*, 38, 397-421.
- USOSKIN, D., FURLAN, A., ISLAM, S., ABDO, H., LONNERBERG, P., LOU, D. & HJERLING-LEFFLER, J. 2015. Unbiased classification of sensory neuron types by large-scale single-cell RNA sequencing. 18, 145-53.
- VRONTOU, S. 2013. Genetic identification of C-fibers that detect massage-like stroking of hairy skin in vivo. 493, 669-73.
- VRONTOU, S., WONG, A. M., RAU, K. K., KOERBER, H. R. & ANDERSON, D. J. 2013. Genetic identification of C fibres that detect massage-like stroking of hairy skin in vivo. *Nature*, 493, 669-73.
- WALL, P., DEVOR, M., INBAL, R., SCADDING, J., SCHONFELD, D., SELTZER, Z. & TOMKIEWICZ, M. 1979. Autotomy following peripheral nerve lesions: experimental anesthesia dolorosa. *Pain*, 7, 103-113.
- WANG, R. & LEWIN, G. R. 2011. The Cav3.2 T-type calcium channel regulates temporal coding in mouse mechanoreceptors. *J Physiol*, 589, 2229-43.
- WANG, X., RATNAM, J., ZOU, B., ENGLAND, P. M. & BASBAUM, A. I. 2009. TrkB signaling is required for both the induction and maintenance of tissue and nerve injury-induced persistent pain. *J Neurosci*, 29, 5508-15.
- WASNER, G., KLEINERT, A., BINDER, A., SCHATTSCHEIDER, J. & BARON, R. 2005. Postherpetic neuralgia: topical lidocaine is effective in nociceptor-deprived skin. *J Neurol*, 252, 677-86.
- WENDE, H., LECHNER, S. G. & BIRCHMEIER, C. 2012a. The transcription factor c-Maf in sensory neuron development. *Transcription*, 3, 285-9.
- WENDE, H., LECHNER, S. G., CHERET, C., BOURANE, S., KOLANCZYK, M. E., PATTYN, A., REUTER, K., MUNIER, F. L., CARROLL, P., LEWIN, G. R. & BIRCHMEIER, C. 2012b. The transcription factor c-Maf controls touch receptor development and function. *Science*, 335, 1373-6.
- WETZEL, C., HU, J., RIETHMACHER, D., BENCKENDORFF, A., HARDER, L., EILERS, A., MOSHOURAB, R., KOZLENKOV, A., LABUZ, D., CASPANI, O., ERDMANN, B., MACHELSKA, H., HEPPENSTALL, P. A. & LEWIN, G. R. 2007. A stomatin-domain protein essential for touch sensation in the mouse. *Nature*, 445, 206-9.
- WILSON, S. R., GERHOLD, K. A., BIFOLCK-FISHER, A., LIU, Q., PATEL, K. N., DONG, X. & BAUTISTA, D. M. 2011. TRPA1 is required for histamine-independent, Mas-related G protein-coupled receptor-mediated itch. *Nat Neurosci*, 14, 595-602.
- WOO, S. H., LUKACS, V., DE NOOIJ, J. C., ZAYTSEVA, D., CRIDDLE, C. R., FRANCISCO, A., JESSELL, T. M. & WILKINSON, K. A. 2015. Piezo2 is the principal mechanotransduction channel for proprioception. 18, 1756-62.
- WOO, S. H., RANADE, S., WEYER, A. D., DUBIN, A. E., BABA, Y., QIU, Z., PETRUS, M., MIYAMOTO, T., REDDY, K., LUMPKIN, E. A., STUCKY, C. L. & PATAPOUTIAN, A. 2014. Piezo2 is required for Merkel-cell mechanotransduction. *Nature*, 509, 622-6.

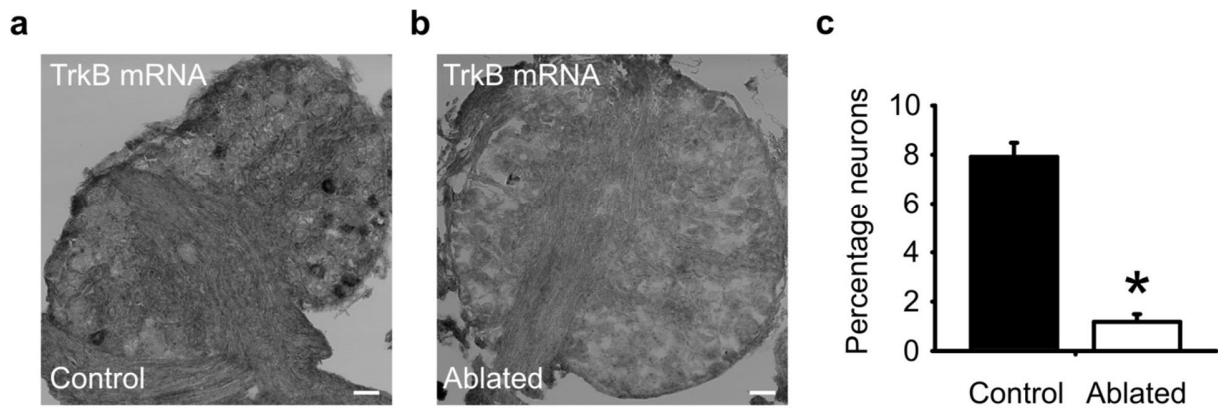
- WOOLF, C. J. 1996. Phenotypic modification of primary sensory neurons: the role of nerve growth factor in the production of persistent pain. *Philos Trans R Soc Lond B Biol Sci*, 351, 441-8.
- WOOLF, C. J. & MA, Q. 2007. Nociceptors--noxious stimulus detectors. *Neuron*, 55, 353-64.
- WOOLF, C. J., SAFIEH-GARABEDIAN, B., MA, Q. P., CRILLY, P. & WINTER, J. 1994. Nerve growth factor contributes to the generation of inflammatory sensory hypersensitivity. *Neuroscience*, 62, 327-31.
- WOOLF, C. J., SHORTLAND, P. & COGGESHALL, R. E. 1992. Peripheral nerve injury triggers central sprouting of myelinated afferents. *Nature*, 355, 75-8.
- XU, Z. Z., KIM, Y. H., BANG, S., ZHANG, Y., BERTA, T., WANG, F., OH, S. B. & JI, R. R. 2015. Inhibition of mechanical allodynia in neuropathic pain by TLR5-mediated A-fiber blockade. *Nat Med*, 21, 1326-31.
- YANG, G., DE CASTRO REIS, F., SUNDUKOVA, M., PIMPINELLA, S., ASARO, A., CASTALDI, L., BATTI, L., BILBAO, D., REYMOND, L., JOHNSON, K. & HEPPENSTALL, P. A. 2015. Genetic targeting of chemical indicators in vivo. *Nat Methods*, 12, 137-9.
- ZEILHOFER, H. U., WILDNER, H. & YEVENES, G. E. 2012. Fast synaptic inhibition in spinal sensory processing and pain control. *Physiol Rev*, 92, 193-235.
- ZELENA, J. 1978. The development of Pacinian corpuscles. *J Neurocytol*, 7, 71-91.
- ZHOU, X. F., DENG, Y. S., XIAN, C. J. & ZHONG, J. H. 2000. Neurotrophins from dorsal root ganglia trigger allodynia after spinal nerve injury in rats. *Eur J Neurosci*, 12, 100-5.
- ZIMMERMANN, K., HEIN, A., HAGER, U., KACZMAREK, J. S., TURNQUIST, B. P., CLAPHAM, D. E. & REEH, P. W. 2009. Phenotyping sensory nerve endings in vitro in the mouse. *Nat Protoc*, 4, 174-96.
- ZIMMERMANN, K., LEFFLER, A., BABES, A., CENDAN, C. M., CARR, R. W., KOBAYASHI, J., NAU, C., WOOD, J. N. & REEH, P. W. 2007. Sensory neuron sodium channel Nav1.8 is essential for pain at low temperatures. *Nature*, 447, 855-8.
- ZOTTERMAN, Y. 1939. Touch, pain and tickling: an electro-physiological investigation on cutaneous sensory nerves. *J Physiol*, 95, 1-28.
- ZYLKA, M. J., RICE, F. L. & ANDERSON, D. J. 2005. Topographically distinct epidermal nociceptive circuits revealed by axonal tracers targeted to Mrgprd. *Neuron*, 45, 17-25.

8 Supplementary figures



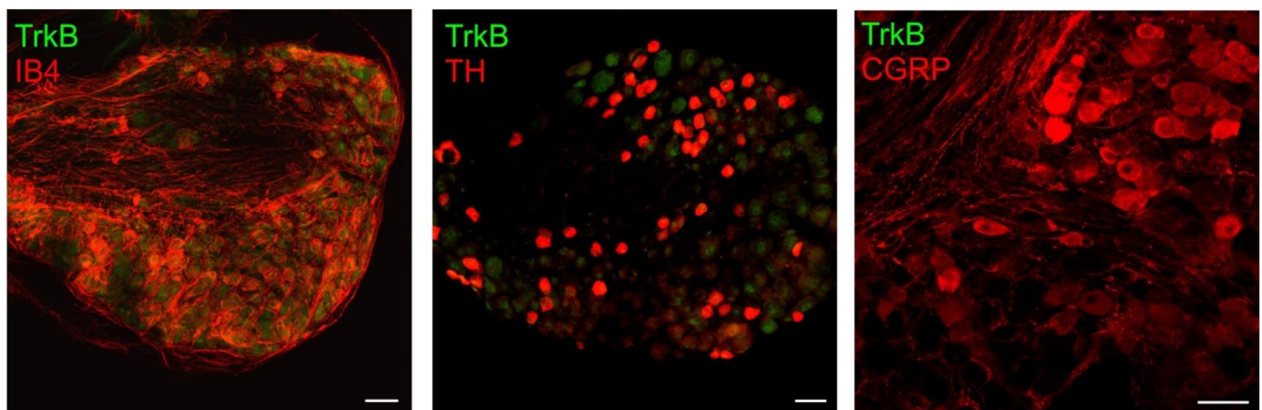
Supplementary figure 22: Generation of $TrkB^{CreERT2}$ and $Avil^{Cherry-hM3DQ}$ mice

Genetic strategy for the generation of (a) $TrkB^{CreERT2}$ BAC transgenic and (b) $Avil^{Cherry-hM3DQ}$ lines. (c) Southern blot for the $Avil^{Cherry-hM3DQ}$ line.



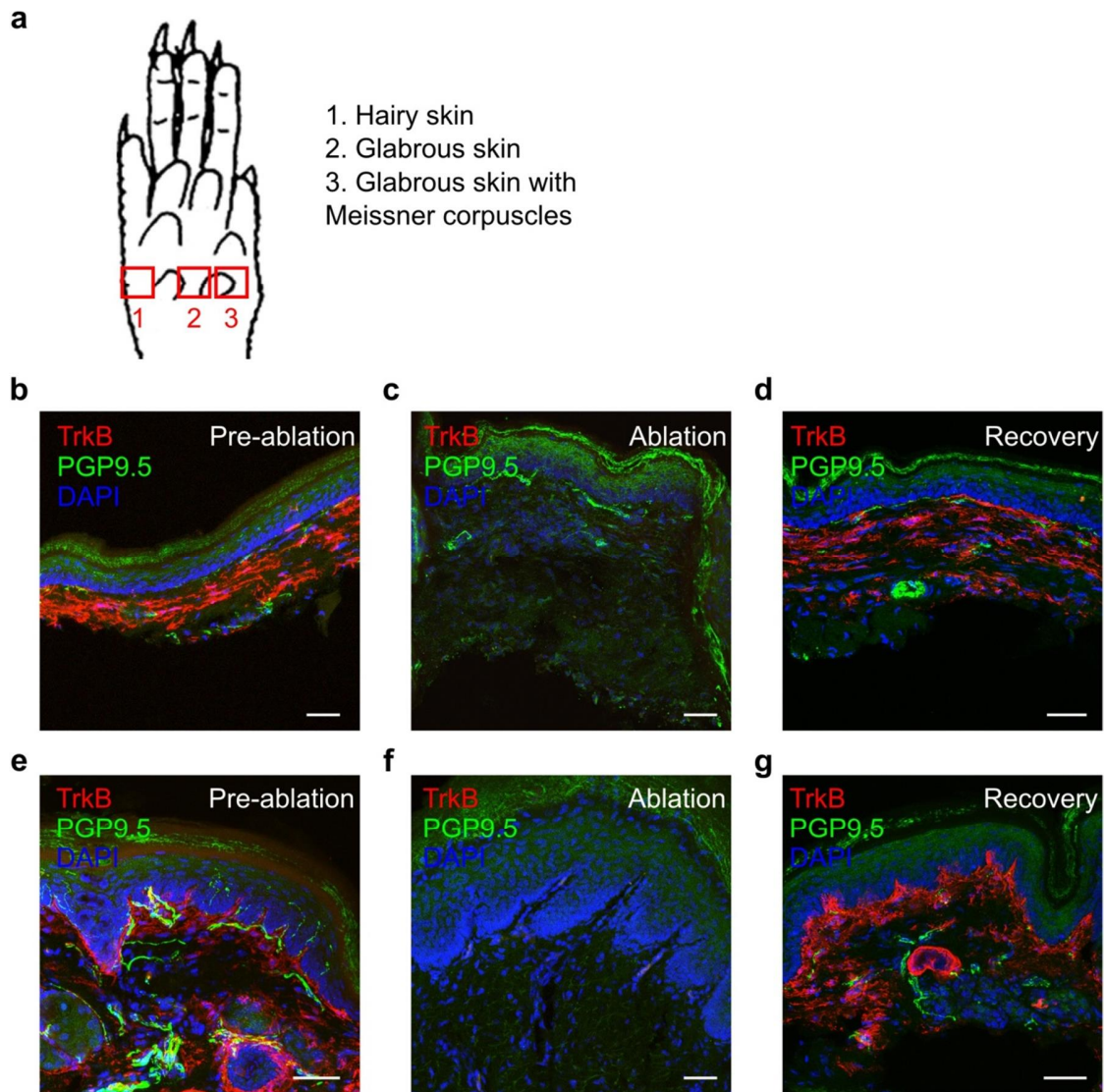
Supplementary figure 23: in-situ hybridization for TrkB

In-situ hybridization for TrkB mRNA in (a) control and (b) ablated mice. (c) Quantification of number of TrkB⁺ cells



Supplementary figure 24: Staining for molecular markers on TrkB ablated mice

Cross-section of DRG from TrkB ablated mice stained with IB4, TH and CGRP shows no difference in numbers on ablation.



Supplementary figure 25: Innervation of hind-paw after BDNF^{SNAP} photoablation

Schematic of the hind-paw of mice showing the (a) different analyzed regions of the glabrous skin under (b-e) baseline conditions, (c-f) after ablation and (d-g) upon re-innervation.